CHALMERS UNIVERSITY OF TECHNOLOGY

MASTER'S THESIS

ENGINEERING MATHEMATICS AND COMPUTATIONAL SCIENCE

# Option Pricing and Exponential Lévy Models

*Author:*
Johan HÅKANSSON

*Supervisor:*
Prof. Patrik ALBIN

April 23, 2015

# ABSTRACT

The aim of this thesis was to capture the stylized facts of the classical Black-Scholes model by utilizing exponential Lévy models. European-style call option prices were retrieved by applying the fractional fast Fourier transform via the characteristic functions of the underlying assets. The underlying assets were the three indices Nasdaq-100, Dow Jones Industrial Average, and Standard & Poor 500. The following exponential Lévy models together with the Black-Scholes model were used to model the price processes of the underlying assets: Merton's and Kou's jump-diffusion models, the variance-gamma model, and the normal-inverse Gaussian model. Furthermore, the method of steepest descent was used to calibrate model prices to market quotes.

It was shown that the exponential Lévy models were better at approximating market quotes than the classical Black-Scholes model. That is, by modeling the possibility of sudden jumps in the asset price process, the exponential Lévy models outperformed the Black-Scholes model.

# ACKNOWLEDGMENTS

I would like to express my gratitude to my supervisor, Prof. Patrik Albin, for introducing me to the subject and for his continuous support and patience during my dissertation.

I would also like to convey my most sincere appreciation for the constant love and encouragement from my father and my mother throughout all my life.

Last but not least, I am deeply grateful to Gullmar and Maj Ekström. Their heartwarming aid and thoughtfulness during the difficult years of my father's illness have given me a vast amount of comfort.

# PREFACE

The Black-Scholes model is a mathematical model of financial markets on which derivatives are being traded. From the model, the Black-Scholes formula can be retrieved which in turn can be used to estimate the price of European-style options based on geometric Brownian motion. However, it has consistently been shown that utilizing the Black-Scholes model in option pricing yields results that are inconsistent with options data. Even though versions of the Black-Scholes model based on the implied volatility are able to perform better, these models are made up of the wrong building blocks. In the late 1980s and early 1990s, Lévy models were proposed as an alternative in order to improve on the results of the Black-Scholes model. A huge benefit of utilizing Lévy models is that they take into account the stylized characteristics of the markets.

This thesis is mainly about the pricing of index options by market models based on Lévy processes. The theory and application of Lévy processes have had a major impact on the finance industry.

This thesis is structured as follows. In Chapter 1 we introduce some basic theory of financial derivatives. We talk about which option markets are included and look at the elements influencing the price of an option.

Chapter 2 deals with basic theory of stochastic calculus. We briefly introduce topics such as measures, filtrations, characteristics of the Brownian motion, and Itô's lemma.

In Chapter 3 we look at the Black-Scholes model. We derive the Black-Scholes equation and talk about the stylized facts of the Black-Scholes model.

In Chapter 4 we derive the price of a European call option based on the fast Fourier transform algorithm. We look at a caveat which concerns the fast Fourier transform which leads us to the introduction of the fractional fast Fourier transform.

Chapter 5 introduces Lévy processes. We talk about Merton's and Kou's jump-diffusion models. We also talk about infinite activity pure jump processes, such as the variance-gamma process and the normal-inverse Gaussian process. An integral part of this chapter concerns with risk-neutral characteristic functions.

Chapter 6 gives a brief overview of the simulation techniques utilized when modeling the various processes.

In Chapter 7 we explain the methods used for estimating the parameters when calibrating the models. We also discuss and list the various model inputs.

In Chapter 8 we present the results. We compare the derived model prices to given market quotes for both the Black-Scholes model and the exponential Lévy models.

Finally, Chapter 9 concludes with a discussion about the results and possible extensions to this work.

# CONTENTS

# 1 Basic Theory of Financial Derivatives

We begin by presenting an elementary introduction to the world of financial derivatives. A more thorough and rigorous treatment of the subject can be found in [10] (Hull, 2011).

## 1.1 Financial Derivatives

A derivative is a financial instrument whose value depends on, or derives from, the values of other underlying variables. The variables underlying the derivative are often the prices of traded assets. In other words, a derivative is a financial contract whose value at the expiration date, $T$ say, is determined by the price process of the underlying assets up to time $T$.

Derivatives have become progressively more important in finance. The market of derivatives is huge, and it is a significant component when transferring risks in the economy from one entity to another ([10], p. 1). In terms of underlying assets, the market of derivatives is much larger than, for example, the stock market.

### 1.1.1 Assets Underlying the Financial Derivatives

The underlying assets in this thesis are stock indices. A stock index is a measurement of the value of a section of the stock market and is generally computed as a weighted average of the underlying stock prices.

A speculator might trade financial derivatives on indices to bet on an overall market development without exposing himself to a particular asset. Furthermore, stock indices are often used by investors and financial managers to describe the market, and to compare the return on particular investments.

### 1.1.2 Interest Rates

An interest rate defines the amount of money a borrower promises to pay to a lender and is a factor in the pricing of nearly all derivatives.

The rates an investor earns on Treasury bills and Treasury bonds are called Treasury rates. Governments use these instruments to borrow in their own currencies. Treasury rates are considered to be risk-free rates since it is usually assumed that the risk of a government defaulting on an obligation denominated in its own currency is negligible. When pricing derivatives, the risk-free rate is used extensively.

In theory, rising interest rates should increase the stock price because a growing economy should yield growing corporate earnings. However, in reality, rising interest rates tend to be detrimental for stocks for various reasons such as [19]:

- When interest rates increase, investors who had previously been buying stocks tend to settle on bonds because their yields are rising.
- When interest rates increase, companies that borrow money have to pay more resulting in a reduction in their earnings.

- Also consumers have to pay more to borrow money when the interest rates increase. This deters them from buying houses, cars, etc. Thus, companies that are dependent on the consumers take a blow.

### 1.1.3 Cash and Stock Dividends

A dividend is an individual share of earnings handed out among stockholders in proportion to their holdings. Usually they are payable in cash, but sometimes also in the form of additional shares of stocks. Most secure and stable companies provide their stockholders with dividends. Even though the companies' share prices might not move much, dividends aim to compensate for this.

## 1.2 European Call and Put Options

There are two types of options: call options and put options. A call option gives the holder the right to buy the underlying asset by a certain date for a certain price. A put option gives the holder the right to sell the underlying asset by a certain date for a certain price. The buyer's profit or loss is the reverse of that for the seller of the option.

The fixed price at which the holder of the option can buy or sell the underlying asset is called the strike price, or the exercise price. The date at which the option expires is called the maturity, or the expiration date.

European options can be exercised only on the expiration date, whereas American options can be exercised at any time up to the expiration date. European call and put options are often known as plain vanilla options since they are so basic. More advanced options are largely called exotic.

### 1.2.1 Exchange-Traded Markets

As was mentioned, the underlying assets in this thesis are stock indices. Throughout the world, many different options trade both on over-the-counter markets and on exchange-traded markets. In the United States, the most popular exchange-traded contracts are those on the S & P 500 Index (SPX), the S & P 100 Index (OEX), the Nasdaq-100 Index (NDX), and the Dow Jones Industrial Average (DJX) ([10], p. 199) . The contracts are mostly European, the exception being the OEX contract on the S & P 100 Index, which is American. Since this thesis solely covers European contracts, this index will be excluded.

### 1.2.2 Volatility as a Measure of Uncertainty

The volatility is, roughly speaking, a measure of the uncertainty about future asset price movements. A higher volatility implies that the value of an asset has the potential to reach a larger range of values, while a lower volatility implies that the value of an asset undergoes minor fluctuations.

### 1.2.3 Moneyness as a Measure of the Intrinsic Value of an Option

Moneyness expresses whether or not exercising an option will produce a profit. It is the relative position of the current price of an underlying asset with respect to the strike price of a derivative. The derivative is said to be in-the-money if it was to expire today and yield a profit. It is said to be out-of-the-money if it was to expire today and yield a loss. Furthermore, it is said to be at-the-money if the current price and the strike price are equal.

### 1.2.4 Elements Influencing Option Prices

Six primary factors influence option prices. These are ([10], pp. 214-218):

- The underlying price: the most prominent factor influencing an option price is the current market price of the underlying asset. As the price of the underlying asset increases, generally the price of a call option increases while the price of a put option decreases, and vice versa if the price of the underlying asset decreases.

- The strike price: the price of an option generally increases as the option gets closer to being in-the-money. This is because the strike price becomes more favorable relative to the current price of the underlying asset. In the same way, the price of an option decreases as the option gets closer to being out-of-the-money, because the strike price is less favorable relative to the price of the underlying asset.

- The time to expiration: the longer time an option has until maturity, the better the chances are that it will end up in-the-money. Hence, as the maturity emerges, the time value of the option decreases. Furthermore, the underlying asset's volatility influences the time value because if the the underlying asset is highly volatile, the price movements are expected to be plentiful.

- Volatility of the underlying asset: the price of an option will typically increase if the underlying asset has higher volatility since the expected price changes will be greater.

- The interest rate: as interest rates increase, the call option premium generally increases, while the put option premium generally decreases, and vice versa if the interest rates decrease. This has to do with the cost connected with owning the underlying asset. If money is borrowed to make the purchase, there is an interest expense. If existing funds are used to make the purchase, there is a loss of interest income. In any case, the buyer will have interest expenses.

- The dividends: the price of the underlying asset typically drops by the amount of any cash dividend on the ex-dividend date. Thus, if the dividend of the underlying asset increases, the price of a call option will decrease, while the price of a put option will increase and vice versa.

### 1.2.5 Pros and Cons of Trading Options

Option strategies can be very risky, but if they are used wisely they can be very helpful. One reason is that the stock leverage can drastically be increased. Another reason is the emerging hedging opportunities against unfavorable markets.

## 1.3 Exploiting the Imbalances in Markets

Arbitrage is the practice of taking advantage of a price difference between two or more markets. The imbalance can be capitalized upon, yielding a risk-free profit where the profit is the difference between the market prices.

The essential part of a no-arbitrage assumption is that with no initial capital, making a profit without exposure to risk should not be possible. If it would be possible, arbitageurs would take advantage of it and use the market as a money-pump to extract arbitrarily large amounts of riskless profit ([9], p. 13).

## 1.4 Number of Trading Days in a Year

Research has shown that when the market is open, the volatility is much higher compared to when the market is closed. As a consequence, days when the market is closed tend to be ignored by practitioners when estimating the volatility from historical data and when valuating an option ([10], pp. 306-307).

Usually the number of trading days in a year is assumed to be 252 for stocks. The remaining life of an option, $T$, is measured in years and is given by

$$T = \frac{\text{Number of trading days until option maturity}}{252}.$$

# 2 Basic Theory of Stochastic Calculus

To be able to understand the evolution of asset prices, particularly in the world of Black-Scholes, one needs a few tools from stochastic calculus. In this section, an overview of the main ideas from a probabilistic perspective will be given. These ideas will later on be used when deriving prices of derivatives within the Black-Scholes setting.

Hence, the aim of this section is to build stochastic processes in continuous time that are able to represent the probabilistic and dynamic performance of assets ([11], p. 21) .

## 2.1 The State Space

A stochastic process is thought of as the result of the state of nature, where each state has the capability to influence the value of the stochastic process. An example of a stochastic process is an asset price process.

Definition 3.1. *The set of all states is denoted by $\Omega$ and is called the state space. An element of $\Omega$ is denoted by $\omega$ and is called a sample path.*

Definition 3.2. *A random variable is a variable whose value is subject to randomness. It assigns numeric values to the outcomes of an experiment. Hence, it is just a function*

$$X : \Omega \to \mathbb{R}^n : \omega \to X(\omega).$$

If the state space is continuous, then the probability that a random variable will assume a particular value will almost always be zero for elements $\omega \in \Omega$, which is of little or no interest ([5], p. 2). Thus, probabilities have to be given to *subsets* of $\Omega$ instead of to *elements* of $\Omega$. Subsets of $\Omega$ on which probabilities can be assigned are called $\sigma$-algebras.

### 2.1.1 $\sigma$-algebras and Information

Definition 3.3. *Let $\Omega$ be some set, and let $2^\Omega$ denote its power set. Then a subset $\mathscr{F} \subset 2^\Omega$ is called a $\sigma$-algebra if it fulfils the following properties:*

- *$\mathscr{F}$ is non-empty. That is, there is at least one $A \subset \Omega \in \mathscr{F}$.*
- *$\mathscr{F}$ is closed under complementation. That is, if $A \in \mathscr{F}$, then also $A^c = \Omega \setminus A \in \mathscr{F}$ holds.*
- *$\mathscr{F}$ is closed under countable unions. That is, if $A_1, A_2, \ldots \in \mathscr{F}$, then also $\bigcup_{i=1}^{\infty} A_i \in \mathscr{F}$.*

Probabilities are just particular instances of an immense class of set functions called *measures*. Generally, measures are defined on $\sigma$-algebras. Elements of $\sigma$-algebras are called *measurable sets*. To reflect that the pair $(\Omega, \mathscr{F})$ can be measured, it is called a *measurable space*.

The smallest $\sigma$-algebra containing all open sets of $\mathbb{R}^n$ is called the *Borel $\sigma$-algebra*.

DEFINITION 3.4. *Let $A$ be an arbitrary family of subsets of $\Omega$. Then there exists a unique smallest $\sigma$-algebra which contains every set in $A$, namely the intersection of all $\sigma$-algebras containing $A$. This $\sigma$-algebra is denoted by $\sigma(A) = \sigma_A$ and is called the $\sigma$-algebra generated by $A$.*

An area that is directly connected to $\sigma$-algebras is information. This is because the information obtained by the realizations of a random variable $X$ is reproduced by the generated $\sigma$-algebra $\sigma_X$.

## 2.2 PROPERTIES OF MEASURES

DEFINITION 3.5 *Let $(\Omega, \mathscr{F})$ be a measurable space. A function $\mu$ from $\mathscr{F}$ to the extended real number line is called a measure if it fulfils the following properties:*

- *The measure of the empty set is zero, that is, $\mu(\emptyset) = 0$.*
- *Non-negativity, that is, $\forall A \in \mathscr{F},\ \mu(A) \geq 0$ holds.*
- *Countable additivity, that is, for all countable collections $\{A_i\}_{i\in\mathbb{N}}$ of pairwise disjoint sets in $\mathscr{F}$ the following holds:*

$$\mu\left(\bigcup_{i\in\mathbb{N}} A_i\right) = \sum_{i\in\mathbb{N}} \mu(A_i).$$

The everyday equivalent of a measure is, for example, the length of a rod, the volume of a ball, etc.

The triplet $(\Omega, \mathscr{F}, \mu)$ is called a *measure space* which is an augmentation of the measurable space with a measure. The reason why the elements of $\mathscr{F}$ that are subsets of $\Omega$ are called measurable sets is that they have the possibility of being able to be measured by $\mu$.

### 2.2.1 PROBABILITY MEASURES

DEFINITION 3.6 *A function $P : \Omega \to \mathbb{R}$ is a probability measure on a probability space if it fulfils the following properties:*

- *$P$ must return results in the unit interval $[0, 1]$. Furthermore, $P(\emptyset) = 0$ and $P(\Omega) = 1$ must hold.*
- *Countable additivity, that is, if $\{A_i\}_{i\in\mathbb{N}}$ is a countable, pairwise disjoint collection of events, then the following holds:*

$$P\left(\bigcup_{i\in\mathbb{N}} A_i\right) = \sum_{i\in\mathbb{N}} P(A_i).$$

A crucial property to keep in mind is that separate probability measures on $\mathbb{R}^n$, derived from separate probability spaces, can be produced by the same random variable.

A typical case where this is applied is when investors are curious about the probabilistic performance of an asset price process. Even though the investors might concur with the true probability measure, they might act as if the probability measure was another one. As will be seen, this can be the result of, for example, the risk aversion among investors or market frictions.

### 2.2.2 Equivalency Between Probability Measures

As was mentioned earlier, random variables can produce a vast number of separate probability measures. These probability measures can be grouped in accordance with some of their properties. One significant property describes the sets which the probability measures attribute zero probability. Measures that concur on these sets are said to be *equivalent* ([20], p. 17).

Furthermore, if a probability measure $Q$ is *absolutely continuous* with respect to another probability measure $P$, then unfeasible events under $P$ are also unfeasible under $Q$.

## 2.3 Stochastic Processes and the Dynamics of Asset Prices

A random variable is adequate if only the uncertainty at a single point in time needs to be described. However, when considering asset prices also the dynamics are vital. By assembling a number of random variables, a stochastic process can be constructed.

Definition 3.7. *A stochastic process is a family of random variables $X = \{X_t\}_{t\in T}$ defined on a given probability space, indexed by a totally ordered set $T$ representing time.*

### 2.3.1 Filtration and Information Flow

As was previously mentioned, information is connected with $\sigma$-algebras. However, in the setting of stochastic processes information undergoes a change. Generally a *filtration* is defined to reflect the accumulation or destruction of information. As time passes, more information is revealed to the observer. In the example of the price of a stock, a filtration characterizes how the stock price information is brought to light.

Definition 3.8. *Given a probability space $(\Omega, \mathscr{F}, P)$, a filtration is a non-decreasing family $\{\mathscr{F}_t\}_{0\le t\le T}$ of sub-$\sigma$-algebras of $\mathscr{F}$ satisfying*

$$\mathscr{F}_s \subset \mathscr{F}_t \subset \mathscr{F}_T \subset \mathscr{F},\ 0 \le s < t \le T,$$

*where $\mathscr{F}_t$ represents the information available at time $t$, and $\{\mathscr{F}_t\}_{0\le t\le T}$ represents the information flow evolving with time.*

If all random variables $X_t$ are $\mathscr{F}_t$-measurable, the stochastic process is said to be *adapted*. Furthermore, each collection of random variables $\{X_s\}_{0\leq s\leq t}$ gives rise to a collection of $\sigma$-algebras called the *natural filtration* of the stochastic process, which is denoted by $\mathscr{F}_t = \sigma(\{X_s\}_{0\leq s\leq t})$ ([5], p. 13). The natural filtration is the smallest filtration causing the stochastic process to be adapted. It embodies the accumulated information by monitoring the stochastic process up to time $t$. In a sense, it is the simplest filtration available for monitoring the stochastic process since only the information regarding the process is included and nothing else.

## 2.4 Brownian Motion

A *Brownian motion* is a continuous-time stochastic process and is one of the best known *Lévy processes*. It often occurs in both pure and applied mathematics. A Brownian motion $B_t$ is characterized by three properties, namely ([9], p. 56):

- $B_0 = 0$.
- The function $t \to B_t$ is continuous everywhere almost surely.
- $B_t$ has independent increments with $B_t - B_s \sim \mathcal{N}(0, t-s)$, where $\mathcal{N}(\mu, \sigma^2)$ denotes a Gaussian distribution with expected value $\mu$ and variance $\sigma^2$.

Note that, by its definition, Brownian motion is Gaussian. A realization of a Brownian motion $B = \{B_t\}_{t\geq 0}$ started at zero is displayed in Figure 1. Even though it is a process lead by pure chance with zero mean, it has regions where it acts as if it has trends.

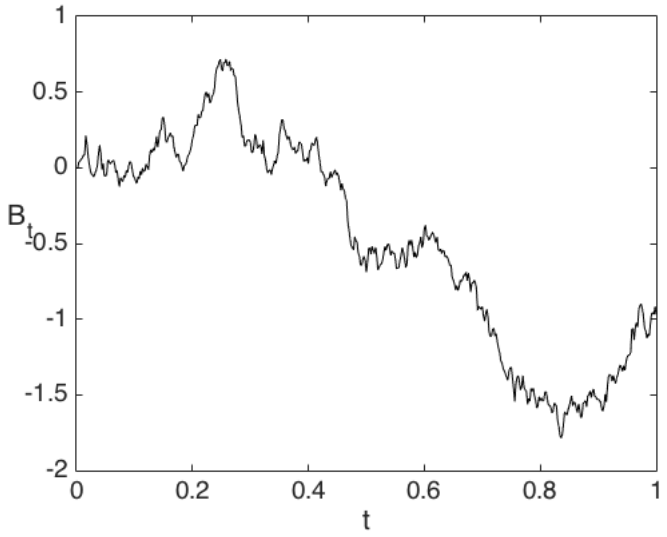


Figure 1: A realization, or path, of a Brownian motion $B_t$ with $\mu = 0$ and $\sigma = 1$.

### 2.4.1 Characteristics of Brownian Motion

It is assumed that the Brownian motion $B = \{B_t\}_{t\geq 0}$ has a natural filtration $\mathscr{F}_t$. Furthermore, the Brownian motion is a *martingale*.

Definition 3.9. *Let $(\Omega, \mathscr{F}, \{\mathscr{F}_t\}_{t\geq 0}, P)$ be a filtered space. A stochastic process $X_t$ is a martingale if it fulfils the following properties:*

- *$X_t$ is adapted to the filtration.*
- *$\mathbb{E}[|X_t|] < \infty \; \forall\, t \geq 0$. That is, the process is integrable.*
- *$\mathbb{E}[X_u|\mathscr{F}_t] = X_t \; \forall\, u \geq t \geq 0$.*

Given an adapted function $\alpha$, every continuous martingale can be represented as a time-changed Brownian motion $B_{\alpha_t}$.

Additionally, the Brownian motion is a *Markov process*. Hence, if the present state of the Brownian motion is known, then its future behavior is independent of its past.

Definition 3.10. *A stochastic process $X = \{X_t\}_{t\geq 0}$ is a Markov process if for any $s, t > 0$ the following property holds:*

$$P(X_{t+s} \leq x|\mathscr{F}_t) = P(X_{t+s} \leq x|X_t) \text{ almost surely.}$$

### 2.4.2 Brownian Motion and Diffusion

A *diffusion* is a Markov process with continuous sample paths and is characterized by its local drift $\mu$ and volatility $\sigma$. Let $X = \{X_t\}_{t\geq 0}$ be a diffusion and let $\Delta t$ be a small time increment. Its *instantaneous drift* is given by

$$\mathbb{E}[X_{t+\Delta t} - X_t|\mathscr{F}_t] = \mu(X_t)\Delta t + o(\Delta t),$$

while its *instantanteous volatility* is given by

$$\mathbb{E}\left[\left(X_{t+\Delta t} - X_t - \mu(X_t)\Delta t\right)^2|\mathscr{F}_t\right] = \sigma^2(X_t)\Delta t + o(\Delta t).$$

Given a Brownian motion $B = \{B_t\}_{t\geq 0}$, the process $X_t = \mu + \sigma B_t$ is a diffusion if both the drift and the volatility are constant. However, in general, the instantaneous drift and the instantaneous volatility do not have to be constant but can depend on both the time $t$ and the location $X_t$ ([5], p. 19).

### 2.4.3 The Erratic Behavior of Brownian Motion

Let $t \mapsto B(t,\omega)$ be a Brownian motion defined as a function of time with a fixed sample point $\omega \in \Omega$. A sample path of this function is continuous almost everywhere but nowhere differentiable.

Let $0 = t_0^{(n)} \leq t_1^{(n)} \leq \ldots \leq t_{k(n)-1}^{(n)} \leq t_{k(n)}^{(n)} = t$ be a nested sequence of partitions of the time

interval $[0, t]$. That is, at each step one or more partition points are added and the mesh given by

$$\Delta(n) = \sup_{1 \le j \le k(n)} \left\{ t_j^{(n)} - t_{j-1}^{(n)} \right\},$$

converges to zero. Then, almost surely, the total variation of a sample path of the Brownian motion is unbounded, and its quadratic variation is finite ([11], p. 63):

$$\lim_{n \to \infty} \sum_{j=1}^{k(n)} \left| B_{t_j^{(n)}} - B_{t_{j-1}^{(n)}} \right| = \infty,$$

$$\lim_{n \to \infty} \sum_{j=1}^{k(n)} \left( B_{t_j^{(n)}} - B_{t_{j-1}^{(n)}} \right)^2 = t.$$

Hence, when examining a path of a Brownian motion, there is no way to find a monotonic interval. A realization of a Brownian motion $B = \{B_t\}_{t \ge 0}$ started at zero and zoomed in three times is displayed in Figure 2.

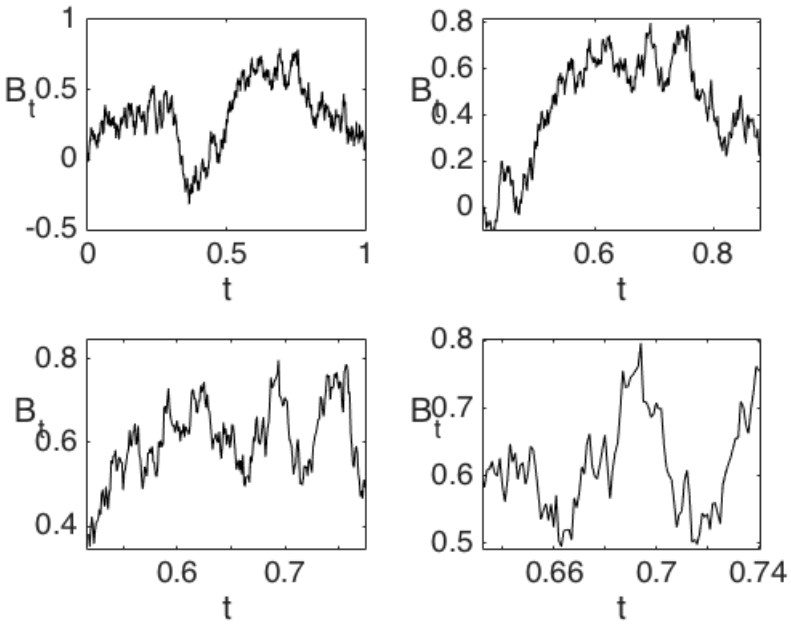


Figure 2: A realization of a Brownian motion $B_t$ zoomed in three times.

## 2.5 Stochastic Differential Equations and Brownian Motion

A *stochastic differential equation* is given by

$$\frac{\mathrm{d}X_t}{\mathrm{d}t} = \mu(t, X_t) + \text{noise}.$$

Let the noise be represented by a Brownian motion $B_t$. Given the drift $\mu$ and the volatility $\sigma$, the resulting process is called an *Itô diffusion* and is denoted by

$$\mathrm{d}X_t = \mu(t, X_t) + \sigma(t, X_t)\,\mathrm{d}B_t.$$

This can also be written as

$$X_t = X_0 + \int_0^t \mu(s, X_s)\,\mathrm{d}s + \int_0^t \sigma(s, X_s)\,\mathrm{d}B_s,$$

where the last integral term is called an *Itô integral* with respect to Brownian motion.

### 2.5.1 Itô's Lemma and Geometric Brownian Motion

One of the most fundamental tools in stochastic calculus is *Itô's formula* or *Itô's lemma*. Consider an Itô process ([11], pp. 91-124)

$$\mathrm{d}X_t = \mu(t, x)\,\mathrm{d}t + \sigma(t, x)\,\mathrm{d}B_t,$$

and a function $h(t, x) \in \mathscr{C}^{(1,2)}$ defining a new Itô process via $Y_t = h(t, X_t)$. What Itô's formula does is to characterize the dynamics of $Y_t$ in connection with the drift and the volatility of $X_t$ and the derivatives of $h$ such that

$$\begin{aligned}\mathrm{d}Y_t &= \partial_t h(t, X_t)\,\mathrm{d}t + \partial_{X_t} h(t, X_t)\,\mathrm{d}X_t + \frac{1}{2}\partial_{X_t X_t} h(t, X_t)(\mathrm{d}X_t)^2 \\ &= \left(\partial_t h(t, X_t) + \mu(t, X_t)\partial_{X_t} h(t, X_t) + \frac{1}{2}\sigma^2(t, X_t)\partial_{X_t X_t} h(t, X_t)\right)\mathrm{d}t \\ &\quad + \sigma(t, X_t)\partial_{X_t} h(t, X_t)\,\mathrm{d}B_t,\end{aligned}$$

since $(\mathrm{d}t)^2 = \mathrm{d}t\,\mathrm{d}B_t = 0$ and $(\mathrm{d}B_t)^2 = \mathrm{d}t$.

A common model for an asset price process $S = \{S_t\}_{t\geq 0}$ comply with the stochastic differential equation for a *geometric Brownian motion* given by

$$\mathrm{d}S_t = \mu S_t\,\mathrm{d}t + \sigma S_t\,\mathrm{d}B_t,$$

with constant expected return $\mu$ and volatility $\sigma$. Applying Itô's formula to the logarithm of the asset price $\ln S_t$ yields

$$\mathrm{d}\ln S_t = \left(\mu - \frac{1}{2}\sigma^2\right)\mathrm{d}t + \sigma\,\mathrm{d}B_t.$$

Hence,

$$\ln S_t = \ln S_0 + \left(\mu - \frac{1}{2}\sigma^2\right)t + \sigma B_t,$$

which gives the result

$$S_t = S_0 \mathrm{e}^{\left(\mu - \frac{1}{2}\sigma^2\right)t + \sigma B_t}.$$

The geometric Brownian motion and the log-normal distribution which it entails form the basis for the Black-Scholes model for asset price dynamics in continuous time. A realization of a geometric Brownian motion $S = \{S_t\}_{t\geq 0}$ started at one is displayed in Figure 3.

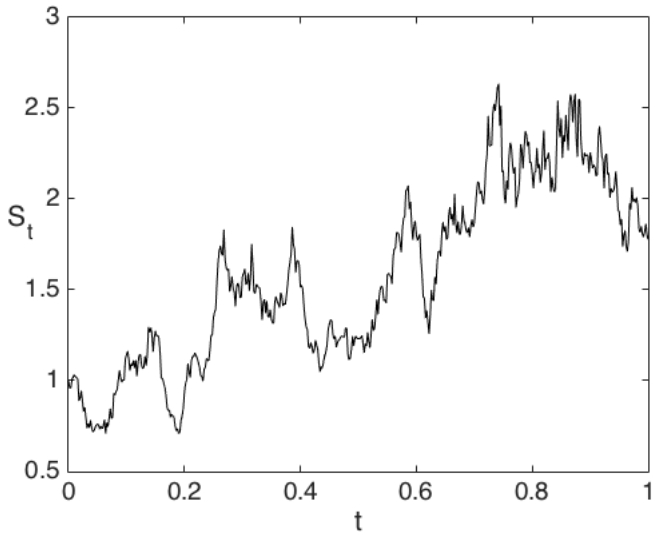


Figure 3: A realization of a geometric Brownian motion $S_t$ where $\mu = 0, \sigma = 1$, and $S_0 = 1$.

# 3 The Black-Scholes Model

The groundbreaking work of Fischer Black and Myron Scholes laid the foundation for the in-depth study of the theory of option pricing. In this section we will study the theory of the Black-Scholes model in some detail due to its monumental significance in the discipline of option pricing.

However, the Black-Scholes model is not perfect since some of its assumptions are not entirely fulfilled in practice. Therefore we will also discuss its imperfections.

## 3.1 Underlying Presumptions of the Black-Scholes Model

When deriving the Black-Scholes partial differential equation, several presumptions are made. In able to understand the limitations of the underlying theory, it is vital to correctly apprehend these presumptions. The Black-Scholes model assumes that the market consists of at least one risky asset and one riskless asset.

The presumptions are ([10], p. 309):

- The rate of return on the riskless asset is constant and is known as the risk-free interest rate.
- The underlying risky asset price process $S_t$ is assumed to follow a geometric Brownian motion such that
$$\mathrm{d}S_t = \mu S_t \,\mathrm{d}t + \sigma S_t \,\mathrm{d}B_t,$$
where the drift $\mu$ and the volatility $\sigma$ are assumed to be constant.
- The risky asset pays no dividend.
- There is no way to make a riskless profit, hence the market has no arbitrage opportunities.
- It is feasible to borrow and to lend fractional amounts of cash at the risk-free rate.
- It is feasible to buy and to sell fractional amounts of the risky asset. Also short-selling is allowed.
- There are neither taxes nor transaction costs, hence the market is frictionless.

Clearly these presumptions cannot be perfectly satisfied in the real world. For example, transaction costs do exist in all markets, and all securities are traded in discrete units.

Despite the imperfections of the Black-Scholes model, it is still important to be able to grasp the theory because the concepts behind the model provide the framework for basic option pricing.

### 3.1.1 A Self-Financing, Replicating Hedging Strategy

Setting up a self-financing, replicating hedging strategy is one way of deriving the Black-Scholes equation [21]. A self-financing portfolio is an important concept in financial mathematics. A portfolio is self-financing if there is no exogenous infusion or withdrawal of money. Hence the sale of an old asset must finance the purchase of every new asset. The initial investment will be the price of the derivative that the strategy is replicating.

A replicating strategy is a dynamic trading strategy that varies the exposure of a portfolio between a risky asset and a riskless asset in order to yield the same payoff function as the derivative being priced.

Furthermore, irrespective of the price changes in the underlying security, the portfolio should consistently produce the same outcome. Hence, besides the stochastic components of the derivative's underlying securities, the portfolio should be deterministic.

By the no-arbitrage concept, any portfolio that is able to replicate the payoff of a derivative is compelled to have the same value as the derivative.

### 3.1.2 The Concept of Risk-Neutral Valuation

The most pivotal concept in derivative valuation is the concept of risk-neutral valuation, which says that the value of a derivative is equal to its expected future value discounted at the risk-free interest rate. This is equivalent to assuming a risk-neutral world. In a risk-neutral world, investors do not crave compensation for risk-taking which implies that the expected return on all securities is the risk-free interest rate. This is an example of a pivotal result known as *Girsanov's theorem* which says that if we move from a world with one set of risk preferences to another world with a different set of risk preferecens, the expected growth rates in variables alter, but their volatilities stay the same. Occasionally, moving from one set of risk preferences to another set of risk preferences is called *changing the measure*. Moreover, the real-world measure is usually called the $P$-measure, while the risk-neutral measure is usually called the $Q$-measure.

## 3.2 Deriving the Black-Scholes Equation

Let $f$ be a derivative whose value is a function of the underlying asset $S = \{S_t\}_{t\geq 0}$ and the time $t$. The underlying asset is assumed to follow a geometric Brownian motion

$$\mathrm{d}S_t = \mu S_t \,\mathrm{d}t + \sigma S_t \,\mathrm{d}B_t, \tag{1}$$

where the average growth rate $\mu$ of the underlying asset and the volatility $\sigma$ are constant.

Applying Itô's formula to $f$ yields ([10], pp. 309-310)

$$\begin{aligned} \mathrm{d}f &= \partial_t f \,\mathrm{d}t + \partial_{S_t} f \,\mathrm{d}S_t + \frac{1}{2}\partial_{S_tS_t} f (\mathrm{d}S_t)^2 \\ &= \left(\partial_t f + \mu S_t \partial_{S_t} f + \frac{1}{2}\sigma^2 S_t^2 \partial_{S_tS_t} f\right)\mathrm{d}t + \sigma S_t \partial_{S_t} f \,\mathrm{d}B_t. \end{aligned} \tag{2}$$

Since $\mathrm{d}f$ contains a stochastic term, $f$ cannot be directly valuated. Let the value of a portfolio be denoted by $\Pi$ and assume that the portfolio is composed of a short position in the derivative $f$ and a long position in $\Delta$ units of the underlying asset $S$ at time $t$, that is

$$\Pi = -f + \Delta S_t.$$

In an infinitesimally small time interval, the value of the portfolio changes by

$$\mathrm{d}\Pi = -\,\mathrm{d}f + \Delta\,\mathrm{d}S_t.$$

The equation for $\mathrm{d}S_t$ is given by Equation (1), whereas the equation for $\mathrm{d}f$ is given by Equation (2). Thus,

$$\begin{aligned}\mathrm{d}\Pi &= -\left(\partial_t f + \mu S_t \partial_{S_t} f + \frac{1}{2}\sigma^2 S_t^2 \partial_{S_t S_t} f\right)\mathrm{d}t - \sigma S_t \partial_{S_t} f\,\mathrm{d}B_t + \Delta\mu S_t\,\mathrm{d}t + \Delta\sigma S_t\,\mathrm{d}B_t \\ &= \left(-\partial_t f - \mu S_t \partial_{S_t} f - \frac{1}{2}\sigma^2 S_t^2 \partial_{S_t S_t} f + \Delta\mu S_t\right)\mathrm{d}t + \left(-\sigma S_t \partial_{S_t} f + \Delta\sigma S_t\right)\mathrm{d}B_t.\end{aligned}$$

To produce a riskless portfolio, the source of randomness has to be taken out. It is clear that the Brownian motion is the source of randomness. Hence, by letting $\Delta = \partial_{S_t} f$, the equation for $\mathrm{d}\Pi$ becomes

$$\mathrm{d}\Pi = \left(-\partial_t f - \frac{1}{2}\sigma^2 S_t^2 \partial_{S_t S_t} f\right)\mathrm{d}t.$$

Without a stochastic component, $\Pi$ is a riskless investment and must thus offer the same return as any other riskless investment, that is, there are no arbitrage opportunities. This implies that the diffusion of the riskless portfolio is equal to $\mathrm{d}\Pi = r\Pi\,\mathrm{d}t$, where $r$ is the risk-free interest rate. Hence,

$$\begin{gathered}\mathrm{d}\Pi = r\Pi\,\mathrm{d}t, \\ \left(-\partial_t f - \frac{1}{2}\sigma^2 S_t^2 \partial_{S_t S_t} f\right)\mathrm{d}t = r\left(-f + S_t \partial_{S_t} f\right)\mathrm{d}t.\end{gathered}$$

Dropping the $\mathrm{d}t$ term from both sides and rearranging yields the Black-Scholes partial differential equation

$$\partial_t f + \frac{1}{2}\sigma^2 S_t^2 \partial_{S_t S_t} f + r S_t \partial_{S_t} f - r f = 0.$$

The final condition $f(T, S_T)$ governs what kind of derivative is being priced. For example, for a European call option, the final condition is $f(T, S_T) = (S_T - K)^+$, where $K$ is the strike price of the option.

Since the Black-Scholes equation is independent of the expected growth rate $\mu$ of the underlying asset price, it is clear that the risk-neutral valuation property holds.

The portfolio $\Pi$ corresponds to a self-financing, replicating hedging strategy since it replicates a riskless investment and its value is deterministic.

The main financial insight behind the Black-Scholes equation is that it is possible to completely hedge the option by buying and selling the underlying asset in a way to eliminate risk. Consequently, this hedge implies that there is solely one correct price for the option, namely the price returned by the Black-Scholes equation.

### 3.2.1 SOLVING THE BLACK-SCHOLES EQUATION

There are many ways of solving the Black-Scholes equation. One way is to solve it numerically using standard methods of numerical analysis. Another way of solving it, which will be demonstrated below, is to apply the risk-neutral valuation property ([10], pp. 311-315).

Employing Itô's formula to $\ln S_t$ yields

$$\mathrm{d}\ln S_t = \frac{1}{S_t}\,\mathrm{d}S_t + \frac{1}{2}\left(-\frac{1}{S_t^2}\right)(\mathrm{d}S_t)^2 = \left(\mu - \frac{\sigma^2}{2}\right)\mathrm{d}t + \sigma\,\mathrm{d}B_t.$$

Hence,

$$\ln S_t \sim \mathcal{N}\left(\ln S_0 + \left(\mu - \frac{\sigma^2}{2}\right)t, \sigma^2 t\right),$$

since $B$ is a standard Brownian motion. Thus, $S_t$ follows a log-normal distribution which is in agreement with the process being a geometric Brownian motion.

The risk-neutral valuation property implies that the present value of the derivative is equal to its expected future value discounted at the risk-free interest rate. In obedience to the risk-neutral valuation property, $\mu$ is substituted with the risk-free interest rate $r$. It is given that $S_T = S_0\mathrm{e}^{X_T}$, where

$$X_T = \left(r - \frac{\sigma^2}{2}\right)T + \sigma B_T = \left(r - \frac{\sigma^2}{2}\right)T + \sigma\sqrt{T}Y,\ Y \sim \mathcal{N}(0,1).$$

The value of a European call option $C$ is derived by

$$\begin{aligned} C &= \mathrm{e}^{-rT}\mathbb{E}\left[(S_T - K)^+\right] \\ &= \mathrm{e}^{-rT}\int_{\ln(K/S_0)}^{\infty}\left(S_0\mathrm{e}^{x} - K\right)f_X(x)\,\mathrm{d}x \\ &= \mathrm{e}^{-rT}\left(S_0\int_{\frac{\ln(K/S_0)-(r-\sigma^2/2)T}{\sigma\sqrt{T}}}^{\infty}\mathrm{e}^{(r-\sigma^2/2)T+\sigma\sqrt{T}y}f_Y(y)\,\mathrm{d}y - K\int_{\ln(K/S_0)}^{\infty}f_X(x)\,\mathrm{d}x\right), \end{aligned}$$

which yields, after some algebraic manipulation,

$$C = S_0\Phi(d_1) - K\mathrm{e}^{-rT}\Phi(d_2) = \mathrm{e}^{-rT}\left(\mathrm{e}^{rT}S_0\Phi(d_1) - K\Phi(d_2)\right), \tag{3}$$

where

$$d_1 = \frac{\ln(S_0/K) + (r+\sigma^2/2)T}{\sigma\sqrt{T}},\ d_2 = \frac{\ln(S_0/K) + (r-\sigma^2/2)T}{\sigma\sqrt{T}} = d_1 - \sigma\sqrt{T},$$

and $\Phi(x)$ is the standard Gaussian cumulative probability distribution function.

Equation (3) can easily be interpreted. The probability that the European call option will be exercised in a risk-neutral world is equal to $\Phi(d_2)$, hence $K\Phi(d_2)$ is simply the strike price times the probability that the strike price will be paid. In a risk-neutral world, $\mathrm{e}^{rT}S_0\Phi(d_1)$ is the expected value of a variable that is equal to $S_T$ if $S_T > K$, otherwise it is equal to zero. Hence, $\mathrm{e}^{rT}S_0\Phi(d_1) - K\Phi(d_2)$ is the expected value of the option at maturity and Equation (3) is simply a demonstration of the risk-neutral valuation property.

## 3.3 Stylized Facts of the Black-Scholes Model

By assumption, all parameters of the Black-Scholes equation are $\mathscr{F}_0$-measurable. But even though the current price, the strike price, the maturity, and the interest rate are observed at time $t = 0$, the volatility $\sigma$ of the asset price is not. However, by inverting the Black-Scholes formula, a series of *implied volatilities* across different maturities and strike prices can be obtained.

The Black-Scholes model bring about many theoretical and practical problems ([5], pp. 66-68). Many of these problems are encapsulated by the patterns of the implied volatilities.

If the underlying presumptions of the Black-Scholes formula were to be true, then all prices would be priced in agreement with the Black-Scholes formula. Therefore, it would be assumed that the implied volatility would be the same across all maturities and all strike prices. However, as it turns out, the implied volatilities are not constant but display evident patterns. These patterns could be the result of the volatilities actually being time varying. Another reason for the patterns to appear could be discontinuities in the asset price process, which is something that will be studied in more detail in subsequent sections.

A plot of the implied volatility with respect to different measures of moneyness is called an implied volatility smile. Furthermore, an implied volatility surface can be constructed by plotting the implied volatility with respect to both moneyness and time to maturity. An example of a realization of an implied volatility surface is displayed in Figure 4.

Possible sources of the implied volatility patterns will subsequently be presented.

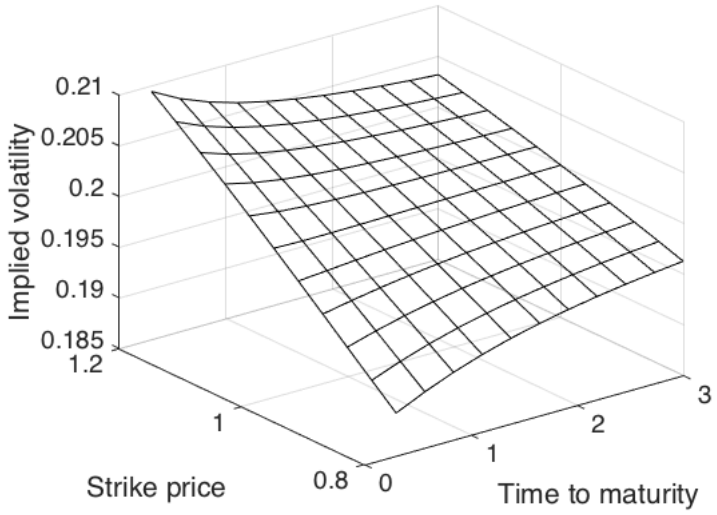


Figure 4: A realization of an implied volatility surface.

### 3.3.1 Leptokurtosis of the Distribution of Returns

It has been shown that asset returns display an extensive degree of excess kurtosis resulting in a higher peak than the curvature found in the Gaussian distribution. The high peak and

the corresponding fat tails yield a more clustured distribution around the mean compared to a mesokurtic or platykurtic distribution. For short maturity investments, the fat tails seem to be more pronounced, while for longer maturity investments they seem to diminish.

A distribution with excess kurtosis is in tune with the existence of an implied volatility smile. The reason is that it gives rise to higher probabilities of extreme events in contrast to the Gaussian distribution. If at-the-money implied volatilities are used then the Black-Scholes formula will consistently undervalue out-of-the-money put and call options.

### 3.3.2 Skewness of the Distribution of Returns

Asset return series can also display considerable skewness. Stocks and indices generally have negative skewness. The reason is that in general the decline rate of stock prices is higher than the growth rate. However, stock prices are apt to grow for longer periods of time than they fall.

The asymmetries displayed in the implied volatility smile can be ascribed to the skewness of the underlying asset returns. In fact, Black [2] argued that falling stock prices can lead to increased volatility. This asymmetry can cause skewed returns. However, this is not enough to shed light on the very steep implied volatility skews observed in option markets. One must also accommodate for sudden jumps in the asset price process resulting in market crashes.

### 3.3.3 Volatility Clustering

Empirical studies have shown that the volatility tend to come in cycles, where periods of low volatility are superseded by periods of high volatility. This can be linked to the surfacing of new information and high trading volume. Since trading does not occur uniformly across time, the arrival of new information will lead to a denser trading pattern with higher trading volumes; the outcome being higher volatilities.

### 3.3.4 Jumps in the Asset Price Process

Simply permitting the volatilities to be time varying is not enough to accommodate for sudden jumps in the asset price process. Even if the volatility would be permitted to fluctuate ferociously, a model with continuous paths such as the Black-Scholes model, would still not be able to accommodate for sudden jumps.

To expand on the Black-Scholes model, Robert Merton introduced in 1976 a *jump-diffusion* model. In this model, the asset price behavior is modeled by incorporating small day-to-day diffusive movements together with larger, randomly occuring jumps. The upside of including jumps is that it allows for more realistic crash scenarios. The downside is that the standard dynamic replicating hedging strategy of the Black-Scholes model is no longer applicable. Compared to the Black-Scholes model, this tends to increase the option prices. It also causes the option prices to depend on the risk aversion among investors.

This and other models will further be explained in Section 5.

# 4 Beyond the Black-Scholes Model

Despite the fact that the Black-Scholes model is neat and easy-to-use, it is somewhat confining in its postulations. For example, one postulation that evidently confute empirical studies is based on the premise that the log-returns are i.i.d. Gaussian ([5], p. 107).

When researchers attempted to find models that tempered with these postulations they realized that scarcely any model, aside from the Black-Scholes model, provided for example European option prices in closed form. It is of great interest to expeditiously be able to determine European option prices since a theoretical model generally is calibrated on a set of prices originating from option markets.

Even though prices of derivatives or risk-neutral densities might not be able to be derivied explicitly, researchers did, however, discover that the characteristic function of the log-returns is unmistakably easy to obtain. Furthermore, via Fourier transforms, researchers such as Carr and Madan [3] connected the characteristic function with European option prices.

## 4.1 Fourier Transforms and Characteristic Functions

Let $S_t$ denote the process of an asset price and let $r$ denote the deterministic rate of return on a riskless asset. Furthermore, let $X_T = \ln(S_T/S_0)$ denote the logarithmic return over the maturity $T$. Since $X_T$ is a random variable, it is distributed in obedience to a probability measure $P$. It is assumed that an equivalent probability measure $Q$, also called the risk-neutral probability measure, exists. Under this measure, the discounted price embodies a martingale:

$$\mathrm{e}^{-rT}\mathbb{E}_Q[S_T] = S_0.$$

Unless the market is complete, $Q$ does not have to be unique. However, every single derivative contract will have a no-arbitrage price corresponding to their discounted expected payoff under $Q$. Thus, the price of a European call option, for example, is given by

$$C = \mathrm{e}^{-rT}\mathbb{E}_Q\left[(S_T - K)^+\right].$$

### 4.1.1 The Fourier Transform

The most general form of the *Fourier transform* of a function $f$ is given by

$$\hat{f}(\omega) = \mathscr{F}[f(x)](\omega) = \sqrt{\frac{|b|}{(2\pi)^{1-a}}}\int_{\mathbb{R}} \mathrm{e}^{\mathrm{i}b\omega x} f(x)\,\mathrm{d}x, \tag{4}$$

where $a$ and $b$ are two arbitrary constants [17]. Furthermore, the *inverse* Fourier transform is given by

$$f(x) = \mathscr{F}^{-1}[\hat{f}(\omega)](x) = \sqrt{\frac{|b|}{(2\pi)^{1+a}}}\int_{\mathbb{R}} \mathrm{e}^{-\mathrm{i}b\omega x} \hat{f}(\omega)\,\mathrm{d}\omega. \tag{5}$$

Since the forthcoming aim is to calculate characteristic functions, the Fourier transform parameters are both set equal to 1. Thus, Equation (4) and Equation (5) become

$$\hat{f}(\omega) = \mathscr{F}[f(x)](\omega) = \int_{\mathbb{R}} \mathrm{e}^{\mathrm{i}\omega x} f(x)\,\mathrm{d}x,$$
$$f(x) = \mathscr{F}^{-1}[\hat{f}(\omega)](x) = \frac{1}{2\pi}\int_{\mathbb{R}} \mathrm{e}^{-\mathrm{i}\omega x} \hat{f}(\omega)\,\mathrm{d}\omega.$$

### 4.1.2 The Characteristic Function

Let $f_X$ be the probability density function measuring a random variable $X$. The Fourier transform of $f_X$ is equal to the *characteristic function* of $X$ given by

$$\phi_X(\omega) = \mathbb{E}[\mathrm{e}^{\mathrm{i}\omega X}] = \int_{\mathbb{R}} \mathrm{e}^{\mathrm{i}\omega x} f_X(x)\,\mathrm{d}x.$$

Characteristic functions possess ample information to recover the probability distribution of a random variable because functions and their Fourier transforms uniquely define each other. In particular, the inverse Fourier transform reclaims the probability density function through

$$f_X(x) = \frac{1}{\pi}\int_{\mathbb{R}_+} \mathrm{Re}\left[\mathrm{e}^{-\mathrm{i}\omega x}\phi_X(\omega)\right]\mathrm{d}\omega.$$

Often it is feasible to solve for the characteristic function of a random variable or a process, as opposed to solving for the probability density itself. In fact, as shall be seen in Section 5, there is a large class of processes, called Lévy processes, which are defined through their characteristic functions.

A valuable feature of the characteristic function is that the moments of a random variable can easily be obtained through

$$\mathbb{E}[X^k] = (-\mathrm{i})^k \frac{\partial^k \phi_X(\omega)}{\partial \omega^k}\Big|_{\omega=0}.$$

As a consequence, the volatility, skewness, and excess kurtosis can straightforwardly be obtained from the characteristic function ([5], p. 110).

## 4.2 Pricing a European Call Option

The characteristic function of the log-return can be used to obtain European option prices. Let the logarithm of the asset price under the risk-neutral measure[1] $Q$ be given by

$$\ln S_T = \ln S_0 + X_T.$$

The reason why the risk-neutral measure is used is that the market might be or is expected to be incomplete. If the market is incomplete, it is not possible to cite no-arbitrage

[1] Also known as the equivalent martingale measure.

option prices based wholly on information under the true measure $P$.

To set up a risk-neutral measure, several techniques can be used. Øksendal [29] utilized Girsanov's theorem, whereas Gerber and Shin [8] employed the Esscher transform. Risk-neutral valuation is described in Subsection 3.1.2.

By *assuming* that the process $\ln S_T$ is defined under $Q$, the only necessary restriction is

$$\mathrm{e}^{-rT}\mathbb{E}_Q[S_T] = S_0 \Leftrightarrow \mathbb{E}_Q\left[\mathrm{e}^{X_T}\right] = \mathrm{e}^{rT}.$$

### 4.2.1 The Fourier Transform of a European Call Option

Let $k = \ln K$ denote the log-strike price of a European call option maturing at time $T$. Furthermore, let the risk-neutral density of the log-price $s_T = \ln S_T$ be denoted by $q(s)$ whose characteristic function is given by

$$\phi(\omega) = \int_{\mathbb{R}} \mathrm{e}^{\mathrm{i}\omega s} q(s)\,\mathrm{d}s.$$

The initial call value is linked to the risk-neutral density by [3]

$$C(k) = \mathrm{e}^{-rT}\mathbb{E}_Q\left[(S_T - K)^+\right] = \mathrm{e}^{-rT}\int_k^\infty (\mathrm{e}^s - \mathrm{e}^k)\,q(s)\,\mathrm{d}s.$$

However, $C(k)$ is not square-integrable because as $k$ tends to $-\infty$, $C(k)$ tends to $S_0$. To make $C(k)$ square-integrable, it is multiplied by $\mathrm{e}^{\eta k}$ for some damping parameter $\eta > 0$ such that

$$C_\eta(k) = \mathrm{e}^{\eta k} C(k).$$

The Fourier transform of $C_\eta(k)$ is given by

$$\psi_\eta(\omega) = \int_{\mathbb{R}} \mathrm{e}^{\mathrm{i}\omega k} C_\eta(k)\,\mathrm{d}k.$$

By applying the inverse Fourier transform, the original call option price can now be obtained:

$$C(k) = \frac{\mathrm{e}^{-\eta k}}{2\pi}\int_{\mathbb{R}} \mathrm{e}^{-\mathrm{i}\omega k}\psi_\eta(\omega)\,\mathrm{d}\omega = \frac{\mathrm{e}^{-\eta k}}{\pi}\int_{\mathbb{R}_+} \mathrm{e}^{-\mathrm{i}\omega k}\psi_\eta(\omega)\,\mathrm{d}\omega, \tag{6}$$

where the second equality holds because $C(k)$ is real, which implies that the function $\psi_\eta(\omega)$ is even in its real part and odd in its imaginary part.

The analytic expression for the Fourier transform of the modified call price is derived as follows:

$$\begin{aligned}
\psi_\eta(\omega) &= \int_{\mathbb{R}} \mathrm{e}^{\mathrm{i}\omega k} C_\eta(k)\,\mathrm{d}k \\
&= \int_{\mathbb{R}} \mathrm{e}^{\mathrm{i}\omega k}\int_k^\infty \mathrm{e}^{\eta k}\mathrm{e}^{-rT}(\mathrm{e}^s - \mathrm{e}^k)\,q(s)\,\mathrm{d}s\,\mathrm{d}k \\
&= \int_{\mathbb{R}} \mathrm{e}^{-rT} q(s)\int_{-\infty}^s \left(\mathrm{e}^{s+\eta k} - \mathrm{e}^{(1+\eta)k}\right)\mathrm{e}^{\mathrm{i}\omega k}\,\mathrm{d}k\,\mathrm{d}s \\
&= \int_{\mathbb{R}} \mathrm{e}^{-rT} q(s)\left(\frac{\mathrm{e}^{(\eta+1+\mathrm{i}\omega)s}}{\eta+\mathrm{i}\omega} - \frac{\mathrm{e}^{(\eta+1+\mathrm{i}\omega)s}}{\eta+1+\mathrm{i}\omega}\right)\mathrm{d}s \\
&= \frac{\mathrm{e}^{-rT}\phi(\omega - (\eta+1)\mathrm{i})}{(\eta+\mathrm{i}\omega)(\eta+1+\mathrm{i}\omega)}.
\end{aligned} \tag{7}$$

By substituting Equation (7) into Equation (6), call option values can numerically be obtained for some appropriate value of the damping parameter $\eta$ which regulates how quickly the integrand converges to zero. For the modified call option value to be square-integrable $\psi_\eta(0)$ must be finite, which implies that $\phi(-(\eta+1)\mathrm{i})$ must be finite. Hence, $\eta$ must satisfy

$$\mathbb{E}_Q\left[S_T^{\eta+1}\right] < \infty.$$

To find an upper limit of integration in Equation (6) we note that, since the modulus of $\phi$ is bounded by $\mathbb{E}_Q\left[S_T^{\eta+1}\right]$, it follows that

$$|\psi_\eta(\omega)|^2 \leq \frac{\mathbb{E}_Q\left[S_T^{\eta+1}\right]}{(\eta^2+\eta-\omega^2)^2+(2\eta+1)^2\omega^2} \leq \frac{D}{\omega^4},$$

for some constant $D$. Hence,

$$|\psi_\eta(\omega)| \leq \frac{\sqrt{D}}{\omega^2}.$$

The integral of the upper tail can be bounded by

$$\int_{\bar{\omega}}^{\infty} |\psi_\eta(\omega)|\,\mathrm{d}\omega < \frac{\sqrt{D}}{\bar{\omega}},$$

making it possible to set up a truncation procedure. Thus, the integral of the tail in Equation (6) is bounded by $\sqrt{D}/\bar{\omega}$ which yields a bound for the truncation error equal to

$$\frac{\mathrm{e}^{-\eta k}}{\pi}\frac{\sqrt{D}}{\bar{\omega}}.$$

This bound can be made smaller than any $\epsilon > 0$ by choosing

$$\bar{\omega} > \frac{\sqrt{D}\mathrm{e}^{-\eta k}}{\epsilon\pi}. \tag{8}$$

### 4.2.2 Utilizing the Trapezoidal Rule

To determine option prices, an integral of the form

$$\int_{\mathbb{R}_+} \mathrm{e}^{-\mathrm{i}\nu k} g(\nu)\,\mathrm{d}\nu,$$

has to be evaluated. This integral can be approximated by, for example, utilizing the trapezoidal rule. The interval to be truncated is $[0,\infty)$. A point $\bar{\nu}$ adequately large is chosen such that the contribution of the integral beyond this point is infinitesimally small. Furthermore, let $\mathbf{v} = \{\nu_j = (j-1)\Delta\nu,\ j = 1,\ldots,N\}$ be a discretization of the interval $[0,\Delta t]$ into $N-1$ subintervals, where $\Delta\nu$ is a given spacing. Finally, the grid point values of the integrand is given by $g_j(k) = \mathrm{e}^{-\mathrm{i}\nu_j k} g(\nu_j)$, yielding the integral approximation

$$\int_{\mathbf{R}_+} \mathrm{e}^{-\mathrm{i}\nu k} g(\nu)\,\mathrm{d}\nu \approx \sum_{j=1}^{N} g_j(k)\Delta\nu - \frac{1}{2}\big(g_1(k)+g_N(k)\big)\Delta\nu.$$

To compute the numerical integration, the upper integration bound $\bar{v}$ and the spacing $\Delta v$ need to be determined. The choice of the upper integration bound was derived in Equation (8). Determining the spacing can be more delicate, since $e^{ivk} = \cos(vk) + i\sin(vk)$ oscillates with frequency that intensifies with $k$ ([5], pp. 118-120).

The connection linking the fat tails and the decay of the characteristic function is of crucial value. To be specific, a higher kurtosis yields a slower decay towards zero as $v$ increases. Thus, an extensive support might have to be used during the integration. Besides, a fine grid is needed to meticulously determine the density close to the tails.

### 4.2.3 The Fast Fourier Transform

The *fast Fourier transform* is an efficient algorithm for simultaneously evaluating $N$ sums of the type

$$h_l^* = \sum_{j=1}^{N} e^{-i\frac{2\pi}{N}(j-1)(k-1)} h_j,\ k = 1,\dots,N,$$

where $N$ generally is a power of 2 [3]. The efficiency of the fast Fourier transform has led to a major breakthrough in computational finance.

As was seen in Equation (6), using the inverse Fourier transform yielded call option prices of the form

$$C(k) = \frac{e^{-\eta k}}{\pi} \int_{\mathbb{R}_+} e^{-ivk} \psi_\eta(v)\, dv,$$

where $\psi_\eta(v)$ is the Fourier transform of the modified call price and $\eta > 0$ is a damping parameter. Utilizing the trapezoidal rule, letting $\mathbf{z} = (1/2, 1, \dots, 1, 1/2)$ and $v_j = (j-1)\Delta v$, produces an approximation to $C(k)$:

$$C(k) \approx \frac{e^{-\eta k}}{\pi} \sum_{j=1}^{N} e^{-iv_j k} \psi_\eta(v_j) z_j \Delta v. \tag{9}$$

The effective upper limit of the integration is $\bar{v} = N\Delta v$. Generally, call option values close to being at-the-money attract most of the attention, which equates to $k = \ln K$ being close to zero if $S_0 = 1$. Assuming a regular log-strike spacing $\Delta k$ yields a log-strike grid of the form

$$k_l = -b + (l-1)\Delta k,\ l = 1,\dots,N, \tag{10}$$

where $b = N\Delta k/2$.

Hence, combining Equation (9) and Equation (10), the call option approximation can be written

$$C(k_l) \approx \frac{e^{-\eta k_l}}{\pi} \sum_{j=1}^{N} e^{-iv_j[-b+(l-1)\Delta k]} \psi_\eta(v_j) z_j \Delta v,\ l = 1,\dots,N.$$

However, since $v_j = (j-1)\Delta v$:

$$C(k_l) \approx \frac{e^{-\eta k_l}}{\pi} \sum_{j=1}^{N} e^{-i\Delta k \Delta v (j-1)(l-1)} e^{ibv_j} \psi_\eta(v_j) z_j \Delta v = \frac{e^{-\eta k_l}}{\pi} \sum_{j=1}^{N} e^{-i\Delta k \Delta v (j-1)(l-1)} h_j,$$

where $h_j = e^{ibv_j}\psi_\eta(v_j)z_j\Delta v$. To apply the fast Fourier transform, the equation $\Delta k\Delta v = 2\pi/N$ must be satisfied, which signifies a restriction between the grid size of the log-strike and the grid size of the characteristic function. Clearly, choosing a small $\Delta v$ in order to acquire a fine integration grid yields a rather large log-strike spacing.

### 4.2.4 A European Call Option Pricing Algorithm

To summarize, European call option prices can be derived by applying the following steps:

- Define the input grid sizes $\Delta v$ and $\Delta k$, and also the number of integration points $N$. The constraint $\Delta k\Delta v = 2\pi/N$ must be fulfilled.
- Establish the vectors $\mathbf{v} = \{(j-1)\Delta v,\ j = 1,\dots,N\}$ and $\mathbf{k} = \{-N\Delta k/2 + (l-1)\Delta k,\ l = 1,\dots,N\}$.
- Define the damping parameter $\eta$ and compute the Fourier transform of the modified call
$$\psi_\eta(\mathbf{v}) = e^{-rT}\phi(\mathbf{v} - (\eta+1)i) \oslash [(\eta + i\mathbf{v}) \odot (\eta + 1 + i\mathbf{v})].$$
- Evaluate the vector $\mathbf{h} = e^{-ik_1\mathbf{v}} \odot \psi_\eta(\mathbf{v})$.
- If the trapezodial rule is used, let $h_1 = h_1/2$ and $h_N = h_N/2$.
- Apply the fast Fourier transform on $\mathbf{h}$, yielding the output $\mathbf{h}^*$.
- Retrieve the option values: $\mathbf{C} = e^{-\eta\mathbf{k}}/\pi \odot \mathrm{Re}(\mathbf{h}^*)$.
- The output is $(\mathbf{k}, \mathbf{C})$, where $\mathbf{C}(l)$ equates to an option value with log-strike price $k_l$, $l = 1,\dots,N$.

## 4.3 The Fractional Fast Fourier Transform

When implementing the fast Fourier transform, the constraint $\Delta k\Delta v = 2\pi/N$ is somewhat impeding. The integration of the characteristic function stipulate the need of a fine grid, however, a fine grid can yield very coarse output grids. For example, integrating over the interval, say $[0, 150]$, using 1024 equidistant points yields $\Delta v = 150/1023 = 0.1466$. To utilize the fast Fourier transform, the constraint $\Delta k = 2\pi/(N\Delta v) = 0.0418$ must be satisfied. This gives $k_1 = -N\Delta k/2 = -21.4\%$, hence merely a fraction of the 1024 output values lie within the, say $\pm 30\%$ interval around the at-the-money strike price.

To decrease the output grid size, one method is to increase $N$. However, since the reason for specifying the upper integration bound was to make the characteristic function infinitesimally small outside this bound, increasing $N$ will simply pad the input vector $\mathbf{h}$ with zeros. It should come as no surprise that this will inevitably impede the speed of the fast Fourier transform.

Chourdakis [4] confronted this matter using the so-called *fractional fast Fourier transform*. Given a parameter $\alpha$, the fractional fast Fourier transform evaluates sums of the type

$$h_l^* = \sum_{j=1}^{N} \mathrm{e}^{-2\pi\alpha(j-1)(l-1)} h_j,\ l = 1,\dots,N.$$

However, invoking the fractional fast Fourier transform is not all sunshine and rainbows, since to do so, a $2N$-point fast Fourier transform has to be implemented three times. But as Chourdakis shows, for a given degree of precision, the liberty of independently being able to choose $\Delta v$ and $\Delta k$ can as a matter of fact ameliorate the speed.

To put the fractional fast Fourier transform into practice, the following outline can be utilized:

- Let $\mathbf{f}_1$ and $\mathbf{f}_2$ be two $(N \times 1)$ vectors defined by

$$\mathbf{f}_1 = \{\mathrm{e}^{-\mathrm{i}\pi\alpha(j-1)^2},\ j = 1,\dots,N\},$$
$$\mathbf{f}_2 = \{\mathrm{e}^{\mathrm{i}\pi\alpha(N-j+1)^2},\ j = 1,\dots,N\}.$$

- Let $\mathbf{h}_1$ and $\mathbf{h}_2$ be two $(2N \times 1)$ vectors defined by

$$\mathbf{h}_1 = \begin{pmatrix} \mathbf{h} \odot \mathbf{f}_1 \\ \mathbf{0} \end{pmatrix},\ \mathbf{h}_2 = \begin{pmatrix} \mathbf{1} \oslash \mathbf{f}_1 \\ \mathbf{f}_2 \end{pmatrix}.$$

- Apply the fast Fourier transform on $\mathbf{h}_1$ and $\mathbf{h}_2$: $\mathbf{h}_1^* = \mathrm{FFT}(\mathbf{h}_1),\ \mathbf{h}_2^* = \mathrm{FFT}(\mathbf{h}_2)$.
- The $N$ first elements of the inverse fast Fourier transform $\mathbf{h}^* = \mathbf{f}_1 \odot \mathrm{IFFT}(\mathbf{h}_1^* \odot \mathbf{h}_2^*)$ correspond to the $N$-point fractional fast Fourier transform.

Furthermore, independently selecting $\Delta v$ and $\Delta k$ yields the fractional parameter $\alpha = \frac{\Delta v \Delta k}{2\pi}$ that can be put to use in the fractional fast Fourier transform.

As was mentioned, many models do not have closed-form solutions. These models do have, on the other hand, existing characteristic functions in closed form. Models of this type are for example *Lévy models*. In Lévy models the log-price follows a *Lévy process* and these models will be the scope of Section 5.

# 5 LÉVY PROCESSES

Exponential Lévy models generalize the Black-Scholes model by allowing the asset prices to jump while maintaining the independence and stationarity of the returns. There are many justifications for introducing jumps in financial modeling. One reason is that asset prices do jump and continuous-path models simply cannot handle this risk. In continuous-path models, the probability that the asset price will move by a large amount over a short period of time is exceptionally small, unless an unrealistically high value of the volatility is established. Another reason for introducing jump models is the existence of the implied volatility smile in option markets, which implies that the risk-neutral returns are non-Gaussian and leptokurtic. A clear indication of the presence of jumps is that the volatility smile becomes much more pronounced for short maturities [25] . In continuous-path models, the law of returns for short maturities becomes more Gaussian, whereas in reality and in models with jumps the law of returns becomes less Gaussian.

Also, continuous-path models correspond to either complete or completable markets. Jump models, on the other hand, correspond to incomplete markets. Thus, from a risk-management perspective, jump models let investors quantify and take into account the risk of large asset price movements over short time intervals, something that is absent in continuous-path models.

## 5.1 BASIC THEORY OF LÉVY PROCESSES

DEFINITION 5.1. *A stochastic process $X = \{X_t\}_{t\geq 0}$ is a Lévy process if it is càdlàg (right-continuous with left limits) and satisfies the following properties:*

- $X_0 = 0$.
- *$X$ has independent and stationary increments.*
- *$X$ is continuous in probability, that is,* $\lim_{s\to 0} P(|X_{t+s} - X_t| > \epsilon) = 0 \ \forall\, t \geq 0, \ \forall \epsilon > 0$.
- *The probability of a jump is zero at any fixed time, that is,* $P(X_{t-} = X_t) = 1 \ \forall\, t$.

Brownian motion is the only non-deterministic continuous-path Lévy process. Other notable examples of Lévy processes are the *Poisson process* and the *compound Poisson process* [25]. These and other processes will be analyzed in the subsequent subsections.

### 5.1.1 INFINITE DIVISIBILITY

DEFINITION 5.2. *A probability distribution $F$ is infinitely divisible if it can be expressed as the probability distribution of the sum of an arbitrary number of i.i.d. random variables $X_1, \ldots, X_n$. The characteristic function of an infinitely divisible distribution is then called an infinitely divisible characteristic function.*

If $X = \{X_t\}_{t\geq 0}$ is a Lévy process then, for any $t \geq 0$, the random variable $X_t$ will be infinitely divisible. The $n$ i.i.d. random variables can, in this case, be represented by the i.i.d.

increments $(X_{t/n} - X_0, X_{2t/n} - X_{t/n}, \ldots, X_t - X_{(n-1)t/n})$. Conversely, for every infinitely divisible distribution $F$, a Lévy process $X = \{X_t\}_{t \geq 0}$ can be constructed such that the law of $X_1$ is given by $F$.

### 5.1.2 The Lévy-Khintchine Representation

When a Lévy process $X = \{X_t\}_{t \geq 0}$ is infinitely divisible, its characteristic function is generally described by the *Lévy-Khintchine formula* [16]

$$\phi_X(\omega) = \mathbb{E}[e^{i\omega X_1}] = \exp\left[ i\mu\omega - \frac{1}{2}\sigma^2\omega^2 + \int_{\mathbb{R}} (e^{i\omega x} - 1 - i\omega x \mathbf{1}_{|x|<1}) \, d\nu(x) \right],$$

which is uniquely defined by the *Lévy triplet* $(\mu, \sigma^2, \nu)$, where $\nu$ is a *Lévy measure* with $\nu(0) = 0$. For the jump process to be a semi-martingale, the Lévy measure has to satisfy

$$\int_{\mathbb{R}} (1 \wedge x^2) \, d\nu(x) < \infty.$$

The measure $\nu$ of a Lévy process is equal to the expected number of jumps of a certain height in a unit time interval. Small jumps and Brownian motion regulates the variation, whereas the activity is regulated by all the jumps. Furthermore, the moment properties are determined by large jumps [18].

### 5.1.3 Finite and Infinite Variation Processes

A Lévy process can be decomposed into a deterministic linear component, a Brownian component, and a pure jump component ([16], p. 506). Setting the Lévy triplet to $(\mu, \sigma^2, 0)$ yields the Lévy characteristic function of a Gaussian distribution:

$$\phi_X(\omega) = e^{i\mu\omega - \frac{1}{2}\omega^2\sigma^2}.$$

Furthermore, setting the Lévy triplet to $(\mu, 0, \nu)$ yields a pure jump process.

In general, Lévy processes are described by their *characteristic exponent* $\psi(\omega)$ satisfying

$$\phi_{X_t}(\omega) = \mathbb{E}[e^{i\omega X_t}] = \left(\mathbb{E}[e^{i\omega X_1}]\right)^t = e^{t\psi(\omega)},$$

where it is assumed that the process $X_t$ is infinitely divisible for any $t$. The characteristic exponent can be decomposed as

$$\psi(\omega) = i\mu\omega - \frac{1}{2}\sigma^2\omega^2 + \int_{|x|\geq 1} (e^{i\omega x} - 1) \, d\nu(x) + \int_{|x|<1} (e^{i\omega x} - 1 - i\omega x) \, d\nu(x),$$

where the component $\int_{|x|\geq 1} (e^{i\omega x} - 1) \, d\nu(x)$ is a *compound Poisson process.* If $\sigma = 0$ and $\int_{|x|\leq 1} |x| \, d\nu(x) < \infty$, then almost all paths have finite variation.

The component $\int_{|x|<1} (e^{i\omega x} - 1 - i\omega x) \, d\nu(x)$ is a square integrable pure jump martingale with a countable number of jumps. Furthermore, the size of each jump is less than 1. A compensating term $i\omega x \mathbf{1}_{|x|<1}$ is needed because the sum of the small jumps does not converge [14]. If $\sigma \neq 0$ or if $\int_{|x|\leq 1} |x| \, d\nu(x) = \infty$ then almost all paths have infinite variation.

### 5.1.4 Finite and Infinite Activity Processes

A finite-activity process has a finite number of jumps in any finite interval, such that $\int_{\mathbb{R}} \mathrm{d}\nu(x) < \infty$ ([20], p. 76). Rare events, such as market crashes, can be modeled by a jump-diffusion finite activity Lévy process. Two common jump-diffusion models are *Merton's model* and *Kou's model*. In Merton's model, the frequency of jumps is determined by a *compound Poisson process*, where each jump size is drawn from a log-normal distribution. In Kou's model, the frequency of jumps is also determined by a compound Poisson process, but each jump size is drawn from a double exponential distribution. Note that the compound Poisson process has a finite measure and hence has a finite variation.

An infinite-activity jump process has an infinite number of jumps in any finite time interval [26]. To construct an infinite activity Lévy process, a Brownian process can be *subordinated* in time to a pure jump process.

Two examples of infinite activity processes are the *variance-gamma* process and the *normal-inverse Gaussian* process. Note that the variance-gamma process has finite variation, whereas the normal-inverse Gaussian process has infinite variation ([16], pp. 506-507).

### 5.1.5 The Poisson Process

Definition 5.3. *Let $(\tau_i)_{i\geq 1}$ be a sequence of exponential random variables with parameter $\lambda$ and let $T_n = \sum_{i=1}^{n} \tau_i$. Then the process*

$$N_t = \sum_{n\geq 1} \mathbf{1}_{t\geq T_n},$$

*is called a Poisson process with parameter $\lambda$.*

The Poisson process is a stochastic process that counts the number of events and the time points at which the events occur in a given time interval. The inter-arrival times are assumed to be independent and exponentially distributed with parameter $\lambda > 0$. The events can represent jumps, hence the Poisson process is a pure-jump process with jumps of size one. The characteristic function of a Poisson process is equal to [25]

$$\phi_{N_t}(\omega) = \mathbb{E}[\mathrm{e}^{\mathrm{i}\omega N_t}] = \mathrm{e}^{\lambda t(\mathrm{e}^{\mathrm{i}\omega}-1)}.$$

A realization of a Poisson process $N = \{N_t\}_{t\geq 0}$ with intensity parameter $\lambda = 10$ is displayed in Figure 5.

### 5.1.6 The Compound Poisson Process

The Poisson process itself is not suitable to model asset prices since the constraint that the jump size is always equal to 1 is too restrictive. However, the Poisson process is still vital in the construction of richer models.

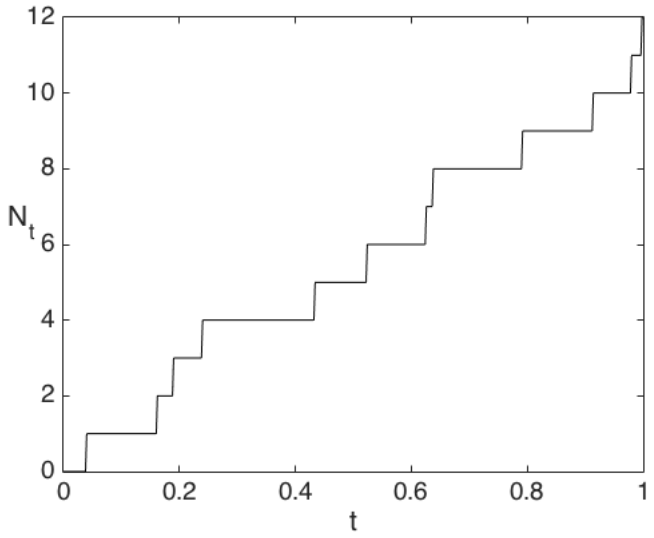


Figure 5: A realization of a Poisson process $N_t$ with intensity parameter $\lambda = 10$.

DEFINITION 5.4. *Let $\{Y_i\}_{i\geq 1}$ be a sequence of independent random variables with law $f$ and let $N = \{N_t\}_{t\geq 0}$ be a Poisson process with parameter $\lambda$ independent from $\{Y_i\}_{i\geq 1}$. Then the process $X = \{X_t\}_{t\geq 0}$ defined by*

$$X_t = \sum_{i=1}^{N_t} Y_i,$$

*is called a compound Poisson process with jump intensity $\lambda$ and jump size distribution $f$.*

In other words, a compound Poisson process is a piecewise constant process where the jump times follow a Poisson process and the jump sizes are i.i.d. random variables with a given distribution [25].

Furthermore, the characteristic function of the compound Poisson process is given by

$$\phi_{X_t}(\omega) = \mathbb{E}[e^{i\omega X_t}] = e^{t\lambda \int_{\mathbb{R}} (e^{i\omega x} - 1)\, df(x)},$$

where the size and the intensity of the jumps are represented by the measure $\lambda\, df(x)$.

A realization of a compound Poisson process $X = \{X_t\}_{t\geq 0}$ with intensity parameter $\lambda = 10$ and a standard Gaussian jump size distribution is displayed in Figure 6.

## 5.2 FINITE ACTIVITY JUMP-DIFFUSION PROCESSES

An exponential Lévy model has the form

$$S_t = S_0 e^{X_t},$$

where the asset price process $\{S_t\}_{t\geq 0}$ is modeled as an exponential of a Lévy process $\{X_t\}_{t\geq 0}$. Saying that an asset price process $S_t$ is modeled as an exponential of a Lévy process $X_t$

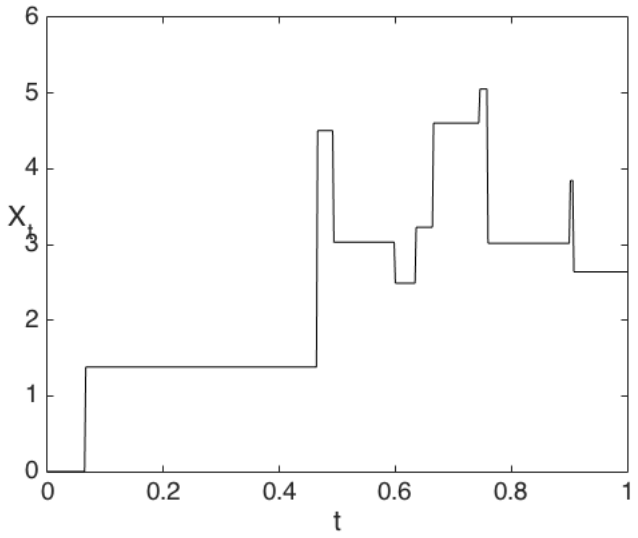


Figure 6: A realization of a compound Poisson process $X_t$ with intensity parameter $\lambda = 10$ and a standard Gaussian jump size distribution.

simply means that its log-return $\ln(S_t/S_0)$ follows a Lévy process, that is,

$$\ln\left(\frac{S_t}{S_0}\right) = X_t.$$

Let $X = \{X_t\}_{t\geq 0}$ be a jump-diffusion process given by

$$X_t = \mu t + \sigma B_t + \sum_{i=1}^{N_t} Y_i,\ \mu \in \mathbb{R}, \sigma \geq 0,$$

where $B = \{B_t\}_{t\geq 0}$ is a standard Brownian motion and $\sum_{i=1}^{N_t} Y_i$ is a compound Poisson process with jump intensity $\lambda$ and jump size distribution $f$ [23].

Since the compound Poisson process and the Brownian motion are independent, the characteristic function of $X_t$ can easily be derived:

$$\begin{aligned}
\phi_{X_t}(\omega) &= \mathbb{E}[e^{i\omega X_t}] \\
&= \mathbb{E}\left[e^{i\omega\left(\mu t+\sigma B_t+\sum_{i=1}^{N_t} Y_i\right)}\right] \\
&= e^{i\mu\omega t}\mathbb{E}\left[e^{i\omega\sigma B_t}\right]\mathbb{E}\left[e^{i\omega\sum_{i=1}^{N_t} Y_i}\right] \\
&= e^{i\mu\omega t}e^{-\frac{1}{2}\sigma^2\omega^2 t}e^{\lambda t\int_{\mathbb{R}}(e^{i\omega x}-1)\,df(x)} \\
&= e^{t\left(i\mu\omega-\frac{1}{2}\sigma^2\omega^2+\int_{\mathbb{R}}(e^{i\omega x}-1)\lambda\,df(x)\right)}.
\end{aligned}$$

### 5.2.1 Merton's Jump-Diffusion Model

Merton's jump-diffusion model tries to capture the negative skewness and excess kurtosis encountered in the Black-Scholes model by simply adding a compound Poisson process.

Merton's jump-diffusion model is an exponential Lévy model where the Lévy process $\{X_t\}_{t\geq 0}$ is given by [17]

$$X_t = \mu t + \sigma B_t + \sum_{i=1}^{N_t} Y_i,$$

where $\{B_t\}_{t\geq 0}$ is a standard Brownian motion. Hence, $\mu t + \sigma B_t$ is a Brownian motion with drift, while $\sum_{i=1}^{N_t} Y_i$ is a compound Poisson process.

The compound Poisson process contains two sources of randomness. One source of randomness is a Poisson process with intensity parameter $\lambda$ which causes random asset price jumps. The other source of randomness is how much the asset price jumps, once it jumps. In Merton's jump-diffusion model, the log-price jump size follows a Gaussian distribution, that is $Y_i \sim \mathcal{N}(\gamma, \delta^2)$, which has a density function of the form

$$f(x;\gamma,\delta) = \frac{1}{\sqrt{2\pi\delta^2}} \mathrm{e}^{-\frac{(x-\gamma)^2}{2\delta^2}}.$$

Furthermore, the two sources of randomness are assumed to be independent of each other. Thus, three extra parameters $\lambda, \gamma$, and $\delta$ are introduced to the Black-Scholes model.

Multiplying the jump intensity $\lambda$ and the jump size density yields the Lévy measure

$$\nu(x;\lambda,\gamma,\delta) = \lambda f(x;\gamma,\delta) = \frac{\lambda}{\sqrt{2\pi\delta^2}} \mathrm{e}^{-\frac{(x-\gamma)^2}{2\delta^2}}.$$

When $X$ is finite, its characteristic function is given by the Lévy-Khintchine formula which is uniquely defined by the Lévy triplet. Hence, substituting the Lévy measure, the characteristic function of $X_t$ is given by

$$\phi_{X_t}(\omega) = \mathrm{e}^{t\left(\mathrm{i}\mu\omega - \frac{1}{2}\sigma^2\omega^2 + \int_{\mathbb{R}} (\mathrm{e}^{\mathrm{i}\omega x} - 1) \frac{\lambda}{\sqrt{2\pi\delta^2}} \mathrm{e}^{-\frac{(x-\gamma)^2}{2\delta^2}} \mathrm{d}x\right)} = \mathrm{e}^{t\psi(\omega)}, \tag{11}$$

where

$$\psi(\omega) = \mathrm{i}\mu\omega - \frac{1}{2}\sigma^2\omega^2 + \lambda\left(\mathrm{e}^{\mathrm{i}\gamma\omega - \frac{1}{2}\delta^2\omega^2} - 1\right).$$

By Equation (11), it is given that

$$\begin{aligned}
\phi_{X_t}(\omega) &= \mathbb{E}\left[\mathrm{e}^{\mathrm{i}\omega X_t}\right] \\
&= \mathrm{e}^{\mathrm{i}\mu\omega t - \frac{\sigma^2\omega^2}{2}t + \lambda t\left(\mathrm{e}^{\mathrm{i}\gamma\omega - \frac{\delta^2\omega^2}{2}} - 1\right)} \\
&= \mathrm{e}^{\mathrm{i}\mu\omega t - \frac{\sigma^2\omega^2}{2}t - \lambda t} \mathrm{e}^{\lambda t \mathrm{e}^{\mathrm{i}\gamma\omega - \frac{\delta^2\omega^2}{2}}} \\
&= \mathrm{e}^{\mathrm{i}\mu\omega t - \frac{\sigma^2\omega^2}{2}t - \lambda t} \sum_{k=0}^{\infty} \frac{\left(\lambda t\left(\mathrm{e}^{\mathrm{i}\gamma\omega - \frac{\delta^2\omega^2}{2}}\right)\right)^k}{k!} \\
&= \sum_{k=0}^{\infty} \frac{\mathrm{e}^{-\lambda t}(\lambda t)^k}{k!} \mathrm{e}^{\mathrm{i}\omega(\mu t + k\gamma) - \frac{\omega^2}{2}(\sigma^2 t + k\delta^2)}.
\end{aligned}$$

By applying the inverse Fourier transform, the probability density function of $X_t$ is obtained such that

$$f_{X_t}(x) = \sum_{k=0}^{\infty} \frac{\mathrm{e}^{-\lambda t}(\lambda t)^k}{k!} \frac{1}{\sqrt{2\pi(\sigma^2 t + k\delta^2)}} \mathrm{e}^{-\frac{(x-(\mu t+k\gamma))^2}{2(\sigma^2 t+k\delta^2)}}.$$

### 5.2.2 Kou's Jump-Diffusion Model

Kou's jump-diffusion model is similar to Merton's model. It is still an exponential Lévy model where the Lévy process $\{X_t\}_{t\geq 0}$ is given by

$$X_t = \mu t + \sigma B_t + \sum_{i=1}^{N_t} Y_i,$$

where $\{B_t\}_{t\geq 0}$ is a standard Brownian motion. Hence, $\mu t + \sigma B_t$ is a Brownian motion with drift, while $\sum_{i=1}^{N_t} Y_i$ is a compound Poisson process. The difference is that in Kou's jump-diffusion model, the log-price jump size follows a double exponential distribution [12]

$$f(x; p_1, p_2, \eta_1, \eta_2) = p_1\eta_1 \mathrm{e}^{-\eta_1 x}\mathbf{1}_{x\geq 0} + p_2\eta_2 \mathrm{e}^{\eta_2 x}\mathbf{1}_{x<0},\ \eta_1, \eta_2 > 1.$$

The probability of an upward jump is denoted by $p_1$, whereas the probability of a downward jump is denoted by $p_2 = 1 - p_1$. Furthermore, the one-sided means are given by $\mu_1 = 1/\eta_1$ and $\mu_2 = 1/\eta_2$. The decay of the tails for positive and negative jump sizes are controlled by $\eta_1$ and $\eta_2$, respectively. Thus, five extra parameters $p_1, p_2, \eta_1, \eta_2$, and $\lambda$ are introduced to the Black-Scholes model.

Multiplying the jump intensity $\lambda$ and the jump size density yields the Lévy measure

$$\nu(x; \lambda, p_1, p_2, \eta_1, \eta_2) = \lambda f(x; p_1, p_2, \eta_1, \eta_2) = \lambda\left(p_1\eta_1 \mathrm{e}^{-\eta_1 x}\mathbf{1}_{x\geq 0} + p_2\eta_2 \mathrm{e}^{\eta_2 x}\mathbf{1}_{x<0}\right).$$

Substituting the Lévy measure, the Lévy-Khintchine formula yields the characteristic function of $X_t$ [16]:

$$\phi_{X_t}(\omega) = \mathrm{e}^{t\psi(\omega)},$$

where

$$\psi(\omega) = \mathrm{i}\mu\omega - \frac{1}{2}\sigma^2\omega^2 + \mathrm{i}\lambda\omega\left(\frac{p_1}{\eta_1 - \mathrm{i}\omega} - \frac{p_2}{\eta_2 + \mathrm{i}\omega}\right).$$

## 5.3 Infinite Activity Pure Jump Processes

Infinite activity processes have an infinite number of jumps in every finite time interval. The dynamics of infinite activity processes are able to replicate small movements typical of diffusion. As a consequence of the dynamics being so rich, there is no need to include Brownian diffusion.

Two common infinite activity processes are the variance-gamma process and the normal inverse Gaussian process.

### 5.3.1 A SUBORDINATOR

Financial markets often exhibit a variety of trading rates. Typical behavior of the trading rates might be long-time segments with a fair degree of tranquility followed by swift short-time price changes. For example, business time might seem to slow down in periods of market instability. This randomness can be reproduced by a drift-diffusion model *subordinated* to a consistently increasing stochastic business time.

DEFINITION 5.1. *A subordinator $X = \{X_t\}_{t\geq 0}$ is a one-dimensional Lévy process such that $t \mapsto X_t$ is non-decreasing.*

Since $X_0 = 0$, all subordinators take non-negative values only. By swapping the time parameter of a Brownian motion with an independent subordinator, a subordinated Brownian motion is obtained. That is, if $B_t$ is a Brownian motion and if $X_t$ is a subordinator, then the process $B_{X_t}$ is called a subordinated Brownian motion ([16], pp. 516-517).

### 5.3.2 THE GAMMA PROCESS

One option for a subordinating, non-decreasing stochastic time process is the *gamma process* $X = \{X_t\}_{t\geq 0}$ ([20], pp. 52-53). The probability density function of the gamma distribution is equal to

$$f(x;\alpha,\beta) = \frac{\beta^\alpha}{\Gamma(\alpha)} x^{\alpha-1} \mathrm{e}^{-\beta x}.$$

Furthermore, the moments of the gamma distribution are:

- Mean: $\dfrac{\alpha}{\beta}$.
- Variance: $\dfrac{\alpha}{\beta^2}$.
- Skewness: $\dfrac{2}{\sqrt{\alpha}}$.
- Kurtosis: $3\left(1+\dfrac{2}{\alpha}\right)$.

The gamma distribution has a semi-heavy right tail. Its characteristic function is given by

$$\phi_X(\omega) = \left(1 - \frac{\mathrm{i}\omega}{\beta}\right)^{-\alpha},$$

and it has a Lévy triplet of the form

$$\left[\frac{\alpha}{\beta}(1-\mathrm{e}^{-\beta}), 0, \frac{\alpha}{x}\mathrm{e}^{-\beta x}\mathbf{1}_{x>0}\,\mathrm{d}x\right].$$

Moreover, the characteristic function of $X_t$ is given by

$$\phi_{X_t}(\omega) = \left(1 - \frac{\mathrm{i}\omega}{\beta}\right)^{-\alpha t}.$$

A realization of a gamma process $X = \{X_t\}_{t\geq 0}$ with shape parameter $\alpha = 3$ and rate parameter $\beta = 4$ is displayed in Figure 7.

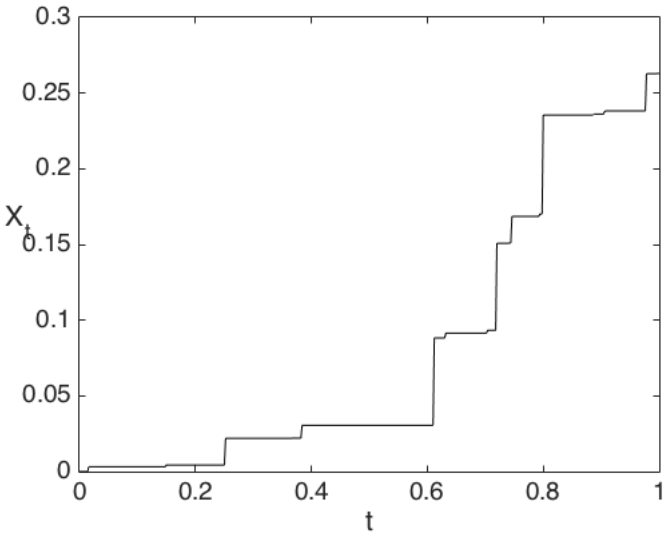


Figure 7: A realization of a gamma process $X_t$ with shape parameter $\alpha = 3$ and rate parameter $\beta = 4$.

### 5.3.3 The Variance-Gamma Process

The variance-gamma process $X = \{X_t\}_{t\geq 0}$ can be seen as a gamma subordinated Brownian motion with drift. Let $G_t$ be a gamma process with parameters $\alpha = \beta = 1/\xi > 0$, where $\xi$ is the volatility of the time change. This way the variance-gamma process can be expressed as ([16], pp. 518-522)

$$X_t = \theta G_t + \sigma B_{G_t}.$$

Since the Lévy measure has finite mass, the variance-gamma process has an infinite number of jumps in every finite time interval ([20], p. 58). The distribution of the variance-gamma process is infinitely divisible and has stationary and independent increments. Furthermore, it is negatively skewed when $\theta < 0$ and positively skewed when $\theta > 0$. The characteristic function of $X$ is given by ([20], pp. 57-59)

$$\phi_X(\omega) = \left(1 - \mathrm{i}\xi\omega\theta + \frac{1}{2}\sigma^2\xi\omega^2\right)^{-1/\xi},$$

whereas the charateristic function of $X_t$ is given by

$$\phi_{X_t}(\omega) = \big(\phi_X(\omega)\big)^t = \left(1 - \mathrm{i}\xi\omega\theta + \frac{1}{2}\sigma^2\xi\omega^2\right)^{-t/\xi}.$$

The moments of the variance-gamma process are:

- Mean: $\theta$.
- Variance: $\sigma^2 + \xi\theta^2$.
- Skewness: $\dfrac{\theta\xi(3\sigma^2 + 2\xi\theta^2)}{(\sigma^2 + \xi\theta^2)^{3/2}}$.
- Kurtosis: $3\left(1 + 2\xi - \dfrac{\xi\sigma^4}{(\sigma^2 + \xi\theta^2)^2}\right)$.

A realization of a variance-gamma process $X = \{X_t\}_{t\geq 0}$ with $\theta = 0.4, \sigma = 5$, and $\xi = 0.01$ is displayed in Figure 8. The subordinating gamma process models the business time or

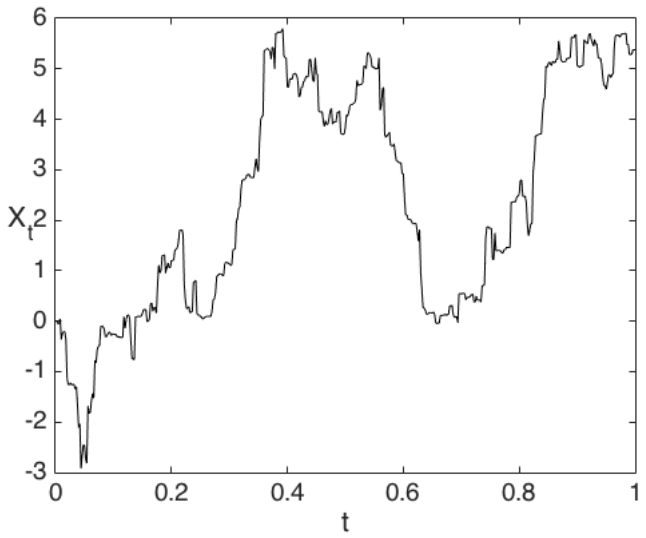


Figure 8: A realization of a variance-gamma process $X_t$ with parameters $\theta = 0.4, \sigma = 5$, and $\xi = 0.01$.

the trading time and is a subordinate input to the drift diffusion process. Even though the conduct of market participants follows a Brownian drift and variance process for a unit of business time, the quota of business time in one unit of real time is stochastic. For instance, the arrival of vital revelations can lead to an increase in the gamma business time relative to one unit of real time. Hence, in one unit of real time, market participants will make more trades which equates to the sensation of time slowing down under periods of increased perceptiveness and stress.

### 5.3.4 The Inverse Gaussian Process

A subordinating time process for the normal-inverse Gaussian process is the *inverse Gaussian process* $X = \{X_t\}_{t\geq 0}$ which outlines the time distribution for a Brownian motion with

positive drift $\beta$ to get to a fixed positive level $\alpha$ ([20], pp. 53-54).

The probability density function of the inverse Gaussian distribution is

$$f(x;\alpha,\beta) = \frac{\alpha}{\sqrt{2\pi}} e^{\alpha\beta} x^{-3/2} e^{-\frac{1}{2}\left(\frac{\alpha^2}{x}+\beta^2 x\right)},\ x>0.$$

The moments of the inverse Gaussian distribution are:

- Mean: $\frac{\alpha}{\beta}$.
- Variance: $\frac{\alpha}{\beta^3}$.
- Skewness: $\frac{3}{\sqrt{\alpha\beta}}$.
- Kurtosis: $3\left(1+\frac{5}{\alpha\beta}\right)$.

The characteristic function of $X$ is given by

$$\phi_X(\omega) = e^{-\alpha\left(\sqrt{-2i\omega+\beta^2}-\beta\right)}.$$

and it has a Lévy triplet of the form

$$\left[\frac{\alpha}{\beta}(2\mathcal{N}(\beta)-1), 0, \frac{1}{\sqrt{2\pi}}\alpha x^{-3/2} e^{-\beta^2 x/2}\mathbf{1}_{x>0}\,dx\right],$$

where $\mathcal{N}(x)$ denotes the standard Gaussian distribution.

Moreover, the characteristic function of $X_t$ is

$$\phi_{X_t}(\omega) = \left(\phi_X(\omega)\right)^t = e^{-\alpha t\left(\sqrt{-2i\omega+\beta^2}-\beta\right)}.$$

A realization of an inverse Gaussian process $X = \{X_t\}_{t\geq 0}$ with parameters $\alpha = 2$ and $\beta = 3$ is displayed in Figure 9.

### 5.3.5 The Normal-Inverse Gaussian Process

The normal-inverse Gaussian process $X = \{X_t\}_{t\geq 0}$ with parameters $\alpha > 0, -\alpha < \beta < \alpha$, and $\delta > 0$ can be seen as an inverse Gaussian subordinated Brownian motion with drift. Let $I_t$ be an inverse Gaussian process with parameters $a = 1$ and $b = \delta\sqrt{\alpha^2-\beta^2}$. $X_t$ is given by ([16], pp. 523-524)

$$X_t = \beta\delta^2 I_t + \delta B_{I_t}.$$

The probability density function of the normal-inverse Gaussian distribution is

$$f(x;\alpha,\beta,\delta) = \frac{\alpha\delta}{\pi} e^{\delta\sqrt{\alpha^2-\beta^2}+\beta x}\frac{K_1\left(\alpha\sqrt{\delta^2+x^2}\right)}{\sqrt{\delta^2+x^2}},$$

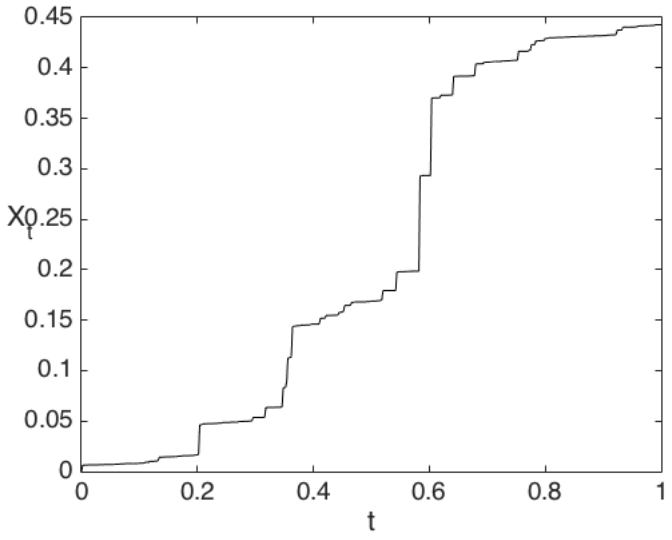


Figure 9: A realization of an inverse Gaussian process $X_t$ with parameters $\alpha = 2$ and $\beta = 3$.

where $K_\lambda$ is the modified Bessel function of the third kind with index $\lambda$.

A large value of $\alpha$ yields light tails, whereas a small value of $\alpha$ yields heavy tails. A positive $\beta$ yields positive skewness, a negative $\beta$ yields negative skewness, whereas $\beta$ equal to zero yields a symmetric distribution. The characteristic function of the normal-inverse Gaussian process is equal to

$$\phi_X(\omega) = \mathrm{e}^{-\delta\left(\sqrt{\alpha^2-(\beta+\mathrm{i}\omega)^2}-\sqrt{\alpha^2-\beta^2}\right)},$$

which is infinitely divisible, and it has a Lévy triplet of the form

$$\left[\frac{2\delta\alpha}{\pi}\int_0^1 \sinh(\beta x)K_1(\alpha x)\,\mathrm{d}x, 0, \frac{\delta\alpha}{\pi}\frac{\mathrm{e}^{\beta x}K_1(\alpha|x|)}{|x|}\,\mathrm{d}x\right].$$

Furthermore, the characteristic function of $X_t$ is given by

$$\phi_{X_t}(\omega) = \big(\phi_X(\omega)\big)^t = \mathrm{e}^{-\delta t\left(\sqrt{\alpha^2-(\beta+\mathrm{i}\omega)^2}-\sqrt{\alpha^2-\beta^2}\right)}.$$

The moments of the normal-inverse Gaussian distribution are:

- Mean: $\dfrac{\delta\beta}{\sqrt{\alpha^2-\beta^2}}$.
- Variance: $\dfrac{\alpha^2\delta}{(\alpha^2-\beta^2)^{3/2}}$.
- Skewness: $\dfrac{3\beta}{\alpha\sqrt{\delta}(\alpha^2-\beta^2)^{1/4}}$.

- Kurtosis: $3\left(1+\dfrac{\alpha^2+4\beta^2}{\delta\alpha^2\sqrt{\alpha^2-\beta^2}}\right)$.

A realization of a normal-inverse Gaussian process $X=\{X_t\}_{t\geq 0}$ with parameters $\alpha=6, \beta=0.8$, and $\delta=1$ is displayed in Figure 10.

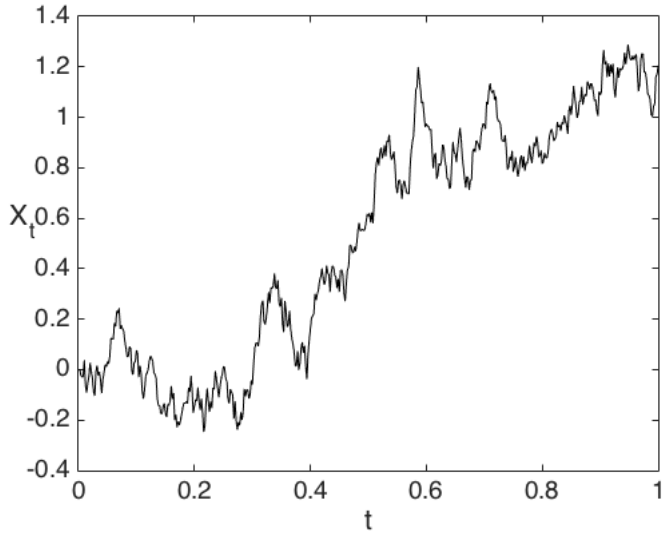


Figure 10: A realization of a normal-inverse Gaussian process $X_t$ with parameters $\alpha=6, \beta=0.8$, and $\delta=1$.

## 5.4 Risk-Neutral Characteristic Functions

One way to procure the equivalent martingale measure under $Q$ for a variety of Lévy processes, is to mean-correct the exponential ([16], pp. 531-536). Since jump-diffusion models are not able to create an admissible self-financing strategy to replicate every contingent claim, they are incomplete. Thus, to price the contingent claims, an equivalent martingale measure is needed. For ease of notation, let $S_0=1$. Under the risk-neutral measure $Q$, it holds that $\mathbb{E}[S_t]=\mathbb{E}[e^{X_t}]=e^{rt}$ and by definition $\phi_{X_t}(\omega)=\mathbb{E}[e^{i\omega X_t}]$.

If $\omega=-i$, then $\phi_{X_t}(-i)=\mathbb{E}[e^{X_t}]=e^{rt}$. Thus, utilizing the characteristic exponent $\psi(\omega)$ yields

$$\psi(-i)=\frac{\ln\phi(-i)}{t}=r.$$

### 5.4.1 The Black-Scholes Model

Under the true measure the characteristic function of $X_t=\mu t+\sigma B_t,\ B_t\sim\mathcal{N}(0,t)$ in the Black-Scholes model is given by

$$\phi_{X_t}(\omega)=e^{t\left(i\mu\omega-\frac{1}{2}\sigma^2\omega^2\right)}=e^{t\psi(\omega)}.$$

The characteristic exponent $\psi(\omega)$ can further be decomposed into a drift part $\psi_{\text{d}}(\omega)$ and a non-drift part $\psi_{\text{n-d}}(\omega)$ such that

$$\psi_{\text{d}}(\omega) = \text{i}\mu\omega,$$
$$\psi_{\text{n-d}}(\omega) = -\frac{1}{2}\sigma^2\omega^2.$$

In risk-neutral valuation, the risk-neutral drift is given by

$$\mu_{\text{r-n}} = r - \psi_{\text{n-d}}(-\text{i}) = r - \left(-\frac{1}{2}\sigma^2(-\text{i})^2\right) = r - \frac{1}{2}\sigma^2,$$

yielding the risk-neutral characteristic exponent

$$\psi_{\text{r-n}}(\omega) = \text{i}\left(r - \frac{1}{2}\sigma^2\right)\omega - \frac{1}{2}\sigma^2\omega^2.$$

Hence, under the risk-neutral measure, the characteristic function of $X_t$ in the Black-Scholes model has the form

$$\phi_{\text{r-n}}(\omega) = \text{e}^{t\left(\text{i}\left(r-\frac{1}{2}\sigma^2\right)\omega - \frac{1}{2}\sigma^2\omega^2\right)}.$$

### 5.4.2 Merton's Jump-Diffusion Model

Under the true measure the characteristic function of $X_t = \mu t + \sigma B_t + \sum_{i=1}^{N_t} Y_i$, $B_t \sim \mathcal{N}(0,t)$, $N_t \sim \text{Pois}(\lambda)$, $Y_i \sim \mathcal{N}(\gamma, \delta^2)$ in Merton's jump-diffusion model is given by

$$\phi_{X_t}(\omega) = \exp\left[t\left(\text{i}\mu\omega - \frac{1}{2}\sigma^2\omega^2 + \lambda\left(\text{e}^{\text{i}\gamma\omega - \frac{1}{2}\delta^2\omega^2} - 1\right)\right)\right] = \text{e}^{t\psi(\omega)}.$$

As before, the characteristic exponent can further be decomposed into a drift part $\psi_{\text{d}}(\omega)$ and a non-drift part $\psi_{\text{n-d}}(\omega)$ such that

$$\psi_{\text{d}}(\omega) = \text{i}\mu\omega,$$
$$\psi_{\text{n-d}}(\omega) = -\frac{1}{2}\sigma^2\omega^2 + \lambda\left(\text{e}^{\text{i}\gamma\omega - \frac{1}{2}\delta^2\omega^2} - 1\right).$$

In risk-neutral valuation, the risk-neutral drift is given by

$$\begin{aligned}\mu_{\text{r-n}} &= r - \psi_{\text{n-d}}(-\text{i}) \\ &= r - \left(-\frac{1}{2}\sigma^2(-\text{i})^2\right) - \lambda\left(\text{e}^{\text{i}\gamma(-\text{i}) - \frac{1}{2}\delta^2(-\text{i})^2} - 1\right) \\ &= r - \frac{1}{2}\sigma^2 - \lambda\left(\text{e}^{\gamma + \frac{1}{2}\delta^2} - 1\right),\end{aligned}$$

yielding the risk-neutral characteristic exponent

$$\psi_{\text{r-n}}(\omega) = \text{i}\mu_{\text{r-n}}\omega - \frac{1}{2}\sigma^2\omega^2 + \lambda\left(\text{e}^{\text{i}\gamma\omega - \frac{1}{2}\delta^2\omega^2} - 1\right).$$

Hence, under the risk-neutral measure, the characteristic function of $X_t$ in Merton's jump-diffusion model has the form

$$\phi_{\text{r-n}}(\omega) = \text{e}^{t\psi_{\text{r-n}}(\omega)}.$$

### 5.4.3 Kou's Jump-Diffusion Model

Under the true measure the characteristic function of $X_t = \mu t + \sigma B_t + \sum_{i=1}^{N_t} Y_i$, $B_t \sim \mathcal{N}(0,t)$, $N_t \sim \text{Pois}(\lambda)$, $f_Y(y; p_1, p_2, \eta_1, \eta_2) = p_1\eta_1 \mathrm{e}^{-\eta_1 y}\mathbf{1}_{y\geq 0} + p_2\eta_2 \mathrm{e}^{\eta_2 y}\mathbf{1}_{y<0}$ in Kou's jump-diffusion model is given by

$$\phi_{X_t}(\omega) = \exp\left[t\left(\mathrm{i}\mu\omega - \frac{1}{2}\sigma^2\omega^2 + \mathrm{i}\lambda\omega\left(\frac{p_1}{\eta_1 - \mathrm{i}\omega} - \frac{p_2}{\eta_2 + \mathrm{i}\omega}\right)\right)\right] = \mathrm{e}^{t\psi(\omega)}.$$

Once again, the characteristic exponent can further be decomposed into a drift part $\psi_{\text{d}}(\omega)$ and a non-drift part $\psi_{\text{n-d}}(\omega)$ such that

$$\begin{aligned}\psi_{\text{d}}(\omega) &= \mathrm{i}\mu\omega,\\ \psi_{\text{n-d}}(\omega) &= -\frac{1}{2}\sigma^2\omega^2 + \mathrm{i}\lambda\omega\left(\frac{p_1}{\eta_1 - \mathrm{i}\omega} - \frac{p_2}{\eta_2 + \mathrm{i}\omega}\right).\end{aligned}$$

In risk-neutral valuation, the risk-neutral drift is given by

$$\begin{aligned}\mu_{\text{r-n}} &= r - \psi_{\text{n-d}}(-\mathrm{i})\\ &= r - \left(-\frac{1}{2}\sigma^2(-\mathrm{i})^2\right) - \mathrm{i}\lambda(-\mathrm{i})\left(\frac{p_1}{\eta_1 - \mathrm{i}(-\mathrm{i})} - \frac{p_2}{\eta_2 + \mathrm{i}(-\mathrm{i})}\right)\\ &= r - \frac{1}{2}\sigma^2 - \lambda\left(\frac{p_1}{\eta_1 - 1} - \frac{p_2}{\eta_2 + 1}\right),\end{aligned}$$

yielding the risk-neutral characteristic exponent

$$\psi_{\text{r-n}}(\omega) = \mathrm{i}\mu_{\text{r-n}}\omega - \frac{1}{2}\sigma^2\omega^2 + \mathrm{i}\lambda\omega\left(\frac{p_1}{\eta - \mathrm{i}\omega} - \frac{p_2}{\eta_2 + \mathrm{i}\omega}\right).$$

Hence, under the risk-neutral measure, the characteristic function of $X_t$ in Kou's jump-diffusion model has the form

$$\phi_{\text{r-n}}(\omega) = \mathrm{e}^{t\psi_{\text{r-n}}(\omega)}.$$

### 5.4.4 The Variance-Gamma Process

Under the true measure the characteristic function of the variance-gamma process $X_t = \theta G_t + \sigma B_{G_t}$, $G_t \sim \Gamma(1/\xi, 1/\xi)$ is given by

$$\begin{aligned}\phi_{X_t}(\omega) &= \big(\phi_X(\omega)\big)^t\\ &= \left(1 - \mathrm{i}\xi\omega\theta + \frac{1}{2}\sigma^2\xi\omega^2\right)^{-t/\xi}\\ &= \mathrm{e}^{-\frac{t}{\xi}\ln\left(1 - \mathrm{i}\xi\omega\theta + \frac{1}{2}\sigma^2\xi\omega^2\right)}\\ &= \mathrm{e}^{t\psi(\omega)}.\end{aligned}$$

The characteristic exponent has no drift part, but it does have a non-drift part $\psi_{\text{n-d}}(\omega)$ of the form

$$\psi_{\text{n-d}}(\omega) = -\frac{1}{\xi}\ln\left(1 - \mathrm{i}\xi\omega\theta + \frac{1}{2}\sigma^2\xi\omega^2\right).$$

In risk-neutral valuation, the risk-neutral drift is given by

$$\begin{aligned}\mu_{\text{r-n}} &= r - \psi_{\text{n-d}}(-\text{i}) \\ &= r - \left(-\frac{1}{\xi}\ln\left(1 - \text{i}\xi(-\text{i})\theta + \frac{1}{2}\sigma^2\xi(-\text{i})^2\right)\right) \\ &= r + \frac{1}{\xi}\ln\left(1 - \xi\theta - \frac{1}{2}\sigma^2\xi\right),\end{aligned}$$

yielding the risk-neutral characteristic exponent

$$\psi_{\text{r-n}}(\omega) = \text{i}\mu_{\text{r-n}}\omega - \frac{1}{\xi}\ln\left(1 - \text{i}\xi\omega\theta + \frac{1}{2}\sigma^2\xi\omega^2\right).$$

Hence, under the risk-neutral measure, the characteristic function of the variance-gamma process $X_t$ has the form

$$\phi_{\text{r-n}}(\omega) = \text{e}^{t\psi_{\text{r-n}}(\omega)}.$$

### 5.4.5 The Normal-Inverse Gaussian Process

Under the true measure the characteristic function of the normal-inverse Gaussian process $X_t = \beta\delta^2 I_t + \delta B_{I_t},\ I_t \sim \text{IG}(1, \delta\sqrt{\alpha^2 - \beta^2})$ is given by

$$\phi_{X_t}(\omega) = \text{e}^{-\delta t\left(\sqrt{\alpha^2 - (\beta + \text{i}\omega)^2} - \sqrt{\alpha^2 - \beta^2}\right)} = \text{e}^{t\psi(\omega)}.$$

Once again the characteristic exponent has no drift part, but it does have a non-drift part $\psi_{\text{n-d}}(\omega)$ of the form

$$\psi_{\text{n-d}}(\omega) = -\delta\left(\sqrt{\alpha^2 - (\beta + \text{i}\omega)^2} - \sqrt{\alpha^2 - \beta^2}\right).$$

In risk-neutral valuation, the risk-neutral drift is given by

$$\begin{aligned}\mu_{\text{r-n}} &= r - \psi_{\text{n-d}}(-\text{i}) \\ &= r - \left(-\delta\left(\sqrt{\alpha^2 - (\beta + \text{i}(-\text{i}))^2} - \sqrt{\alpha^2 - \beta^2}\right)\right) \\ &= r + \delta\left(\sqrt{\alpha^2 - (\beta + 1)^2} - \sqrt{\alpha^2 - \beta^2}\right),\end{aligned}$$

yielding the risk-neutral characteristic exponent

$$\psi_{\text{r-n}}(\omega) = \text{i}\mu_{\text{r-n}}\omega - \delta\left(\sqrt{\alpha^2 - (\beta + \text{i}\omega)^2} - \sqrt{\alpha^2 - \beta^2}\right).$$

Hence, under the risk-neutral measure, the characteristic function of the normal-inverse Gaussian process $X_t$ has the form

$$\phi_{\text{r-n}}(\omega) = \text{e}^{t\psi_{\text{r-n}}(\omega)}.$$

# 6 Computer Simulation

In this section, the procedures used to simulate the preceding processes will be presented. It is assumed that random number generators providing standard Gaussian and uniform random numbers are available.

## 6.1 Simulating Basic Processes

First the simulation of the standard Brownian motion and the Poisson process will be presented ([20], p. 101) since they lay the foundation for more intricate processes.

### 6.1.1 Brownian Motion

A standard Brownian motion $B = \{B_t\}_{t\geq 0}$ is effortless to simulate since it has stationary, independent, and Gaussian distributed increments.

Let $\Delta t$ denote a small time step and let $\{Y_i\}_{i\geq 1}$ denote a series of standard Gaussian random variates. It follows that a standard Brownian motion can be simulated by

- $B_0 = 0$,
- $B_{i\Delta t} = B_{(i-1)\Delta t} + \sqrt{\Delta t}\, Y_i,\ i \geq 1$.

### 6.1.2 The Poisson Process

A Poisson process $N = \{N_t\}_{t\geq 0}$ with intensity parameter $\lambda$ is simulated by utilizing the method of exponential spacings. The method of exponential spacings makes use of the fact that the inter-arrival times of the jumps follow an exponential distribution with mean $\lambda^{-1}$.

To obtain a series of exponentially distributed random variates $\{Y_i\}_{i\geq 1}$ with mean $\lambda^{-1}$, the following transform can be made

$$Y_i = -\frac{\ln(U_i)}{\lambda},$$

where $\{U_i\}_{i\geq 1}$ is a series of uniformly distributed random variates on the unit interval.

Let $\Delta t$ denote a small time step and let

- $S_0 = 0$,
- $S_i = S_{i-1} + Y_i,\ i \geq 1$,

where $S_i$ is the $i$th arrival time and $Y_i$ is the $i$th inter-arrival time. Then a sample path of the Poisson process $N$ is given by

- $N_0 = 0$,
- $N_{i\Delta t} = \sup(k : S_k \leq i\Delta t),\ i \geq 1$.

## 6.2 Simulating Lévy Processes

### 6.2.1 The Compound Poisson Process

To simulate a sample path of the compound Poisson process $X = \{X_t\}_{0 \le t \le T}$, the following procedure is applied:

- Generate a Poisson distributed random variate $N$ with intensity parameter $\lambda T$. $N$ corresponds to the total number of jumps on the interval $[0, T]$.
- Generate a series of uniformly distributed random variates $U = \{U_i\}_{i=1}^{N}$ on an interval of length $T$. $U$ corresponds to the the jump times.
- Generate a series of independent jump sizes $Y = \{Y_i\}_{i=1}^{N}$ with law $f$.

A sample path of the compound Poisson process is then given by

$$X_t = \sum_{i=1}^{N} Y_i \mathbf{1}_{U_i \le t}.$$

### 6.2.2 Merton's and Kou's Jump-Diffusion Models

As has been mentioned, a general jump-diffusion process $X = \{X_t\}_{t \ge 0}$ corresponds to a Brownian motion with drift coupled with a compound Poisson process, that is,

$$X_t = \mu t + \sigma B_t + \sum_{i=1}^{N_t} Y_i, \; Y_i \sim f.$$

Let $t_1, \ldots, t_n$ be a set of equally spaced fixed time points, i.e., $\Delta t = t_i - t_{i-1}$. A discretized trajectory of the Lévy jump-diffusion $X$ is simulated by ([18], p. 29):

- Generate a Poisson distributed random variate $N$ with intensity parameter $\lambda T$.
- Generate a series of uniformly distributed random variates $U = \{U_i\}_{i=1}^{N}$ on an interval of length $T$. $U$ corresponds to the jump times.
- Generate a standard normal random variate and transform it into a normal variate, say $G_i$. The variance of $G_i$ is equal to $\sigma \Delta t$.
- Simulate the law of of the jump size $Y$. In other words, simulate the random variates $Y_i$ with law $f$.

A sample path of $X$ is then given by

$$X_{i\Delta t} = \mu i \Delta t + \sum_{j=1}^{i} G_j + \sum_{k=1}^{N} Y_i \mathbf{1}_{U_i \le t_i}.$$

### 6.2.3 The Gamma Process

Let $Y = \{Y_i\}_{i\geq 1}$ be a series of random numbers following a $\Gamma(a\Delta t, b)$ distribution, where $\Delta t$ denotes a small time step. A sample path of a gamma process $G = \{G_t\}_{t\geq 0}$ following a $\Gamma(at, b)$ distribution is then given by ([20], p. 109)

- $G_0 = 0$,
- $G_{i\Delta t} = G_{(i-1)\Delta t} + Y_i,\ i \geq 1$.

### 6.2.4 The Variance-Gamma Process

Earlier it was noted that a variance-gamma process $X = \{X_t\}_{t\geq 0}$ with parameters $\sigma > 0$, $\xi > 0$, and $\theta$ can be seen as a gamma subordinated Brownian motion with drift.

Let $B = \{B_t\}_{t\geq 0}$ denote a standard Brownian motion and let $G = \{G_t\}_{t\geq 0}$ denote a gamma process with parameters $\alpha = \beta = 1/\xi$. A sample path of a variance-gamma process is then given by ([20], pp. 109-110)

$$X_t = \theta G_t + \sigma B_{G_t}.$$

### 6.2.5 The Inverse Gaussian Process

In able to simulate a sample path of an inverse Gaussian process, an inverse Gaussian random number generator has to be utilized. The following procedure generates inverse Gaussian random numbers from an $\mathrm{IG}(\alpha, \beta)$ distribution ([20], pp. 111-113):

- Generate a random variate $v \sim \mathcal{N}(0, 1)$.
- Set $y = v^2$.
- Set $x = \dfrac{\alpha}{\beta} + \dfrac{y - \sqrt{4\alpha\beta y + y^2}}{2\beta^2}$.
- Generate a random variate $u$ uniformly distributed on the unit interval.
- If $u \leq \dfrac{\alpha}{\alpha + \beta x}$ return $x$, otherwise return $\dfrac{\alpha^2}{\beta^2 x}$.

Let $g = \{g_i\}_{i\geq 1}$ be a series of random numbers following an $\mathrm{IG}(\alpha\Delta t, \beta)$ distribution, where $\Delta t$ denotes a small time step. A sample path of an inverse Gaussian process $I = \{I_t\}_{t\geq 0}$ following an $\mathrm{IG}(\alpha t, \beta)$ distribution is then given by

- $I_0 = 0$,
- $I_{i\Delta t} = I_{(i-1)\Delta t} + g_i,\ i \geq 1$.

### 6.2.6 THE NORMAL-INVERSE GAUSSIAN PROCESS

As was mentioned, a normal-inverse Gaussian process $X = \{X_t\}_{t\geq 0}$ with parameters $\alpha > 0, -\alpha < \beta < \alpha$, and $\delta > 0$ can be seen as an inverse Gaussian subordinated Brownian motion with drift.

Let $B = \{B_t\}_{t\geq 0}$ denote a standard Brownian motion and let $I = \{I_t\}_{t\geq 0}$ denote an inverse Gaussian process with parameters $a = 1$ and $b = \delta\sqrt{\alpha^2 - \beta^2}$. A sample path of a normal-inverse Gaussian process is then given by ([18], p. 59)

$$X_t = \beta\delta^2 I_t + \delta B_{I_t}.$$

# 7 Model Calibration

To calculate option prices, it is necessary to calibrate the models with respect to option quotes found on the market. The option quotes that will be used come from plain vanilla options.

## 7.1 Model Inputs

The option quotes will be based on index options. Index options are calls and puts where the underlying asset is a stock market index. The indices being treated in this thesis are NDX, DJX, and SPX. The reason is that they are European style indices.

Other significant calibration inputs are interest rates and dividends, both of which are not straightforwardly obtained. The interest rate cannot be assumed to be constant because we will calculate option prices across many different maturities. Moreover, one of the major difficulties for traders pricing index options is to retrieve dividend estimates. How to acquire interest rates and dividends will be discussed in the subsequent subsections.

### 7.1.1 The Risk-Free Interest Rate

The risk-free interest rate is the theoretical rate of return on investment with zero risk and thus represents the interest an investor would expect from a perfectly riskless investment over a given period of time. The risk-free rate is in theory an investor's minimum expected return on any investment since additional risk is not acceptable unless the potential rate of return is greater than the risk-free rate. In practice the risk-free rate does not exist because even the most secure investments involve a small amount of risk.

Since the options are priced across different maturities, the interest rate cannot be assumed to be constant. In the case of USD investments, rates on U.S. Treasury bills, bonds, and notes are often used as an estimate of the varying risk-free interest rate. Since we will consider maturities ranging from 94 days to 1004 days, the Treasury yield curve will be based on rates on Treasury bills and short-term over-the-counter Treasury notes, both of which are quoted in Table 1[2]. If longer maturities would have been considered, then also rates on Treasury bonds would have been included when constructing the Treasury yield curve. Figure 11 displays the resulting Treasury yield curve.

Table 1: U.S. Treasury quotes on Tuesday, March 17, 2015.

| Maturity | Yield | Maturity | Yield | Maturity | Yield |
|---|---|---|---|---|---|
| Mar. 19, 2015 | 0.025 | Dec. 15, 2015 | 0.261 | Mar. 15, 2017 | 0.683 |
| Mar. 26, 2015 | 0.033 | Dec. 31, 2015 | 0.260 | Mar. 31, 2017 | 0.713 |
| Apr. 2, 2015 | 0.025 | Jan. 15, 2016 | 0.262 | Apr. 15, 2017 | 0.727 |
| Apr. 9, 2015 | 0.028 | Jan. 31, 2016 | 0.276 | Apr. 30, 2017 | 0.756 |
| Apr. 16, 2015 | 0.043 | Feb. 15, 2016 | 0.298 | May 15, 2017 | 0.762 |

Continued on next page

[2]Recovered from online.wsj.com.

Table 1 – continued from previous page

| Maturity | Yield | Maturity | Yield | Maturity | Yield |
|---|---|---|---|---|---|
| Apr. 23, 2015 | 0.033 | Feb. 29, 2016 | 0.308 | May 31, 2017 | 0.797 |
| Apr. 30, 2015 | 0.025 | Mar. 15, 2016 | 0.328 | June 15, 2017 | 0.805 |
| May 7, 2015 | 0.025 | Mar. 31, 2016 | 0.337 | June 30, 2017 | 0.816 |
| May 14, 2015 | 0.028 | Apr. 15, 2016 | 0.374 | July 15, 2017 | 0.834 |
| May 21, 2015 | 0.030 | Apr. 30, 2016 | 0.389 | July 31, 2017 | 0.847 |
| May 28, 2015 | 0.023 | May 15, 2016 | 0.419 | Aug. 15, 2017 | 0.854 |
| June 4, 2015 | 0.020 | May 31, 2016 | 0.434 | Aug. 31, 2017 | 0.887 |
| June 11, 2016 | 0.028 | June 15, 2016 | 0.431 | Sep. 15, 2017 | 0.898 |
| June 18, 2015 | 0.033 | June 30, 2016 | 0.427 | Sep. 30, 2017 | 0.919 |
| June 25, 2015 | 0.033 | July 15, 2016 | 0.454 | Oct. 15, 2017 | 0.927 |
| July 2, 2015 | 0.038 | July 31, 2016 | 0.449 | Oct. 31, 2017 | 0.941 |
| July 9, 2015 | 0.038 | Aug. 15, 2016 | 0.503 | Nov. 15, 2017 | 0.961 |
| July 16, 2015 | 0.038 | Aug. 31, 2016 | 0.505 | Nov. 30, 2017 | 0.977 |
| July 23, 2015 | 0.053 | Sep. 15, 2016 | 0.517 | Dec. 15, 2017 | 0.985 |
| July 30, 2015 | 0.056 | Sep. 30, 2016 | 0.526 | Dec. 31, 2017 | 0.998 |
| Aug. 6, 2015 | 0.081 | Oct. 15, 2016 | 0.555 | Jan. 15, 2018 | 1.015 |
| Aug. 13, 2015 | 0.089 | Oct. 31, 2016 | 0.560 | Jan. 31, 2018 | 1.038 |
| Aug. 20, 2015 | 0.099 | Nov. 15, 2016 | 0.573 | Feb. 15, 2018 | 1.046 |
| Aug. 27, 2015 | 0.107 | Nov. 30, 2016 | 0.578 | Feb. 28, 2018 | 1.065 |
| Sep. 15, 2015 | 0.186 | Dec. 15, 2016 | 0.593 | Mar. 15, 2018 | 1.067 |
| Sep. 30, 2015 | 0.192 | Dec. 31, 2016 | 0.605 | Mar. 31, 2018 | 1.102 |
| Oct. 15, 2015 | 0.196 | Jan. 15, 2017 | 0.634 | Apr. 30, 2018 | 1.118 |
| Oct. 31, 2015 | 0.212 | Jan. 31, 2017 | 0.639 | May 15, 2018 | 1.108 |
| Nov. 15, 2015 | 0.233 | Feb. 15, 2017 | 0.670 | May 31, 2018 | 1.149 |
| Nov. 30, 2015 | 0.261 | Feb. 28, 2017 | 0.662 | | |

### 7.1.2 Option Quotes

Out of all index options available, not all are well-priced. For example, deep-in-the-money and deep-out-of-the-money options are often illiquid, or have a price close to nothing. Hence, for calibration purposes, some option quotes have to be excluded. Which option quotes to be kept for calibration will be based on the following guideline:

- Solely options in the vicinity of being at-the-money will be included. The cut-off point will be approximately ±25% in the neighborhood of the strike price.
- Options with little time to maturity have a price close to their intrinsic values. Hence, we will solely include options with a time to maturity being no less than one month.
- A large bid-ask spread may exist when a market is not being actively traded on and has low volume. Therefore the options may not be well-priced. Hence, solely options for which the relative spread[3] is less than or equal to, say 12%, will be included.

[3]Relative spread: $2 \times \frac{\text{ask price}-\text{bid price}}{\text{ask price}+\text{bid price}}$.

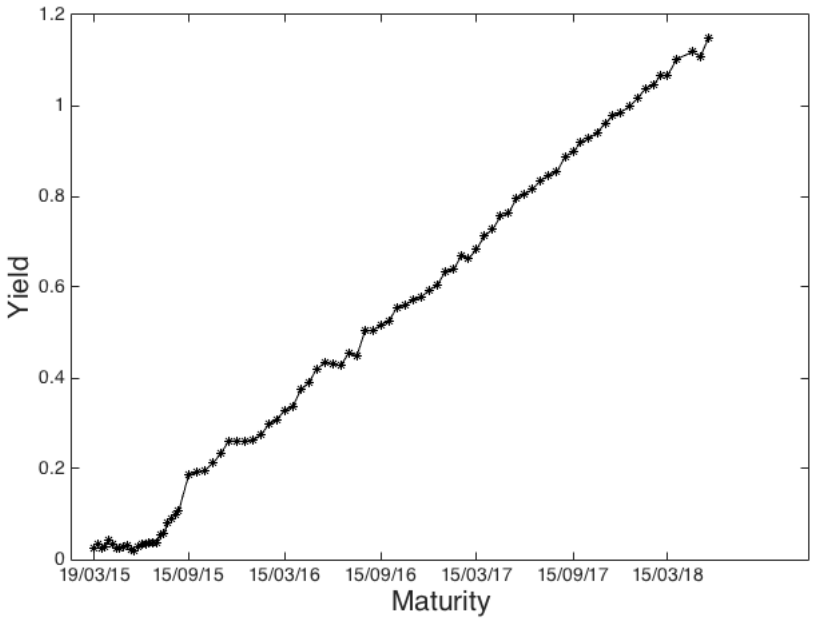


Figure 11: U.S. Treasury yield curve on Tuesday, March 17, 2015.

All the data, such as index option quotes, index futures quotes, and rates on Treasury bills and short-term over-the-counter Treasury notes were collected on Tuesday, March 17, 2015. The reason why index futures quotes were collected is that they will be used when estimating the dividends as will be seen in the next subsection.

Tables 2-4[4] present option quotes across a variety of maturities.

Table 2: NDX market quotes on Tuesday, March 17, 2015[5].

| Strike price | 94 days | 185 days | 277 days |
|---|---|---|---|
| 3300 | 1082.80 | 1091.80 | 1104.60 |
| 3325 | 1048.30 | 1067.80 | 1081.80 |
| 3350 | 1033.90 | 1047.40 | 1059.90 |
| 3375 | 1009.70 | 1020.80 | 1037.10 |
| 3400 | 985.30 | 999.50 | 1013.90 |
| 3425 | 961.00 | 974.10 | 990.70 |
| 3450 | 936.70 | 951.30 | 968.40 |
| 3475 | 912.50 | 928.10 | 947.30 |
| 3500 | 888.30 | 905.10 | 924.70 |
| 3525 | 863.60 | 882.10 | 903.20 |
| 3550 | 839.30 | 859.20 | 881.10 |

Continued on next page

[4]Recovered from oic.ivolatility.com.

[5]On Tuesday, March 17, 2015, 361 NDX call option prices were quoted on the market, out of which 210 market quotes fulfilled the above preconditions.

Table 2 – continued from previous page

| Strike price | 94 days | 185 days | 277 days |
|---|---|---|---|
| 3575 | 815.30 | 836.40 | 859.00 |
| 3600 | 789.90 | 813.80 | 837.70 |
| 3625 | 766.30 | 791.30 | 815.90 |
| 3650 | 742.40 | 768.60 | 794.30 |
| 3675 | 718.60 | 745.50 | 772.90 |
| 3700 | 696.50 | 723.30 | 751.90 |
| 3725 | 673.00 | 701.50 | 731.20 |
| 3730 | 666.90 | | |
| 3735 | 663.60 | | |
| 3740 | 659.00 | | |
| 3745 | 654.30 | | |
| 3750 | 648.50 | 679.70 | 710.00 |
| 3755 | 643.70 | | |
| 3760 | 640.30 | | |
| 3765 | 634.50 | | |
| 3770 | 629.70 | | |
| 3775 | 625.10 | 658.70 | 689.30 |
| 3780 | 621.40 | | |
| 3785 | 617.10 | | |
| 3790 | 612.50 | | |
| 3795 | 607.90 | | |
| 3800 | 602.00 | 637.10 | 669.20 |
| 3805 | 598.70 | | |
| 3810 | 594.10 | | |
| 3815 | 588.30 | | |
| 3820 | 584.90 | | |
| 3825 | 580.40 | 615.30 | 648.40 |
| 3830 | 575.80 | | |
| 3835 | 569.80 | | |
| 3840 | 565.50 | | |
| 3850 | 557.60 | 594.00 | 628.20 |
| 3875 | 533.50 | 574.10 | 608.80 |
| 3900 | 512.50 | 552.20 | 588.40 |
| 3925 | 488.70 | 532.80 | 568.20 |
| 3950 | 467.70 | 512.50 | 549.60 |
| 3975 | 445.00 | 491.60 | 530.30 |
| 4000 | 424.70 | 472.40 | 511.50 |
| 4025 | 402.30 | 452.70 | 493.30 |
| 4050 | 381.20 | 433.30 | 475.00 |
| 4075 | 360.80 | 413.50 | 456.20 |
| 4080 | | 410.60 | |
| 4085 | | 406.00 | |
| 4090 | | 402.80 | |
| 4095 | | 399.00 | |
| 4100 | 340.30 | 394.60 | 439.10 |
| 4105 | | 391.60 | |
| 4110 | | 387.20 | |
| 4115 | | 383.70 | |
| 4120 | | 380.00 | |

Continued on next page

Table 2 – continued from previous page

| Strike price | 94 days | 185 days | 277 days |
|---|---|---|---|
| 4125 | 320.20 | 376.30 | 421.50 |
| 4150 | 300.60 | 358.70 | 403.20 |
| 4155 | | 354.30 | |
| 4160 | | 350.90 | |
| 4165 | | 347.60 | |
| 4170 | | 343.60 | |
| 4175 | 280.80 | 340.60 | 386.30 |
| 4180 | | 336.60 | |
| 4185 | | 334.00 | |
| 4190 | | 329.30 | |
| 4195 | | 325.60 | |
| 4200 | 266.50 | 322.40 | 369.80 |
| 4225 | 246.20 | 304.90 | 353.10 |
| 4250 | 227.00 | 288.50 | 336.60 |
| 4275 | 210.20 | 271.70 | 321.40 |
| 4300 | 191.20 | 255.80 | 305.90 |
| 4325 | 178.70 | 240.20 | 290.70 |
| 4350 | 162.70 | 225.00 | 274.80 |
| 4375 | 147.50 | 210.70 | 262.30 |
| 4400 | 133.20 | 196.30 | 246.60 |
| 4425 | 119.50 | 183.00 | 232.80 |
| 4450 | 104.00 | 169.90 | 219.90 |
| 4475 | 93.40 | 157.40 | 207.50 |
| 4500 | 83.00 | 144.60 | 195.20 |
| 4525 | 70.70 | 133.60 | 183.40 |
| 4550 | 61.80 | 122.00 | 172.00 |
| 4575 | 52.10 | 110.60 | 160.90 |
| 4600 | 44.10 | 100.40 | 150.50 |
| 4625 | 37.20 | 91.10 | 139.90 |
| 4650 | 31.20 | 82.50 | 123.50 |
| 4675 | | 74.10 | 121.50 |
| 4700 | | 66.60 | |
| 4725 | | | 101.50 |
| 4750 | | 52.30 | 93.70 |
| 4775 | | 46.30 | 86.00 |
| 4800 | | 40.30 | 78.70 |

Table 3: DJX market quotes on Tuesday, March 17, 2015[6].

| Strike price | 94 days | 185 days | 277 days |
|---|---|---|---|
| 130 | 48.25 | 48.10 | 49.50 |
| 135 | 43.30 | 43.35 | 45.30 |
| 136 | 42.35 | | |

Continued on next page

[6]On Tuesday, March 17, 2015, 175 DJX call option prices were quoted on the market, out of which 101 market quotes fulfilled the above preconditions.

Table 3 – continued from previous page

| Strike price | 94 days | 185 days | 277 days |
|---|---|---|---|
| 137 | 41.35 | | |
| 138 | 40.40 | | |
| 139 | 39.40 | | |
| 140 | 38.40 | 38.60 | 39.95 |
| 141 | 37.45 | | |
| 142 | 36.50 | | |
| 143 | 35.50 | | |
| 144 | 34.55 | | |
| 145 | 33.60 | 33.95 | 36.25 |
| 146 | 32.60 | | |
| 147 | 31.65 | | |
| 148 | 30.70 | 31.25 | |
| 149 | 29.75 | 30.35 | |
| 150 | 28.80 | 29.45 | |
| 151 | 27.85 | 28.50 | |
| 152 | 26.90 | 27.60 | |
| 153 | 25.95 | 26.75 | |
| 154 | 25.05 | 25.85 | |
| 155 | 24.00 | 24.95 | 26.10 |
| 156 | 23.05 | 24.15 | |
| 157 | 22.15 | 23.25 | |
| 158 | 21.25 | 22.40 | |
| 159 | 20.30 | 21.55 | |
| 160 | 19.40 | 20.70 | 21.95 |
| 161 | 18.55 | 19.85 | |
| 162 | 17.65 | 19.05 | |
| 163 | 16.80 | 18.20 | |
| 164 | 15.90 | 17.40 | |
| 165 | 15.05 | 16.60 | 18.05 |
| 166 | 14.20 | 15.85 | |
| 167 | 13.35 | 15.05 | |
| 168 | 12.55 | 14.30 | |
| 169 | 11.75 | 13.50 | |
| 170 | 10.95 | 12.75 | 14.25 |
| 171 | 10.15 | 12.05 | |
| 172 | 9.40 | 11.30 | |
| 173 | 8.65 | 10.65 | |
| 174 | 7.95 | 9.85 | |
| 175 | 7.25 | 9.20 | 10.70 |
| 176 | 6.60 | 8.55 | |
| 177 | 5.90 | 7.90 | |
| 178 | 5.30 | 7.30 | |
| 179 | 4.65 | 6.70 | |
| 180 | 4.10 | 6.10 | |
| 181 | 3.55 | 5.55 | |
| 182 | 3.05 | 5.05 | |
| 183 | 2.57 | 4.55 | |
| 184 | 2.14 | 4.05 | |

Table 4: SPX market quotes on Tuesday, March 17, 2015[7].

| Strike price | 94 days | 185 days | 277 days | 458 days | 640 days | 1004 days |
|---|---|---|---|---|---|---|
| 1550 | 514.30 | 515.50 | 524.10 | 532.00 | 546.80 | 575.40 |
| 1560 | 504.50 | | | | | |
| 1570 | 495.50 | | | | | |
| 1575 | 490.30 | 491.80 | 501.20 | 510.30 | 526.30 | 556.70 |
| 1580 | 485.50 | | | | | |
| 1590 | 475.90 | | | | | |
| 1600 | 465.90 | 468.30 | 478.50 | 488.90 | 506.10 | 538.30 |
| 1610 | 456.40 | | | | | |
| 1620 | 446.50 | | | | | |
| 1625 | 441.60 | 445.00 | 455.90 | 467.90 | 486.00 | 520.00 |
| 1640 | 436.80 | | | | | |
| 1650 | 427.10 | 422.00 | 433.60 | 446.70 | 466.20 | 502.00 |
| 1660 | 417.70 | | | | | |
| 1670 | 407.80 | | | | | |
| 1675 | 398.10 | 398.90 | 411.40 | 426.00 | 446.60 | 484.30 |
| 1680 | 393.30 | | | | | |
| 1690 | 388.50 | | | | | |
| 1700 | 378.90 | 375.50 | 389.50 | | 427.30 | 466.70 |
| 1710 | 369.40 | | | | | |
| 1720 | 359.90 | | | | | |
| 1725 | 350.40 | 353.60 | 367.80 | 385.30 | 408.20 | 449.40 |
| 1730 | 345.60 | | | | | |
| 1740 | 340.90 | | | | | |
| 1750 | 331.40 | 330.70 | 346.50 | 365.50 | 389.40 | 432.40 |
| 1760 | 321.80 | | | | | |
| 1770 | 312.40 | | | | | |
| 1775 | 303.10 | 309.40 | 325.20 | 345.90 | 370.90 | 415.60 |
| 1780 | 298.50 | | | | | |
| 1790 | 294.00 | | | | | |
| 1800 | 284.80 | 288.10 | 304.60 | 326.60 | 352.60 | 399.00 |
| 1810 | 275.60 | | | | | |
| 1820 | 266.50 | | | | | |
| 1825 | 257.40 | 266.80 | 284.20 | 307.70 | 334.70 | 382.80 |
| 1830 | 252.60 | | | | | |
| 1840 | 248.10 | | | | | |
| 1850 | 239.60 | 245.40 | 264.20 | 289.20 | 317.10 | 366.80 |
| 1860 | 230.40 | | | | | |
| 1870 | 221.40 | | | | | |
| 1875 | 213.00 | 225.00 | 244.60 | 271.00 | 299.90 | 351.10 |
| 1880 | 208.80 | | | | | |
| 1885 | 204.30 | | | | | |
| 1890 | 199.80 | | | | | |
| 1895 | 195.30 | | | | | |
| 1900 | 191.20 | 204.80 | 225.40 | 253.30 | 282.80 | 335.70 |
| 1905 | 187.10 | | | | | |

Continued on next page

[7] On Tuesday, March 17, 2015, 636 SPX call option prices were quoted on the market, out of which 249 market quotes fulfilled the above preconditions.

Table 4 – continued from previous page

| Strike price | 94 days | 185 days | 277 days | 458 days | 640 days | 1004 days |
|---|---|---|---|---|---|---|
| 1910 | 183.00 | | | | | |
| 1915 | 178.80 | | | | | |
| 1920 | 174.60 | | | | | |
| 1925 | 170.10 | 185.90 | 203.20 | 236.00 | 266.40 | 320.60 |
| 1930 | 166.00 | | 199.60 | | | |
| 1935 | 161.70 | | | | | |
| 1940 | 157.80 | | 192.30 | | | |
| 1945 | 153.50 | | | | | |
| 1950 | 149.30 | 166.40 | 185.20 | 216.40 | 250.30 | 305.70 |
| 1955 | 145.50 | | | | | |
| 1960 | 141.40 | | 178.10 | | | |
| 1965 | 138.00 | | | | | |
| 1970 | 133.70 | | 171.10 | | | |
| 1975 | 129.90 | 148.40 | 167.70 | 199.30 | 234.60 | 291.20 |
| 1980 | 125.80 | | | | | |
| 1985 | 122.60 | | | | | |
| 1990 | 118.80 | | | | | |
| 1995 | 114.60 | | | | | |
| 2000 | 111.00 | 128.50 | 150.90 | 183.50 | 215.40 | 277.00 |
| 2005 | 107.00 | | | | | |
| 2010 | 101.10 | | | | | |
| 2015 | 97.50 | | | | | |
| 2020 | 93.80 | | | | | |
| 2025 | 90.50 | 111.30 | 134.80 | 168.20 | 200.80 | 262.90 |
| 2030 | 86.90 | | | | | |
| 2035 | 83.30 | | | | | |
| 2040 | 79.90 | | 125.50 | | | |
| 2045 | 76.80 | | | | | |
| 2050 | 73.40 | 95.60 | | 153.60 | 186.40 | 249.70 |
| 2055 | 70.10 | | | | | |
| 2060 | 67.10 | | | | | |
| 2065 | 63.90 | | | | | |
| 2070 | 60.80 | | | | | |
| 2075 | 57.80 | 80.40 | 101.80 | 139.50 | 172.50 | 236.50 |
| 2080 | 54.80 | | | | | |
| 2085 | 51.90 | | | | | |
| 2090 | 49.00 | | 94.00 | | | |
| 2095 | 46.40 | | | | | |
| 2100 | 43.70 | 66.60 | 88.60 | | 159.20 | 220.10 |
| 2105 | 41.10 | | | | | |
| 2110 | 38.50 | | | | | |
| 2115 | 36.00 | | | | | |
| 2120 | 33.60 | | | | | |
| 2125 | 31.30 | 54.00 | 75.60 | 111.00 | 146.60 | 207.80 |
| 2130 | 29.30 | | | | | |
| 2135 | 27.10 | | | | | |
| 2140 | 25.10 | | | | | |
| 2145 | 23.10 | | | | | |
| 2150 | 21.30 | 42.60 | | 98.70 | 134.50 | 195.60 |

Continued on next page

Table 4 – continued from previous page

| Strike price | 94 days | 185 days | 277 days | 458 days | 640 days | 1004 days |
|---|---|---|---|---|---|---|
| 2155 | 19.50 | | | | | |
| 2160 | 17.80 | | | | | |
| 2165 | 16.20 | | | | | |
| 2170 | 14.80 | | | | | |
| 2175 | 13.40 | 32.60 | | 87.30 | | 184.10 |
| 2180 | 12.00 | | | | | |
| 2200 | | 24.20 | | | 109.50 | 172.90 |
| 2225 | | 17.30 | | | 99.10 | 162.30 |
| 2250 | | 11.90 | | | 89.40 | 151.80 |
| 2275 | | | | | 80.30 | 141.70 |
| 2300 | | | | | | 132.10 |
| 2325 | | | | | | 123.00 |
| 2350 | | | | | | 111.40 |
| 2375 | | | | | | 103.20 |
| 2400 | | | | | | 95.20 |
| 2425 | | | | | | 87.80 |
| 2450 | | | | | | 80.70 |
| 2475 | | | | | | 74.00 |

### 7.1.3 Futures Quotes and Dividends

One of the main difficulties for traders pricing index options is to estimate the expected dividends. A workaround to this problem is to not use any dividend estimates at all but instead derive the expected dividends from futures contracts. Futures quotes for a variety of maturities are available on the market and the goal is to derive dividend yields from futures prices.

Let $S_0$ be the price of an asset that pays a continuous dividend yield $q$ per annum and let $r$ be the risk-free interest rate. The price of a futures contract $F_0$ maturing at $T$ is then given by ([20], pp. 21-22)

$$F_0 = S_0 e^{(r-q)T}.$$

Since $F_0, S_0, r$, and $T$ are easily retrievable, the expected dividend yield $q$ can straightforwardly be found. In the event of an option maturing between two futures maturities, interpolation can be used to retrieve $q$.

Table 5-7[8] display futures quotes of the indices NDX, DJX, and SPX across a variety of maturities and the resulting discount factors.

| Maturity | Futures prices | Discount factor |
|---|---|---|
| June, 2015 | 4,370.50 | -0.00030 |
| September, 2015 | 4,243.50 | -0.01554 |
| December, 2015 | 4,244.00 | -0.02318 |

Table 5: NDX futures quotes. The spot price is equal to 4,375.63.

[8]Recovered from www.barchart.com.

| Maturity | Futures prices | Discount factor |
|---|---|---|
| June, 2015 | 17,777 | -0.00104 |
| September, 2015 | 17,617 | -0.00663 |
| December, 2015 | 17,527 | -0.01382 |

Table 6: DJX futures quotes on Tuesday, March 17, 2015. The spot price is equal to 17,849.08.

| Maturity | Futures prices | Discount factor |
|---|---|---|
| June, 2015 | 2,066.20 | -0.00101 |
| September, 2015 | 2,059.60 | -0.00360 |
| December, 2015 | 2,053.30 | -0.00771 |
| June, 2016 | 2,043.90 | -0.01851 |
| December, 2016 | 2,039.00 | -0.03008 |
| December, 2017 | 2,046.50 | -0.03709 |

Table 7: SPX futures quotes. The spot price is equal to 2,074.28.

## 7.2 Parameter Estimation

Estimating the parameters in able to calibrate the models is not always easy. However, one way to do it is to simply utilize the option prices at hand.

Let $\mathbf{C}_{\text{q}} = \{C(k), k = 1,\dots,N\}$ be a collection of option quotes and let $\mathbf{C}_{\text{m}} = \{C(k;\theta), k = 1,\dots,N\}$ be a collection of option prices derived from the given model. To retrieve the set of parameters $\theta$, we simply minimize a sum of $N$ squared residuals with respect to $\theta$, such that [23]

$$\hat{\theta} = \arg\min_{\theta} \sum_{k=1}^{N} \left(C(k) - C(k;\theta)\right)^2.$$

### 7.2.1 The Method of Steepest Descent

The method of steepest descent is based on the idea that if the multivariable function $F(\mathbf{x})$ is defined and differentiable in a neighborhood of a point $\mathbf{a}$, then $F(\mathbf{x})$ experiences the most rapid decrease if one goes from $\mathbf{a}$ in the direction of the negative gradient of $F$ at $\mathbf{a}$, that is, in the direction of $-\nabla F(\mathbf{a})$ [27]. Hence, if

$$\mathbf{b} = \mathbf{a} - \gamma \nabla F(\mathbf{a}),$$

for $\gamma$ adequately small, then $F(\mathbf{a}) \geq F(\mathbf{b})$.

Thus, assuming an initial guess $\mathbf{x}_0$ for the local minimum of $F$, one can generate a sequence[9]

$$\mathbf{x}_{n+1} = \mathbf{x}_n - \gamma \nabla F(\mathbf{x}_n),\ n \geq 0,$$

which hopefully converges to the wanted local minimum such that

$$F(\mathbf{x}_0) \geq F(\mathbf{x}_1) \geq F(\mathbf{x}_2) \geq \dots.$$

[9]The value of $\gamma$ is allowed to change at every iteration.

The value of $\gamma$ is allowed to change at every iteration. In fact, robust gradient descent methods must always rescale the step size empirically depending on local properties of the function:

- If after a step the function value increases, the step size was too large. Thus, the step must be undone and the step size must be decreased.
- If after a step the function value decreases, the step size might have been too small. Hence, one can try to increase the step size.

The function $F$ to minimize is of course the difference between the option quotes and the model option prices, and the vector $\mathbf{x}_0$ is an initial guess of the model parameters. Since we do not have a closed-form expression for $F$, the gradient of $F$ has to be approximated which can be done by utilizing the finite difference method. Hence, using this method with a forward difference step size $h$, the elements of $\nabla F$ are approximated by

$$\frac{\partial F}{\partial x} = \frac{F(x+h) - F(x)}{h}, \ h > 0.$$

In the mathematical formulation the gradient is defined in the limit as $h$ goes to zero. However, in practice it is often sufficient to choose a very small value for $h$, and ideally it should be chosen in a way such as to avoid numerical issues. Thus to utilize the method of steepest descent in this setting, two step sizes need to be established, namely $\gamma$ and $h$. It should be noted that the gradient descent method is fairly slow close to the minimum.

# 8 RESULTS

## 8.1 THE BLACK-SCHOLES MODEL

As has been mentioned, the goal of this thesis is to show that the utilization of exponential Lévy models in option pricing can produce better results compared to the utilization of the classical Black-Scholes model.

Figures 12-17 display the results of the Black-Scholes model applied to the Nasdaq-100 Index, the Dow Jones Industrial Average, and the S & P 500 Index. Historical volatilities used as input are given in Table 8[10].

| Index | 10 days | 20 days | 30 days |
|---|---|---|---|
| NDX | 0.1466 | 0.1181 | 0.1200 |
| DJX | 0.1792 | 0.1364 | 0.1311 |
| SPX | 0.1584 | 0.1169 | 0.1178 |

Table 8: Current historical volatilities on Tuesday, March 17, 2015.

It is clear that even though some of the model prices fit the market quotes quite well, the general impression is that overall the model's ability to capture the option prices is inadequate. This also holds true when trying to calibrate the model by changing the volatility input. Furthermore, the mean absolute percentage errors of the Black-Scholes model are given in Table 9.

| Index | Mean absolute percentage error |
|---|---|
| NDX | 0.1283 |
| DJX | 0.0946 |
| SPX | 0.1988 |

Table 9: The mean absolute percentage errors of the Black-Scholes model applied to the given indices.

[10] Recovered from oic.ivolatility.com.

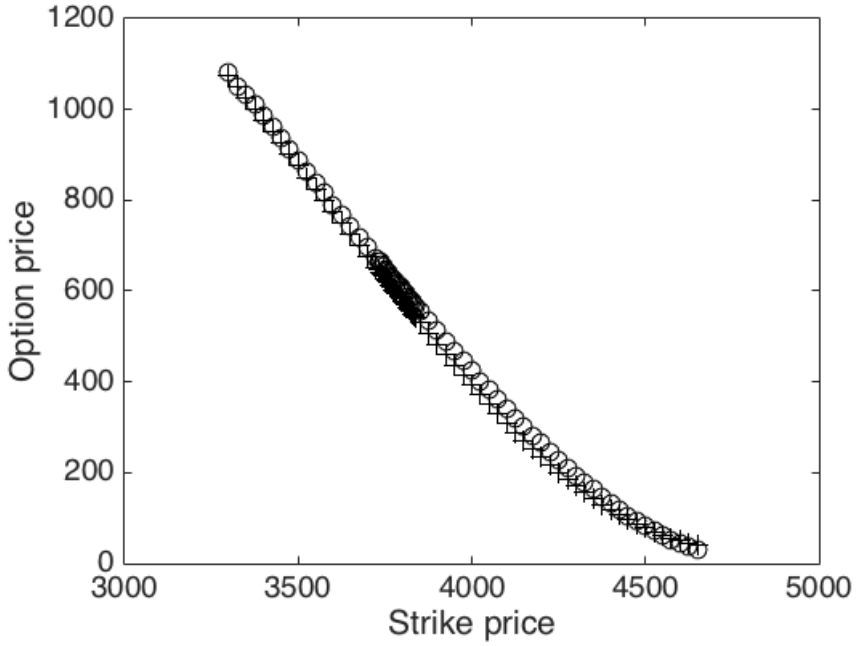


(a) The Nasdaq-100 Index. 94 days to maturity.

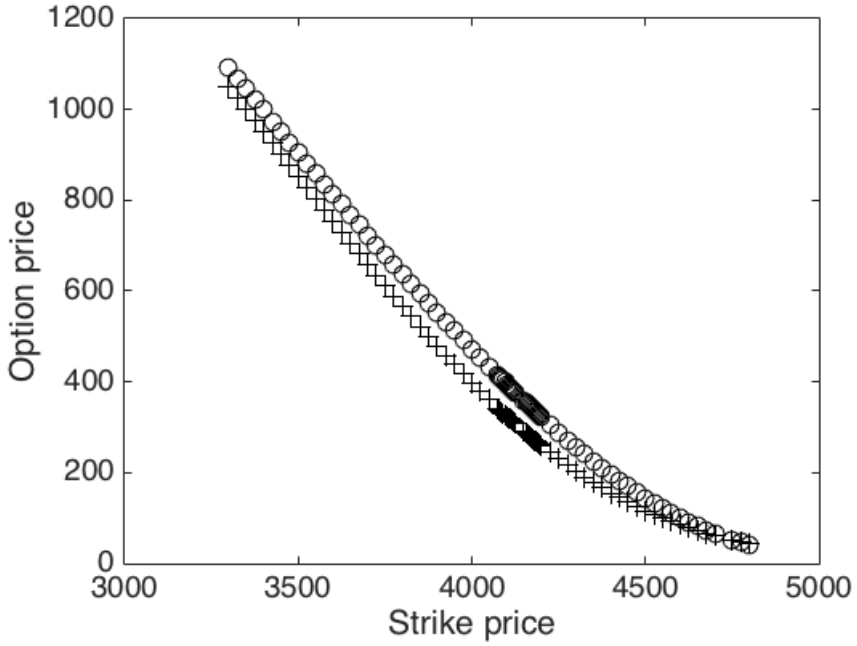


(b) The Nasdaq-100 Index. 185 days to maturity.

Figure 12: The Black-Scholes model applied to the Nasdaq-100 Index. Rings are market quotes, crosses are model prices.

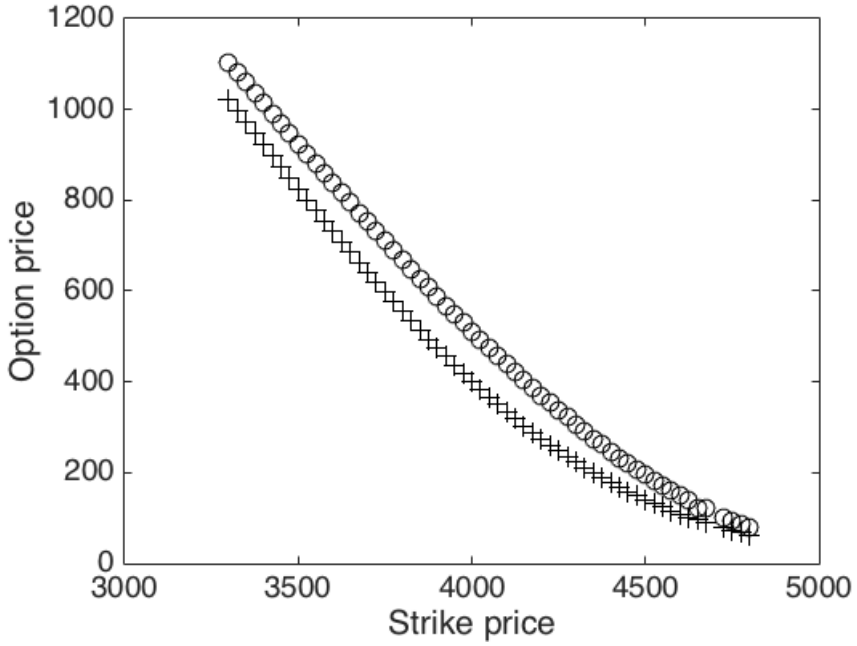


(a) The Nasdaq-100 Index. 277 days to maturity.

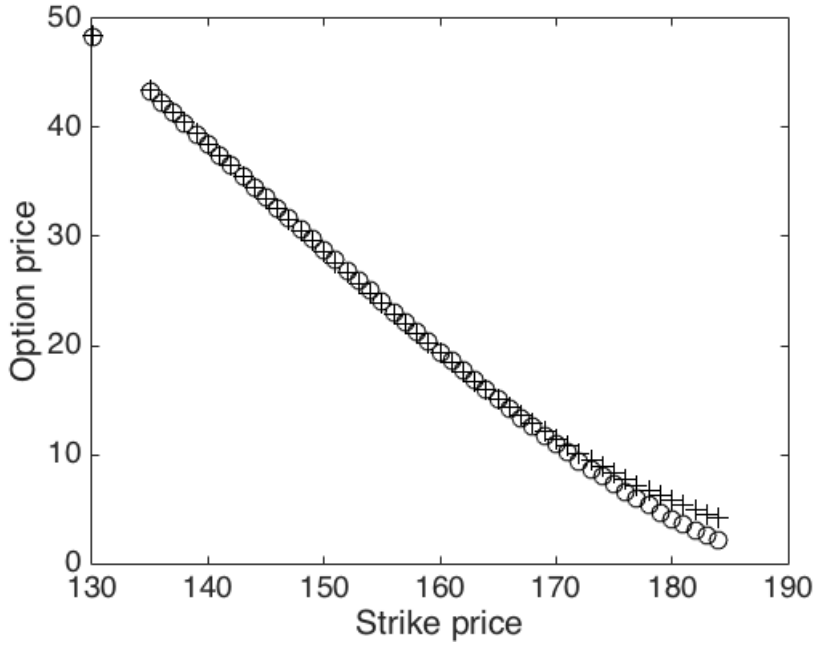


(b) The Dow Jones Industrial Average. 94 days to maturity.

Figure 13: The Black-Scholes model applied to the Nasdaq-100 Index and the Dow Jones Industrial Average. Rings are market quotes, crosses are model prices.

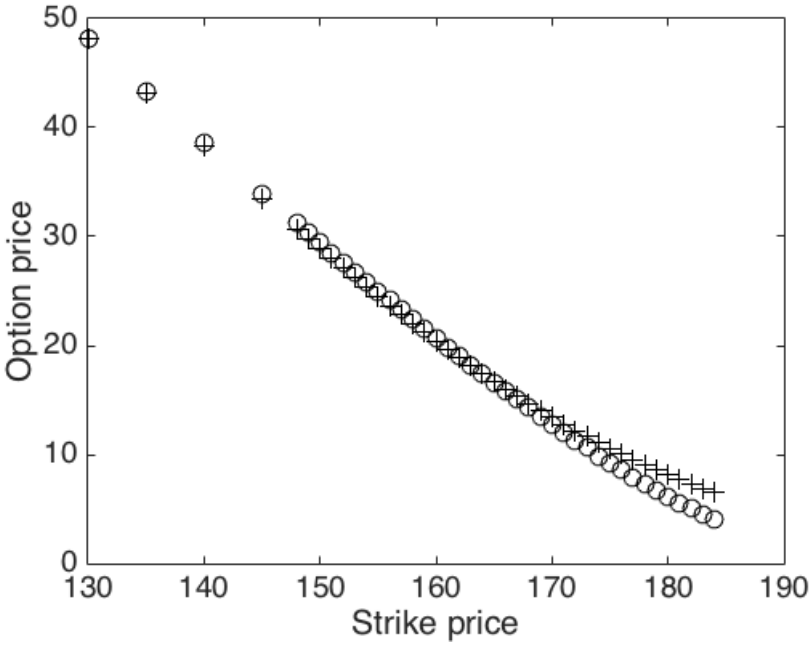


(a) The Dow Jones Industrial Average. 185 days to maturity.

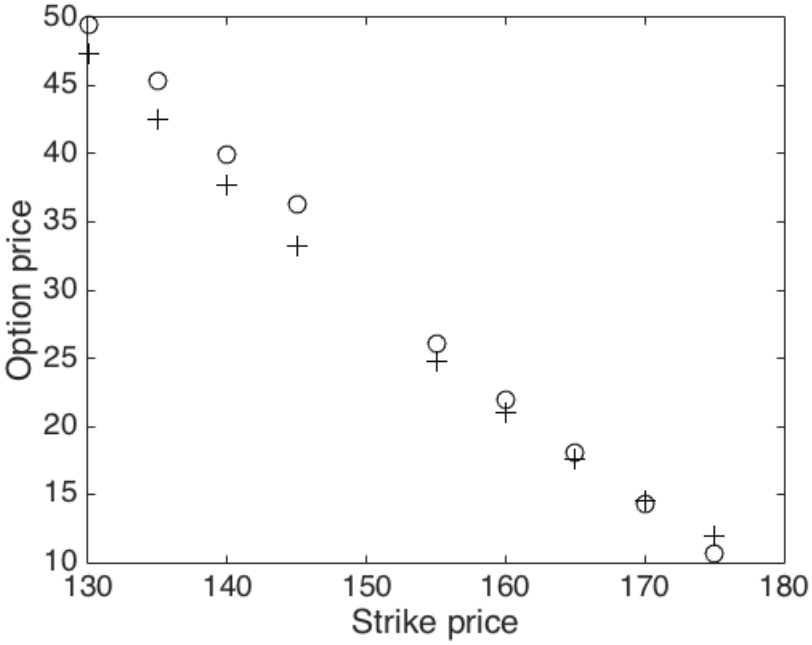


(b) The Dow Jones Industrial Average. 277 days to maturity.

Figure 14: The Black-Scholes model applied to the Dow Jones Industrial Average. Rings are market quotes, crosses are model prices.

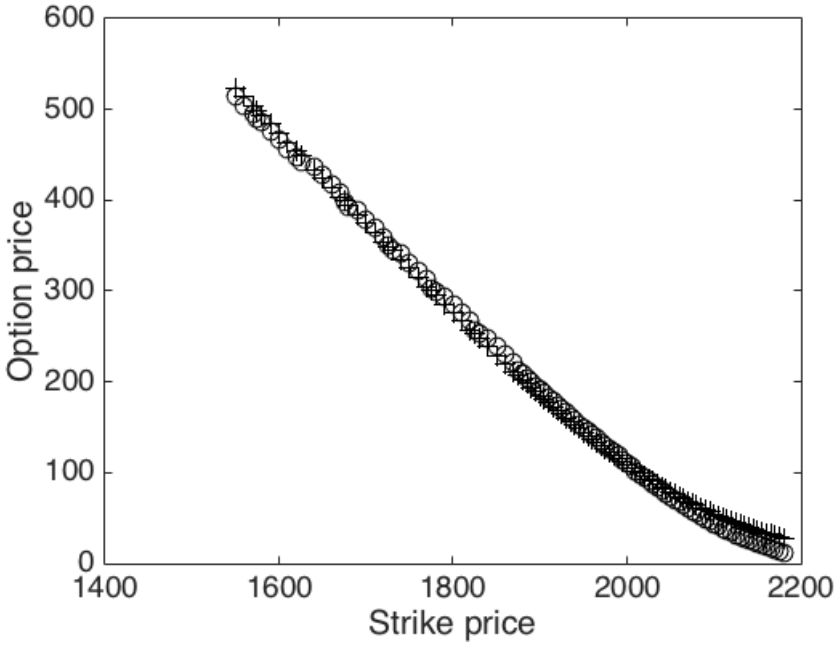


(a) The S & P 500 Index. 94 days to maturity.

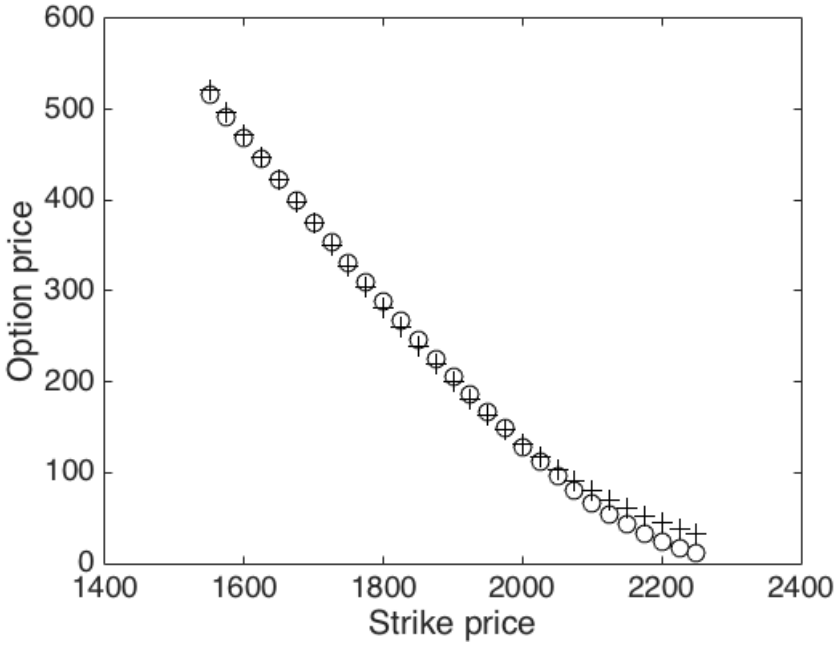


(b) The S & P 500 Index. 185 days to maturity.

Figure 15: The Black-Scholes model applied to the S & P 500 Index. Rings are market quotes, crosses are model prices.

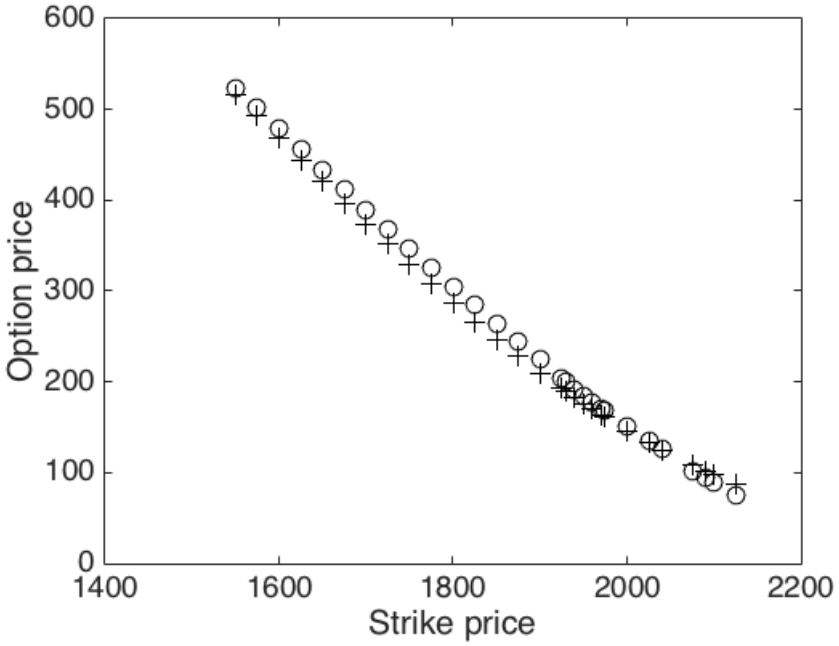


(a) The S & P 500 Index. 277 days to maturity.

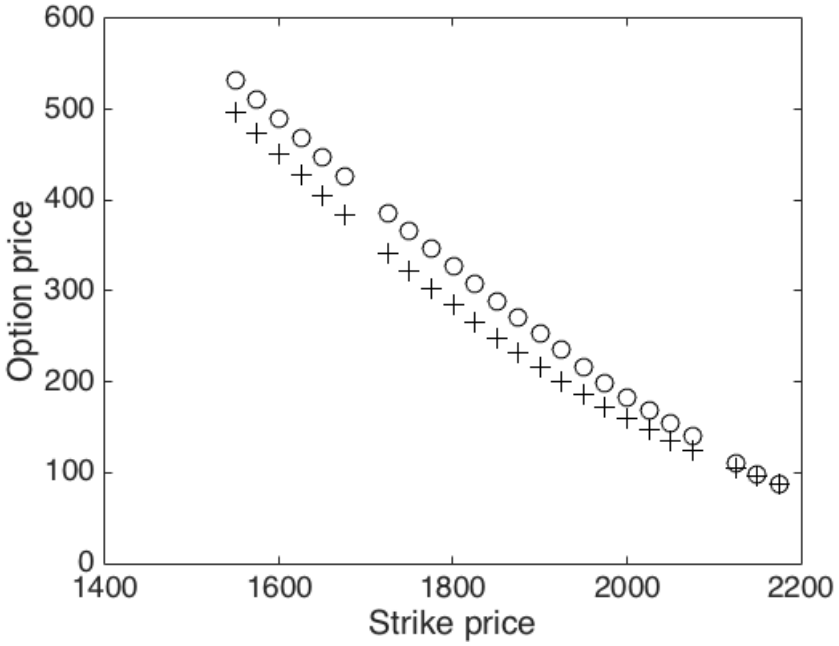


(b) The S & P 500 Index. 458 days to maturity.

Figure 16: The Black-Scholes model applied to the S & P 500 Index. Rings are market quotes, crosses are model prices.

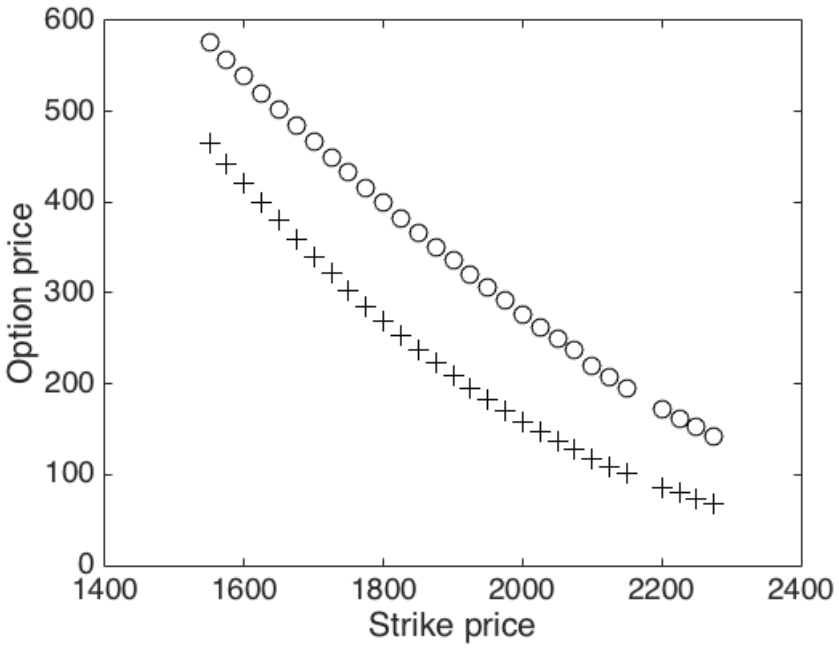


(a) The S & P 500 Index. 640 days to maturity.

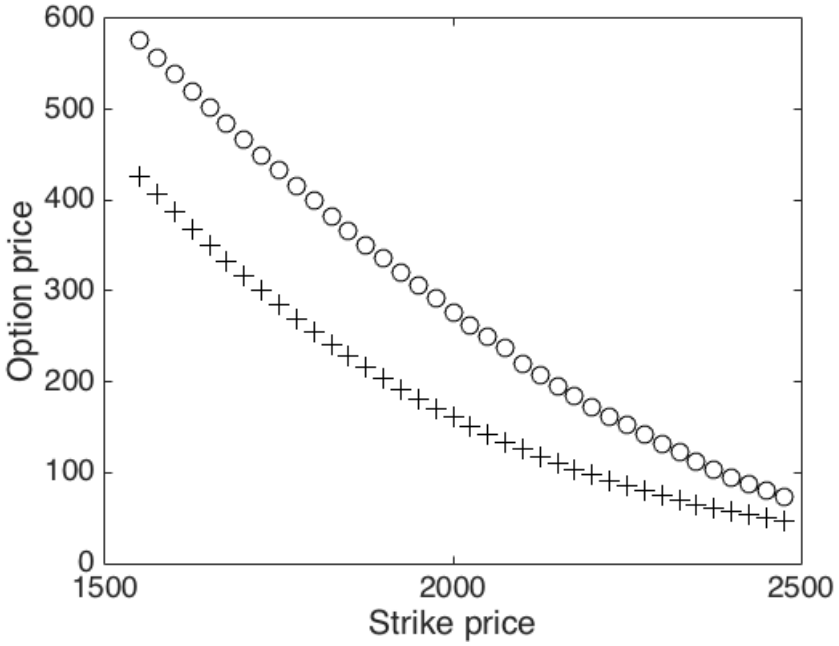


(b) The S & P 500 Index. 1004 days to maturity.

Figure 17: The Black-Scholes model applied to the S & P 500 Index. Rings are market quotes, crosses are model prices.

Employing the method of steepest descent, all of the exponential Lévy models were calibrated and their parameters were estimated and improved until their respective mean squared error was sufficiently small. The step size $h$ of the finite difference derivative was held fixed at a small, constant value.

Figures 18-41 display the results of Merton's jump-diffusion model, Kou's jump-diffusion model, the variance-gamma model, and the normal-inverse Gaussian model. The improvements with respect to the Black-Scholes model are clearly apparent. The mean absolute percentage errors for each model are given in Table 10.

It should be noted that the method of steepest descent is a first-order optimization algo-

| Index | Merton | Kou | Variance-gamma | Normal-inverse Gaussian |
|---|---|---|---|---|
| NDX | 0.0709 | 0.0654 | 0.0732 | 0.0143 |
| DJX | 0.0311 | 0.0540 | 0.0432 | 0.0126 |
| SPX | 0.0591 | 0.0448 | 0.0176 | 0.0873 |

Table 10: The mean absolute percentage errors of the exponential Lévy models applied to the given indices.

rithm which finds local minima[11], hence the results are very much connected to the initial guess of the parameters. Consulting the tables, it is clear that the model which is best at mimicking both the Nasdaq-100 Index market quotes and the Dow Jones Industrial Average market quotes under the given framework is the normal-inverse Gaussian model. The variance-gamma model has the smallest mean absolute percentage error for the S & P 500 Index.

[11] Since steps are taken proportional to the negative of the gradient of the function at the current point.

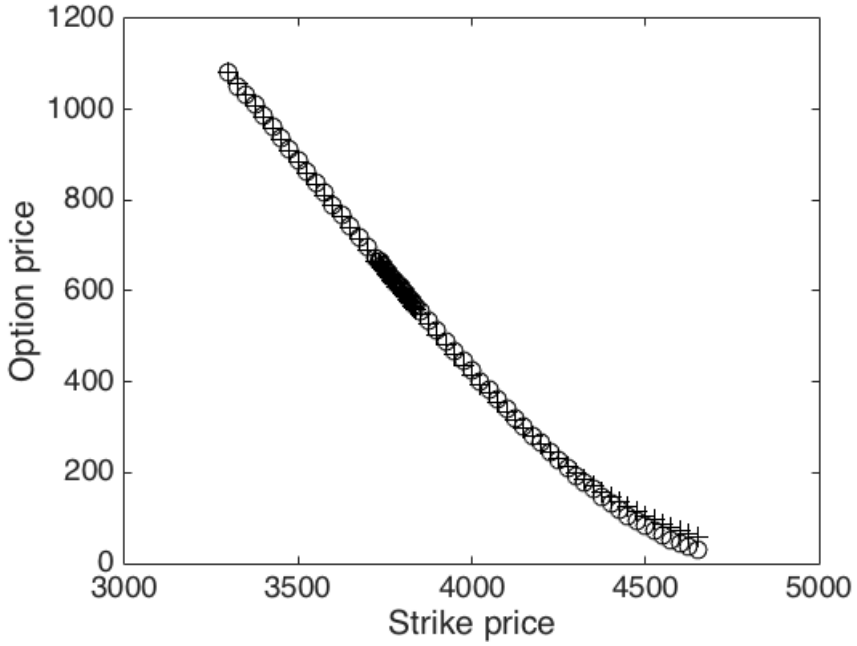


(a) The Nasdaq-100 Index. 94 days to maturity.

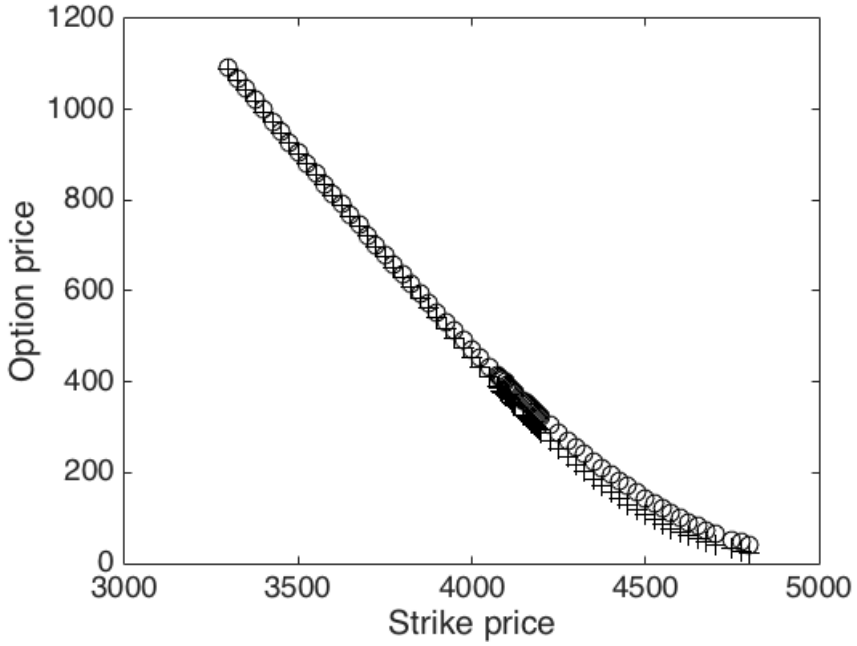


(b) The Nasdaq-100 Index. 185 days to maturity.

Figure 18: Merton's jump-diffusion model applied to the Nasdaq-100 Index. Rings are market quotes, crosses are model prices.

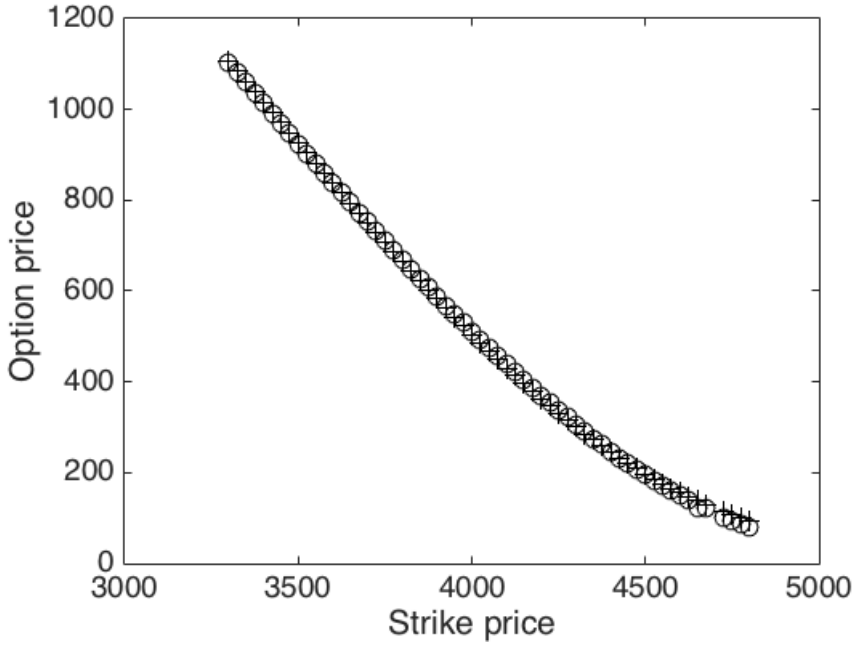


(a) The Nasdaq-100 Index. 277 days to maturity.

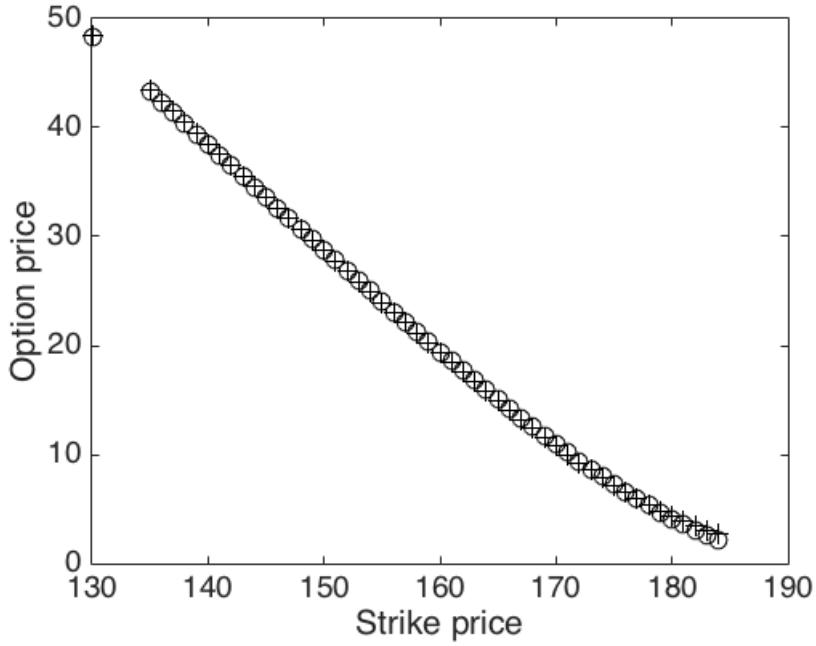


(b) The Dow Jones Industrial Average. 94 days to maturity.

Figure 19: Merton's jump-diffusion model applied to the Nasdaq-100 Index and the Dow Jones Industrial Average. Rings are market quotes, crosses are model prices.

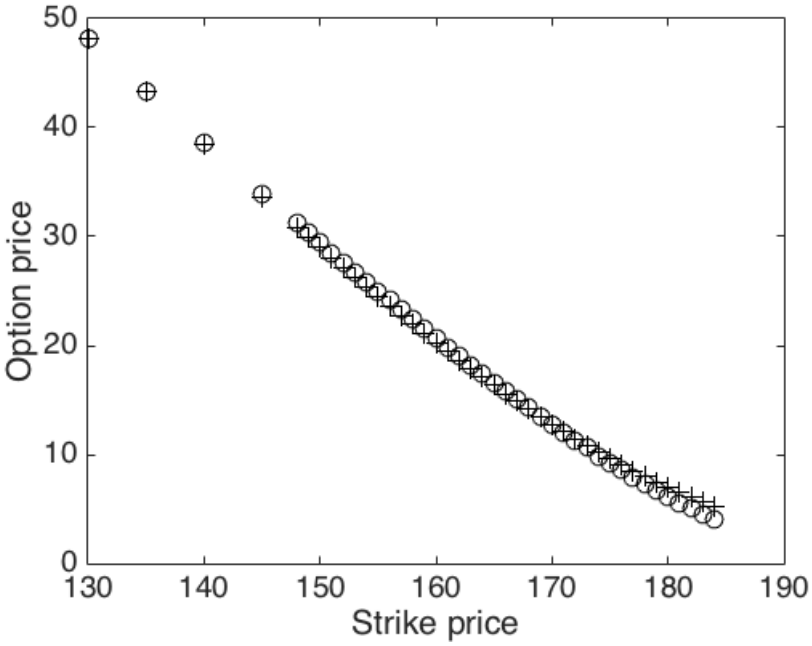


(a) The Dow Jones Industrial Average. 185 days to maturity.

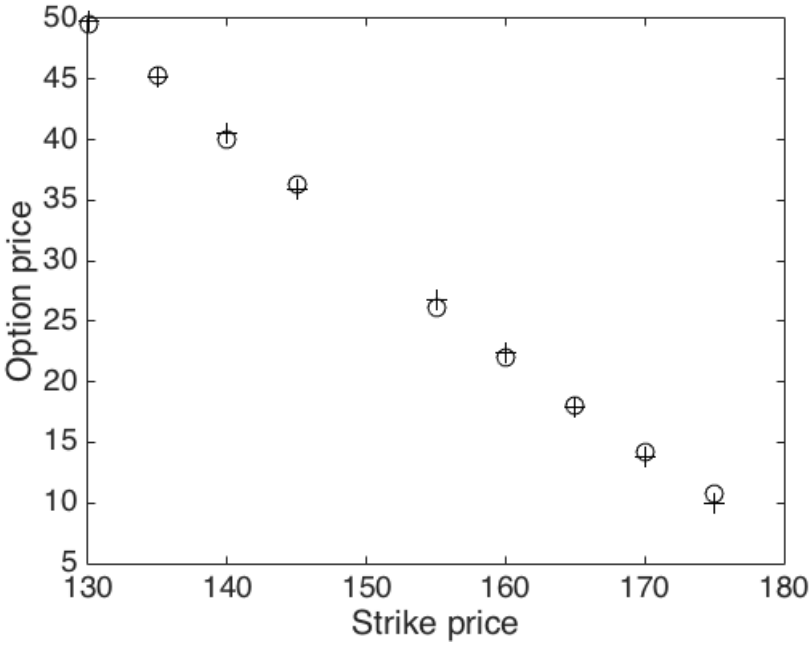


(b) The Dow Jones Industrial Average. 277 days to maturity.

Figure 20: Merton's jump-diffusion model applied to the Dow Jones Industrial Average. Rings are market quotes, crosses are model prices.

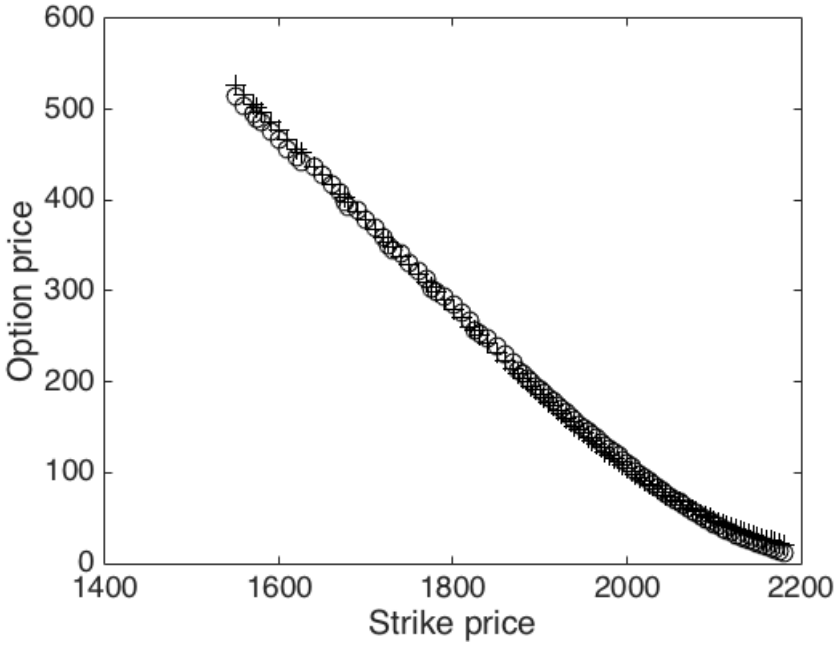


(a) The S & P 500 Index. 94 days to maturity.

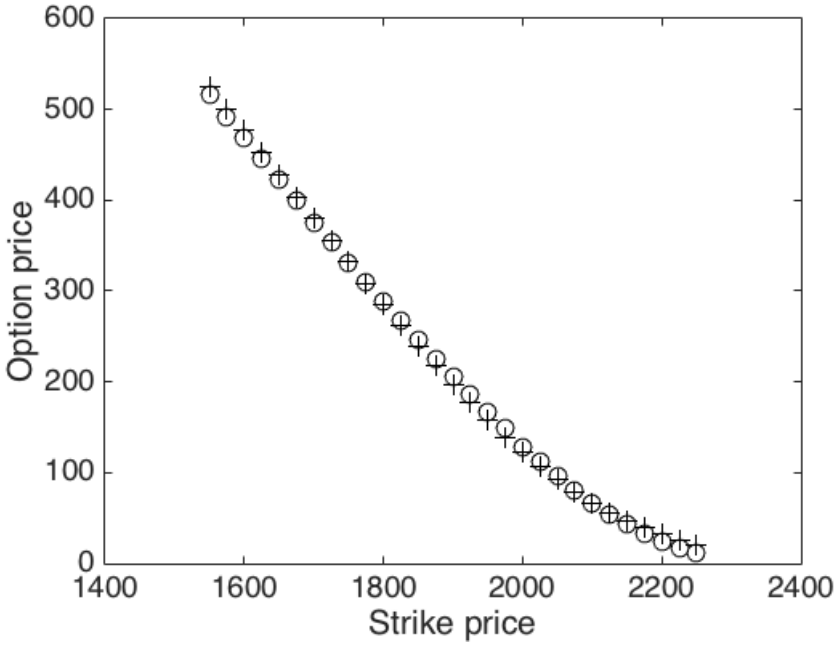


(b) The S & P 500 Index. 185 days to maturity.

Figure 21: Merton's jump-diffusion model applied to the S & P 500 Index. Rings are market quotes, crosses are model prices.

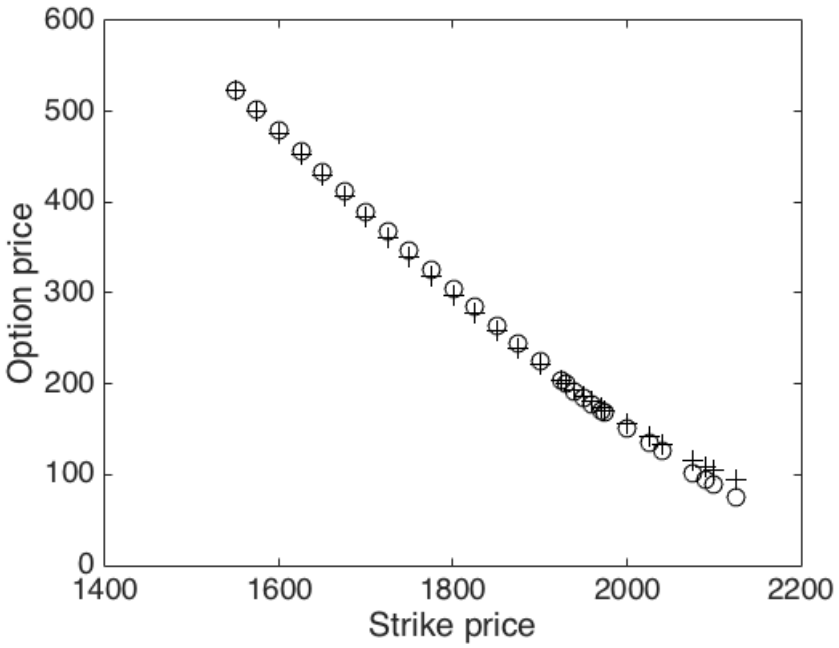


(a) The S & P 500 Index. 277 days to maturity.

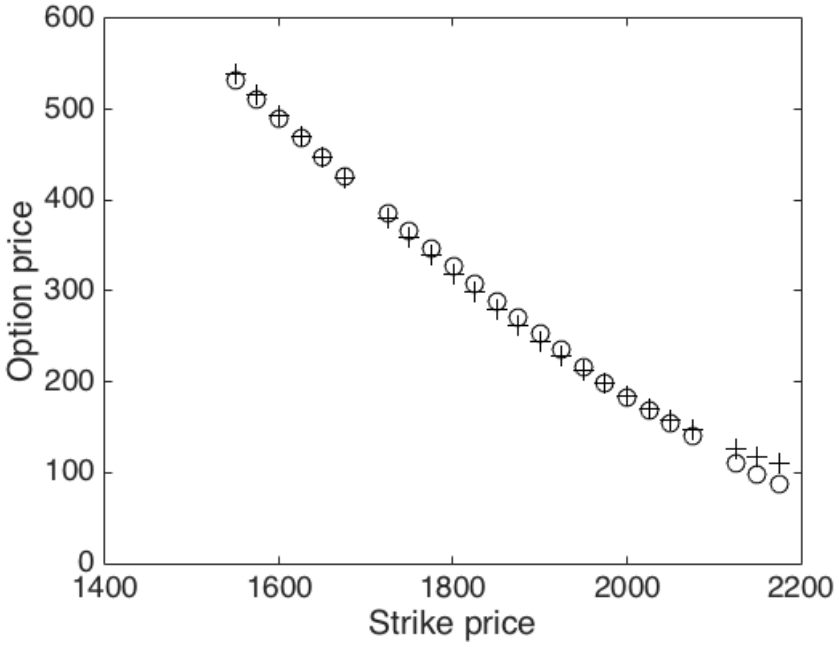


(b) The S & P 500 Index. 458 days to maturity.

Figure 22: Merton's jump-diffusion model applied to the S & P 500 Index. Rings are market quotes, crosses are model prices.

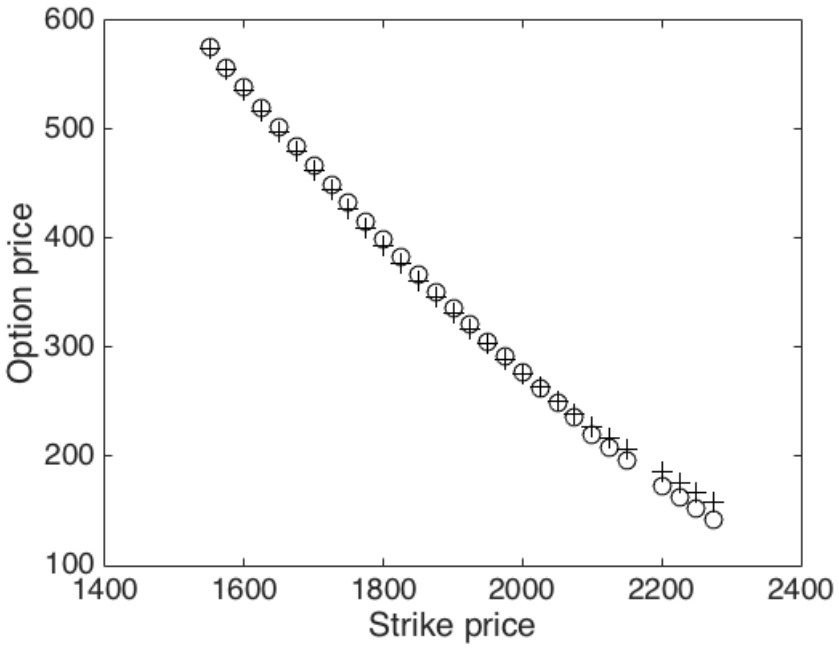


(a) The S & P 500 Index. 640 days to maturity.

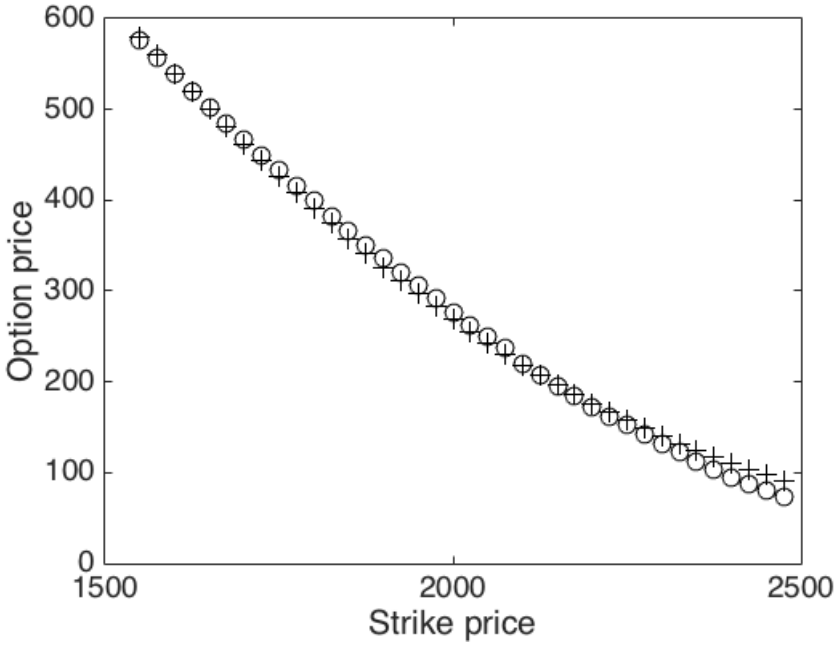


(b) The S & P 500 Index. 1004 days to maturity.

Figure 23: Merton's jump-diffusion model applied to the S & P 500 Index. Rings are market quotes, crosses are model prices.

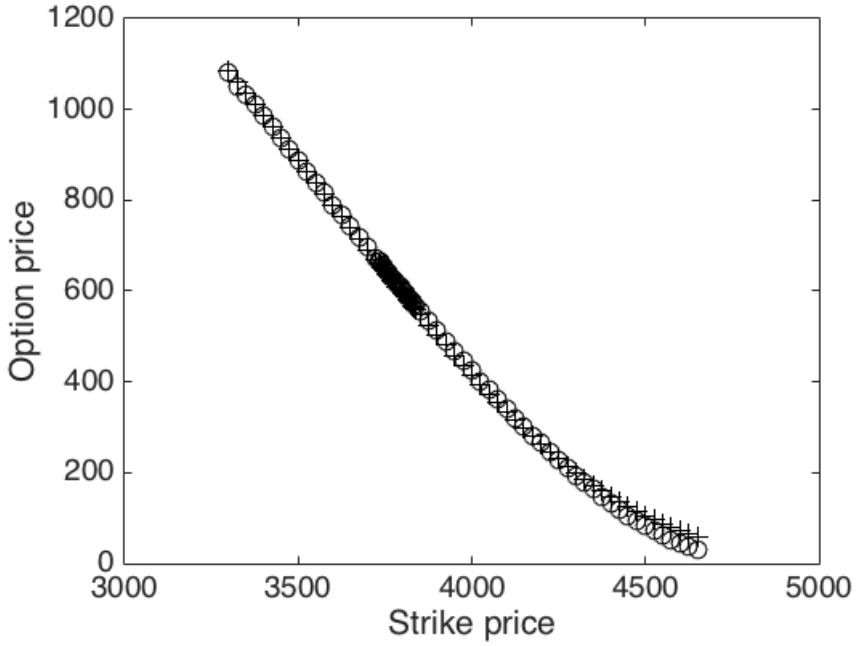


(a) The Nasdaq-100 Index. 94 days to maturity.

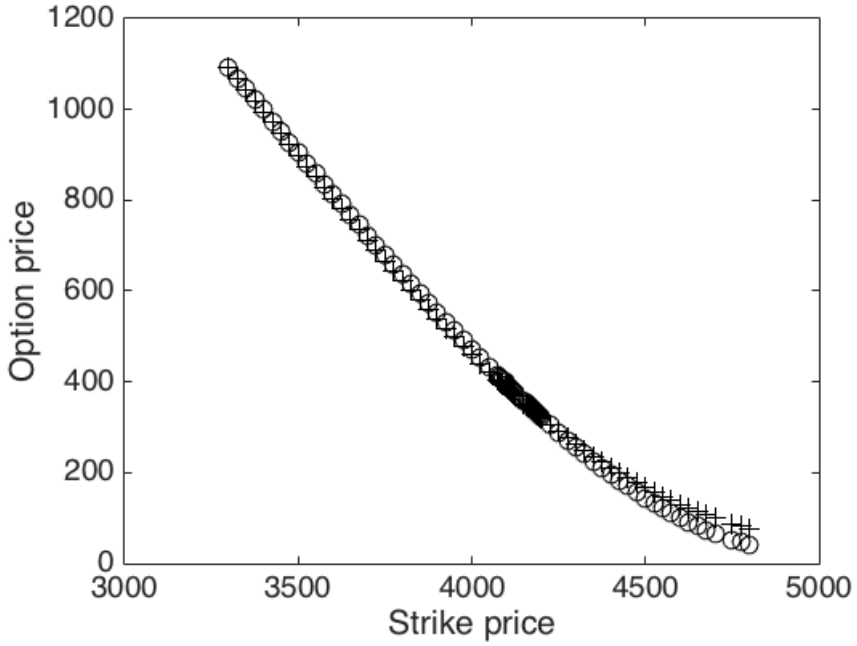


(b) The Nasdaq-100 Index. 185 days to maturity.

Figure 24: Kou's jump-diffusion model applied to the Nasdaq-100 Index. Rings are market quotes, crosses are model prices.

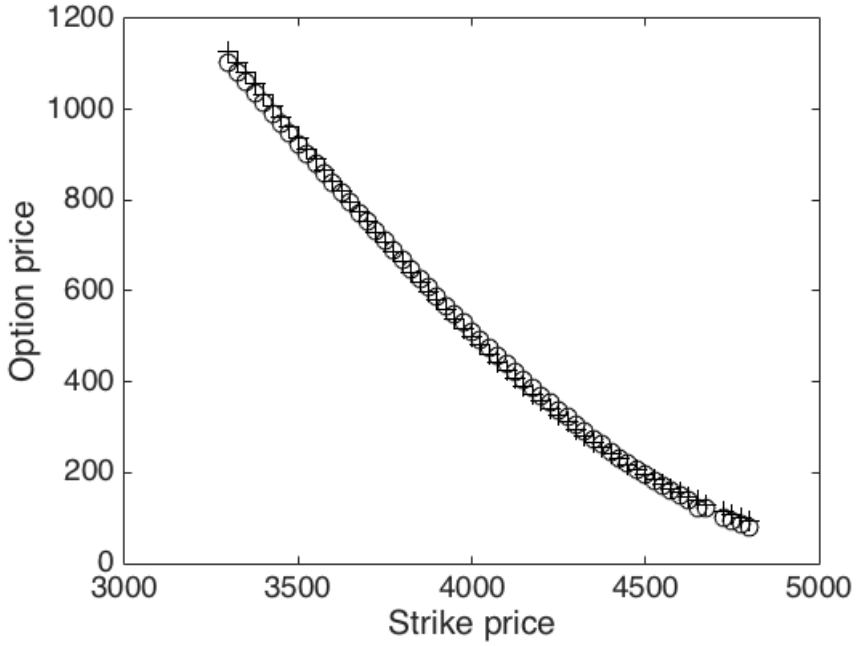


(a) The Nasdaq-100 Index. 277 days to maturity.

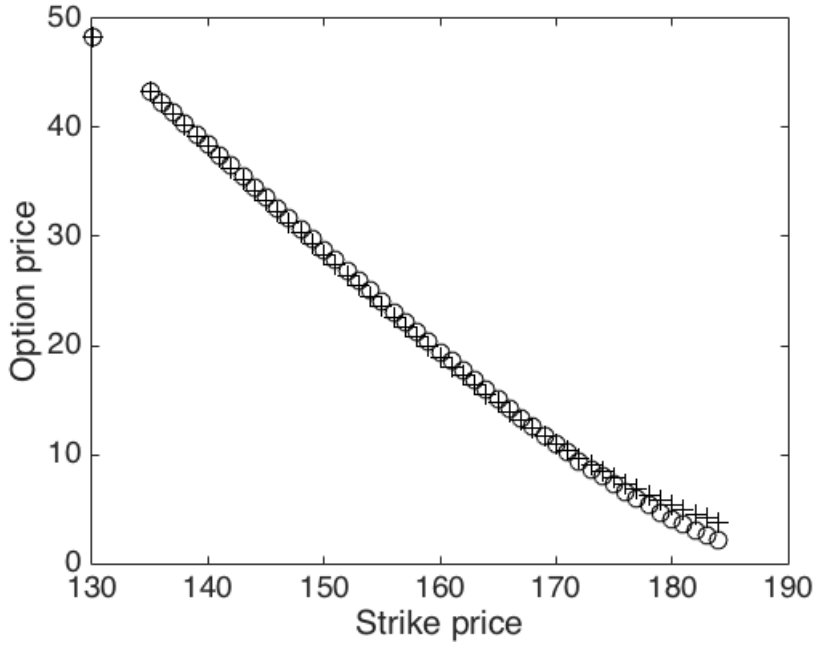


(b) The Dow Jones Industrial Average. 94 days to maturity.

Figure 25: Kou's jump-diffusion model applied to the Nasdaq-100 Index and the Dow Jones Industrial Average. Rings are market quotes, crosses are model prices.

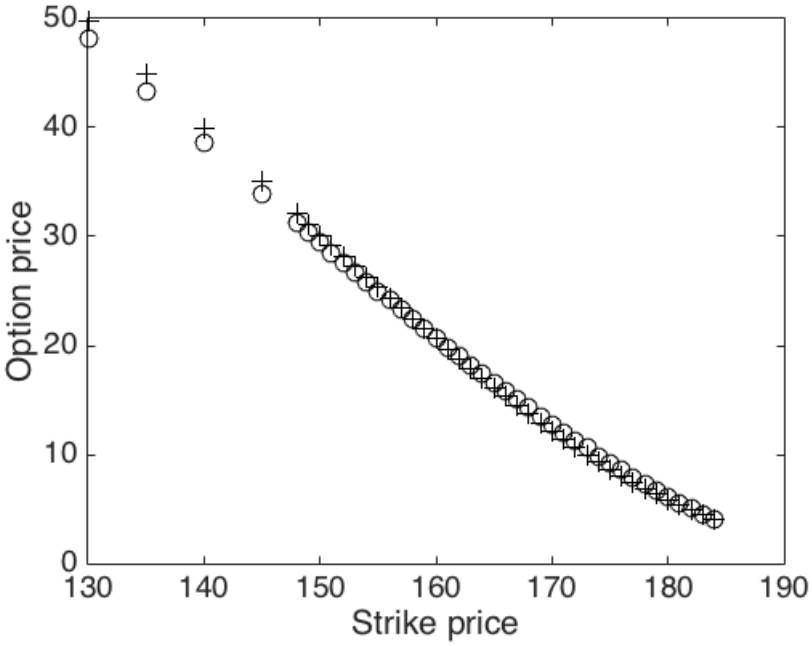


(a) The Dow Jones Industrial Average. 185 days to maturity.

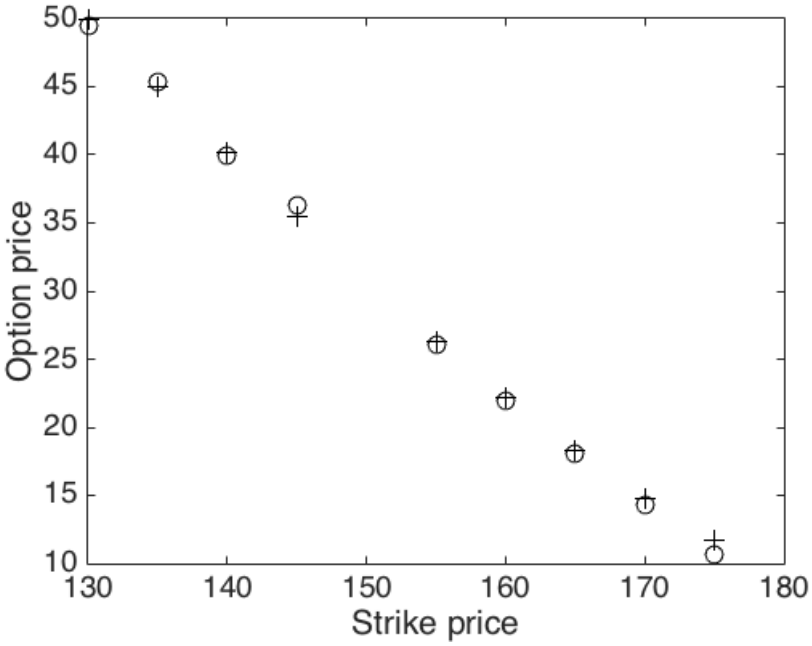


(b) The Dow Jones Industrial Average. 277 days to maturity.

Figure 26: Kou's jump-diffusion model applied to the Dow Jones Industrial Average. Rings are market quotes, crosses are model prices.

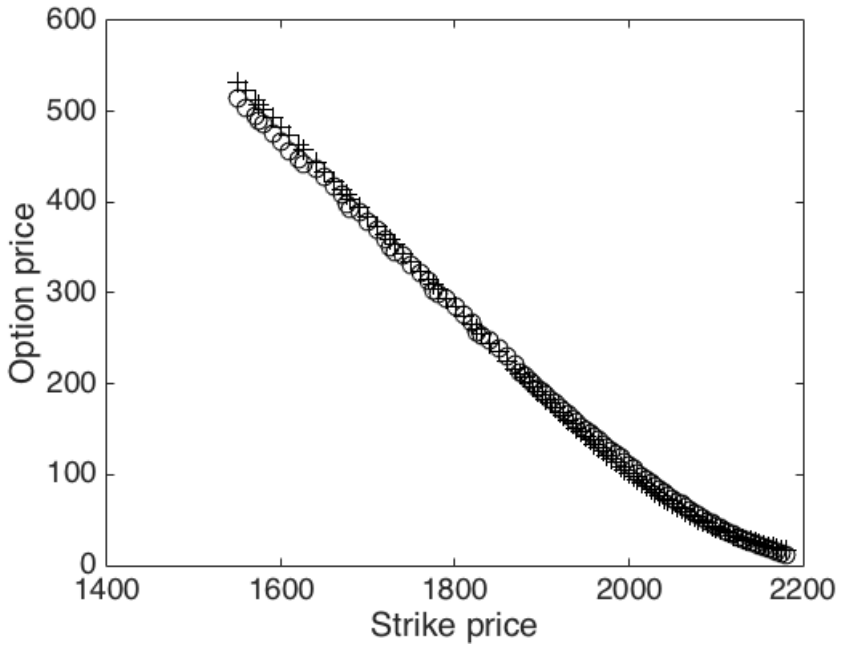


(a) The S & P 500 Index. 94 days to maturity.

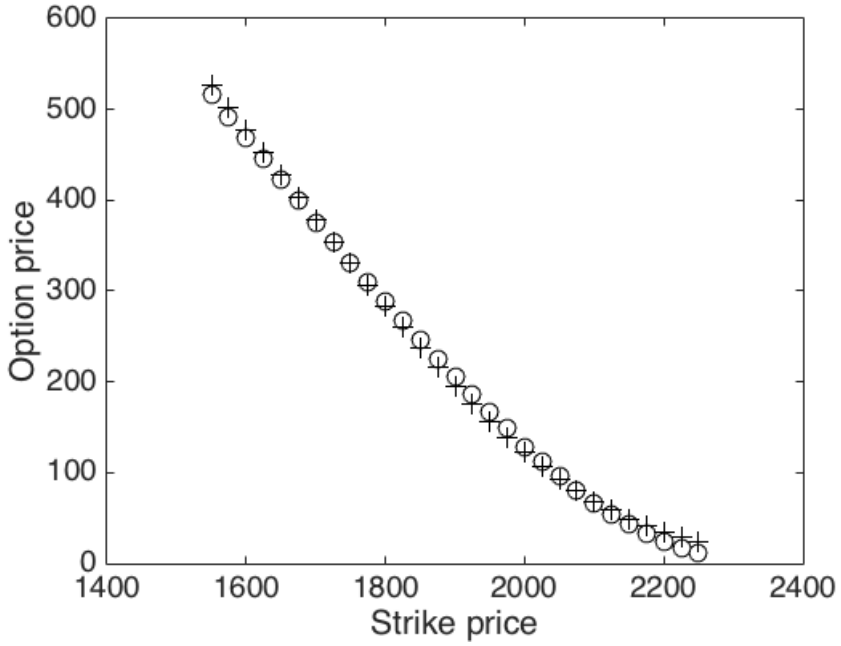


(b) The S & P 500 Index. 185 days to maturity.

Figure 27: Kou's jump-diffusion model applied to the S & P 500 Index. Rings are market quotes, crosses are model prices.

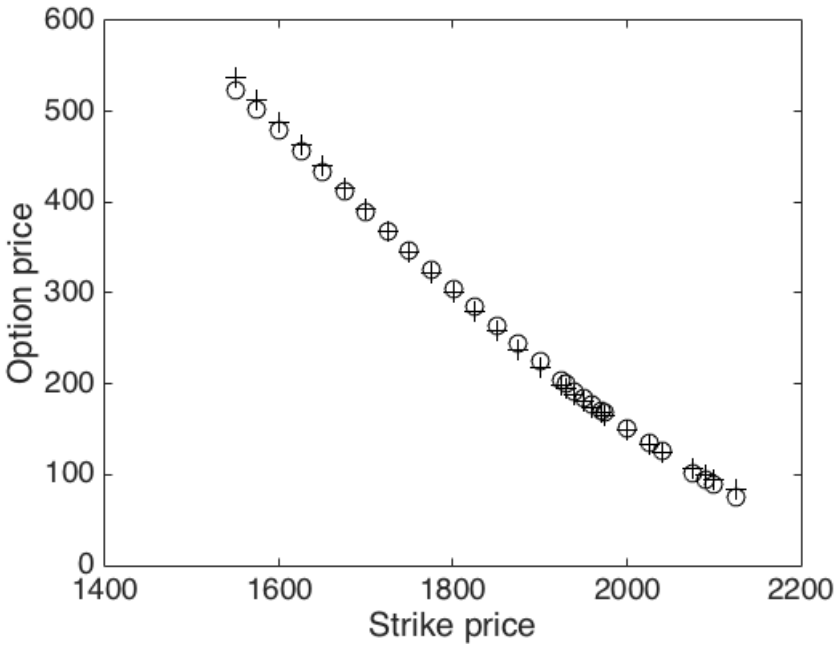


(a) The S & P 500 Index. 277 days to maturity.

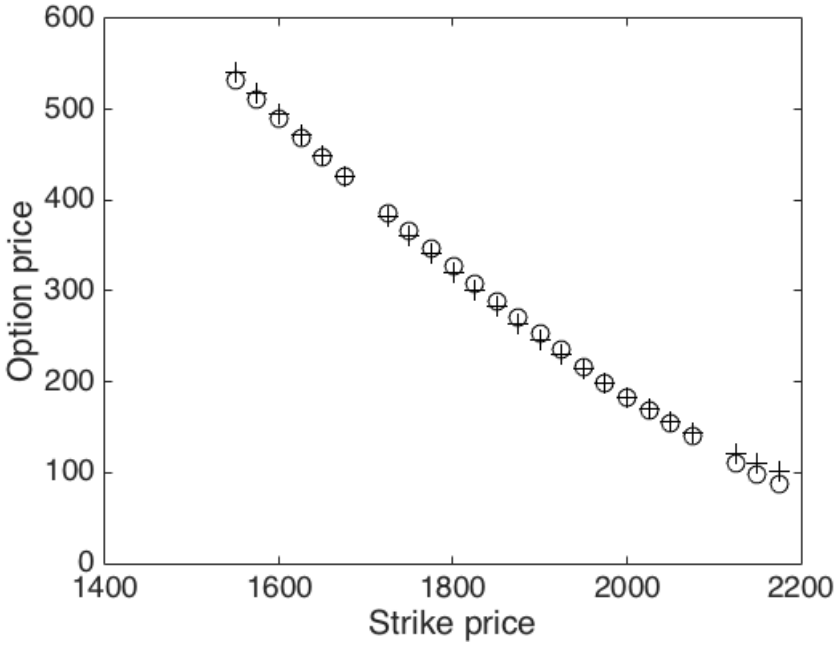


(b) The S & P 500 Index. 458 days to maturity.

Figure 28: Kou's jump-diffusion model applied to the S & P 500 Index. Rings are market quotes, crosses are model prices.

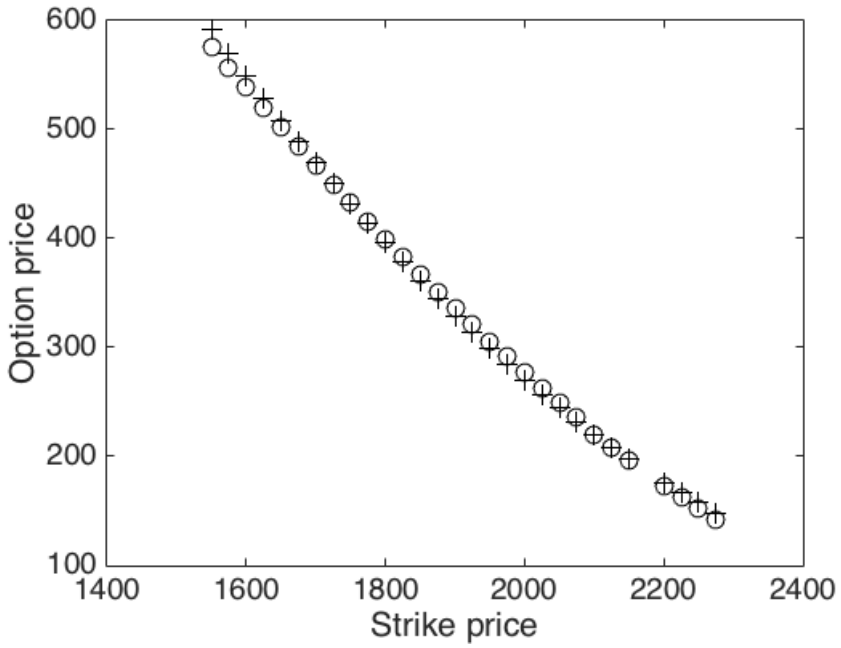


(a) The S & P 500 Index. 640 days to maturity.

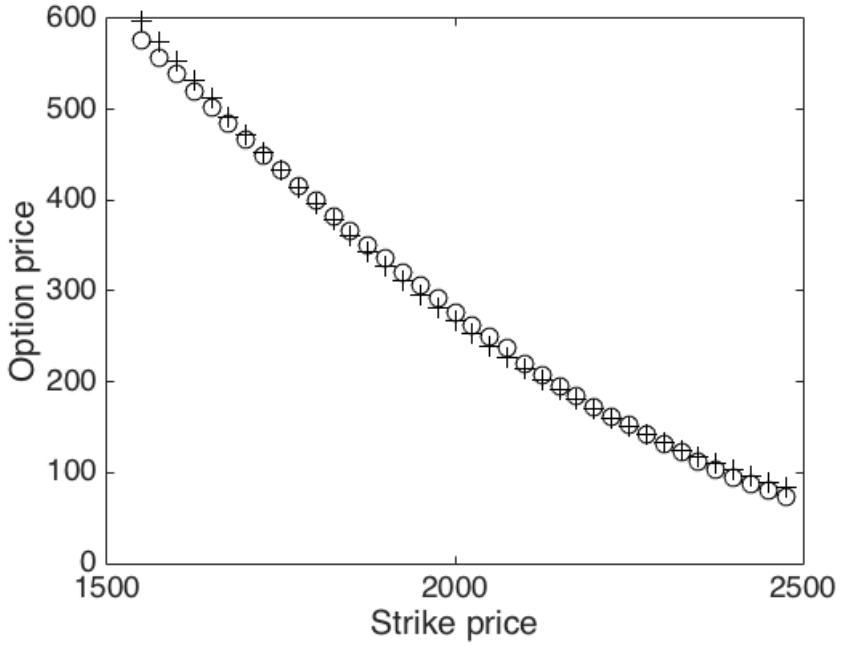


(b) The S & P 500 Index. 1004 days to maturity.

Figure 29: Kou's jump-diffusion model applied to the S & P 500 Index. Rings are market quotes, crosses are model prices.

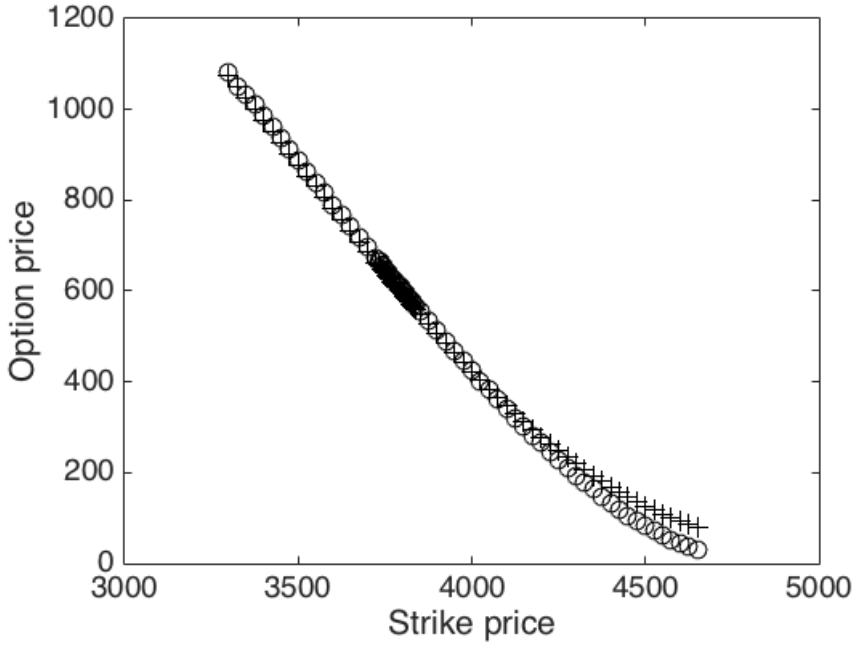


(a) The Nasdaq-100 Index. 94 days to maturity.

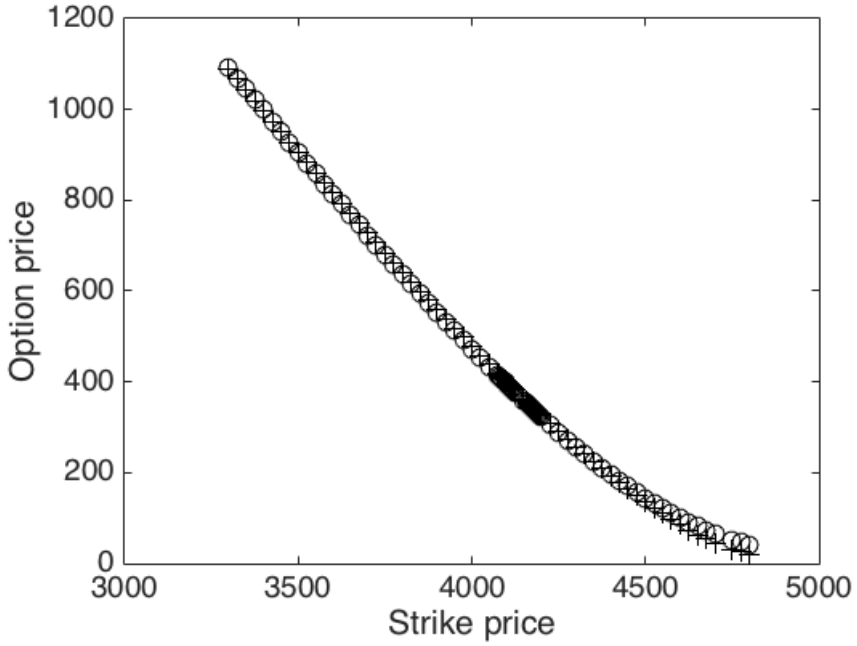


(b) The Nasdaq-100 Index. 185 days to maturity.

Figure 30: The variance-gamma model applied to the Nasdaq-100 Index. Rings are market quotes, crosses are model prices.

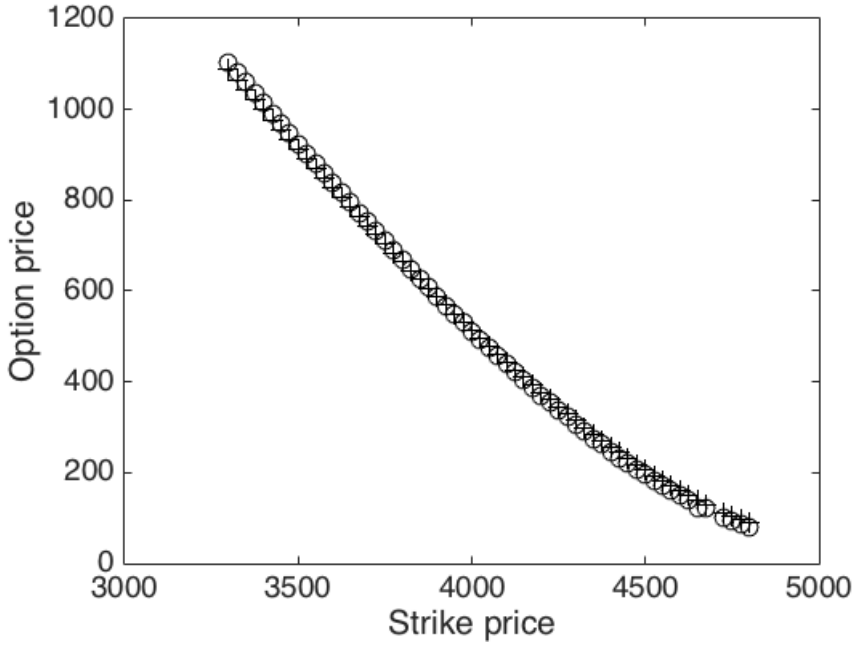


(a) The Nasdaq-100 Index. 277 days to maturity.

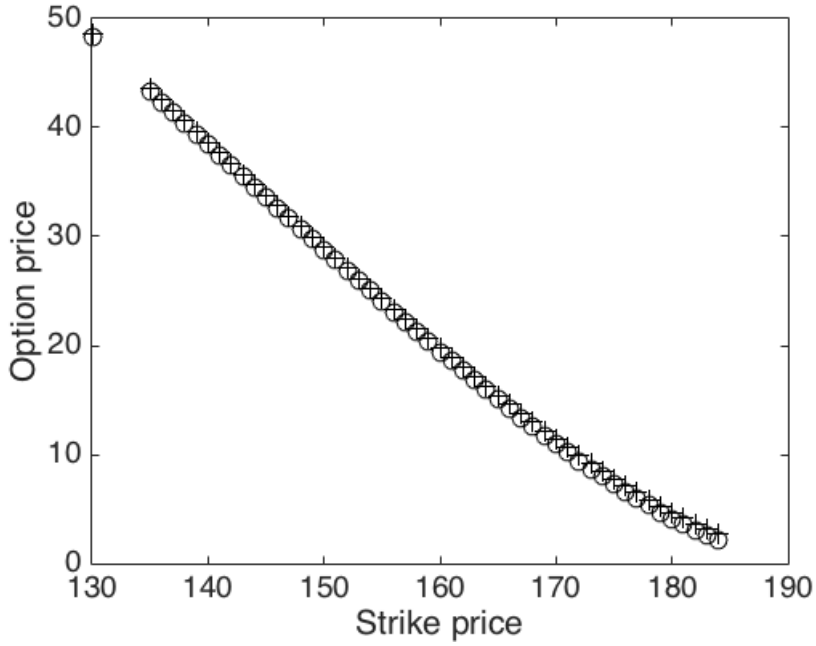


(b) The Dow Jones Industrial Average. 94 days to maturity.

Figure 31: The variance-gamma model applied to the Nasdaq-100 Index and the Dow Jones Industrial Average. Rings are market quotes, crosses are model prices.

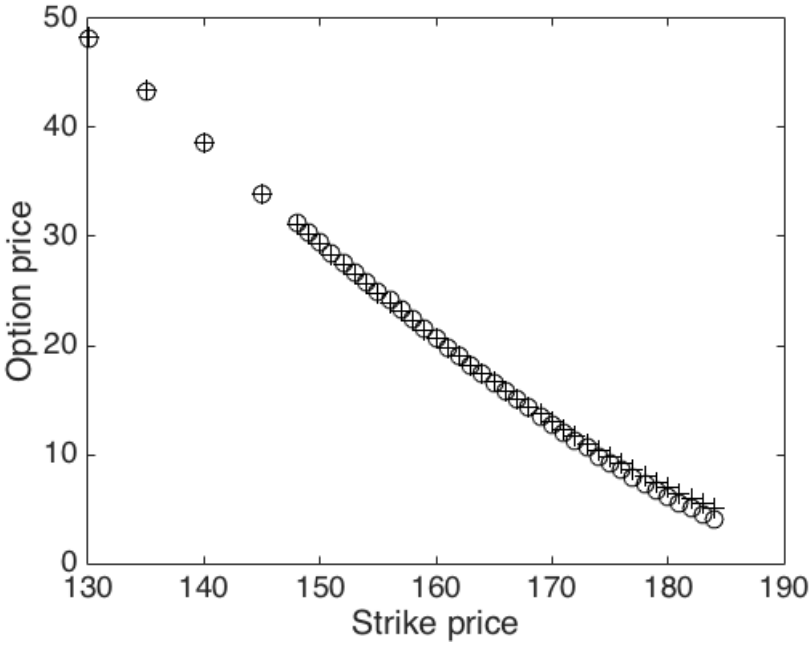


(a) The Dow Jones Industrial Average. 185 days to maturity.

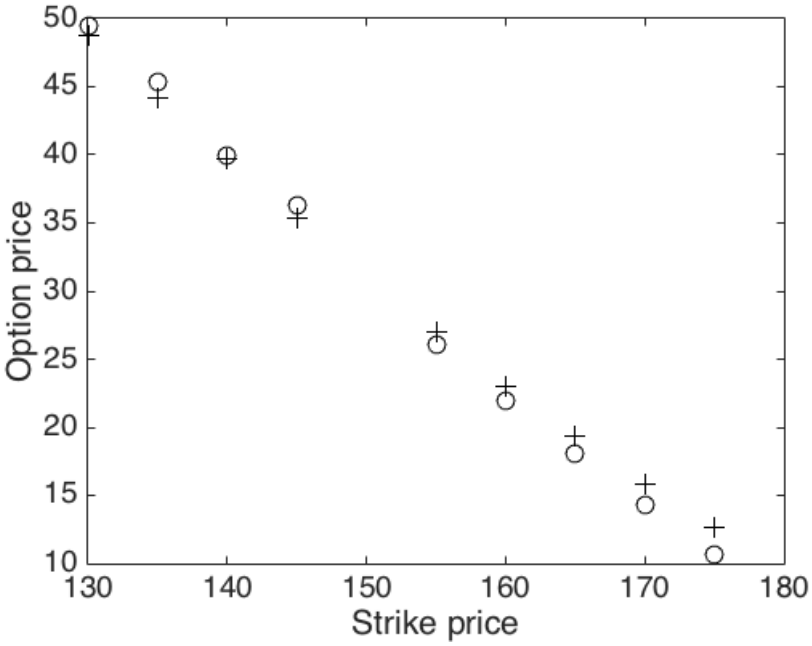


(b) The Dow Jones Industrial Average. 277 days to maturity.

Figure 32: The variance-gamma model applied to the Dow Jones Industrial Average. Rings are market quotes, crosses are model prices.

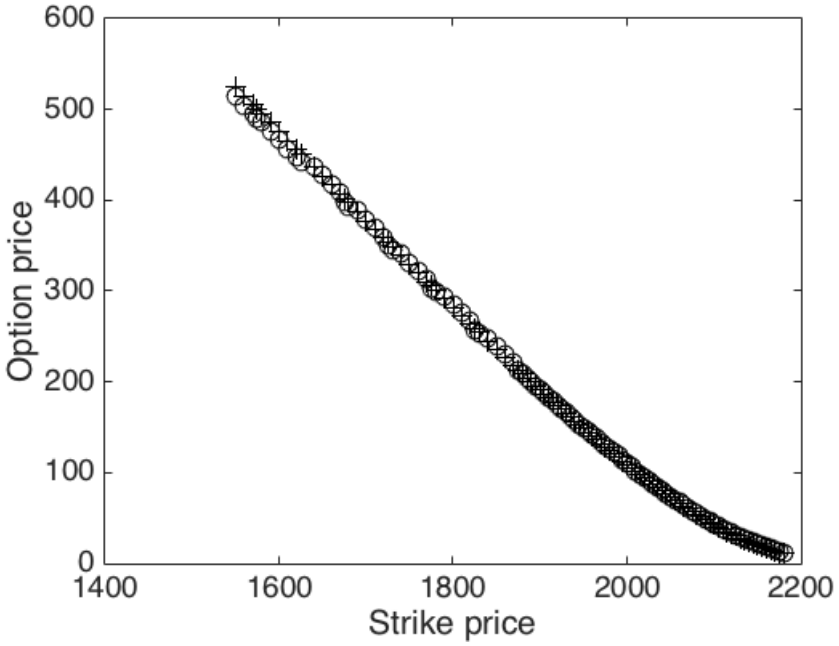


(a) The S & P 500 Index. 94 days to maturity.

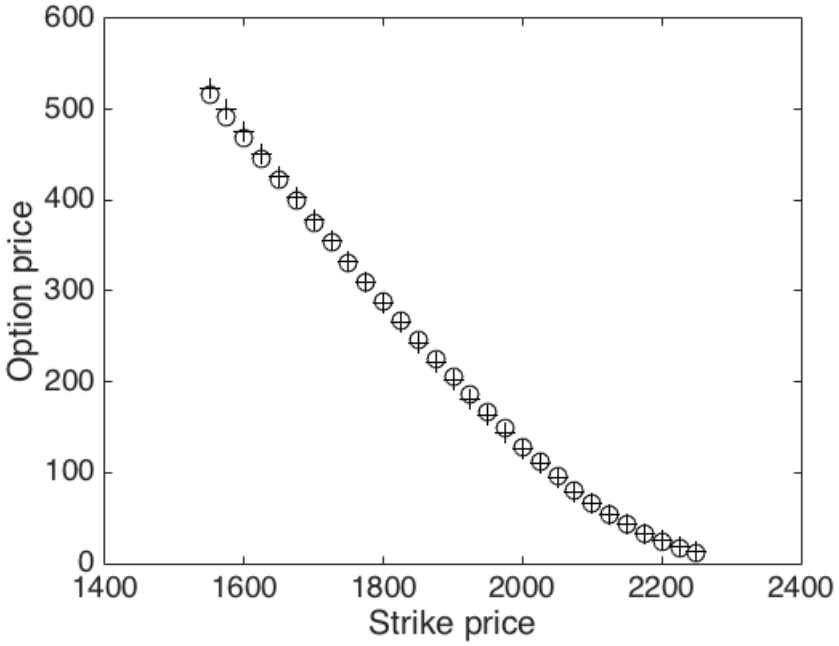


(b) The S & P 500 Index. 185 days to maturity.

Figure 33: The variance-gamma model applied to the S & P 500 Index. Rings are market quotes, crosses are model prices.

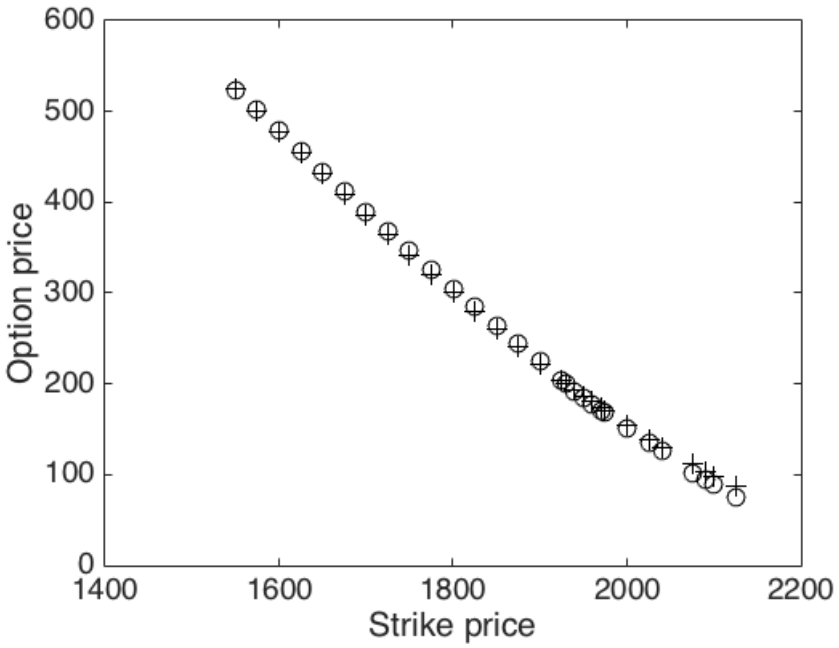


(a) The S & P 500 Index. 277 days to maturity.

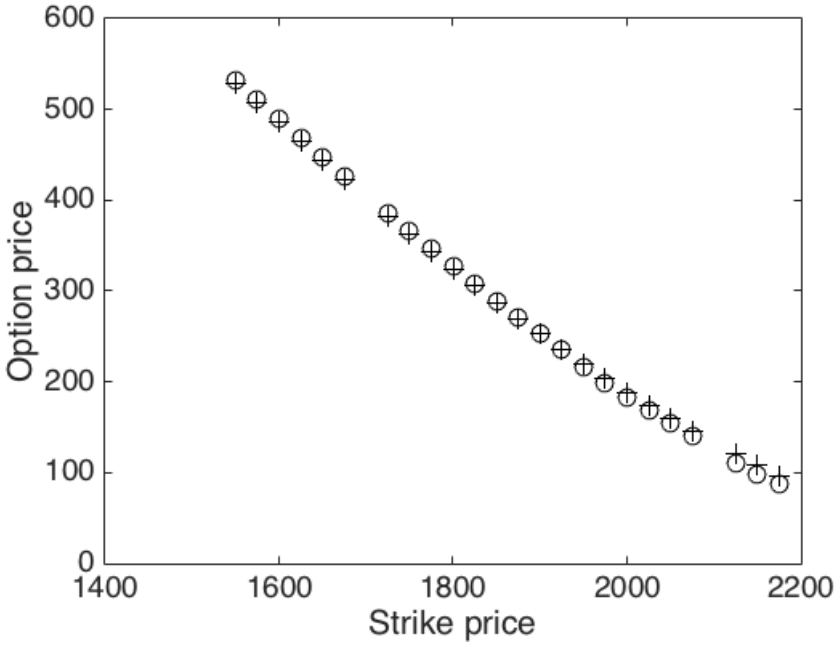


(b) The S & P 500 Index. 458 days to maturity.

Figure 34: The variance-gamma model applied to the S & P 500 Index. Rings are market quotes, crosses are model prices.

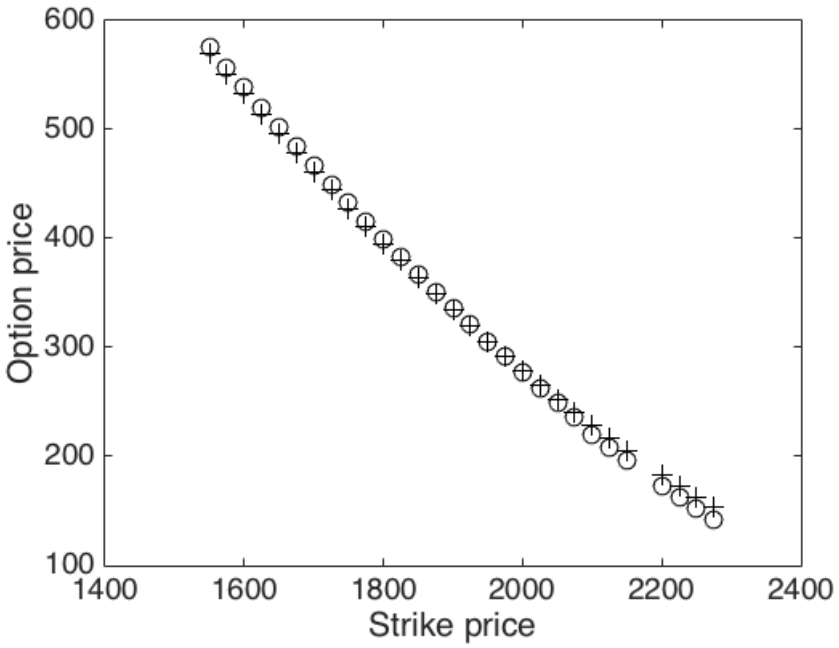


(a) The S & P 500 Index. 640 days to maturity.

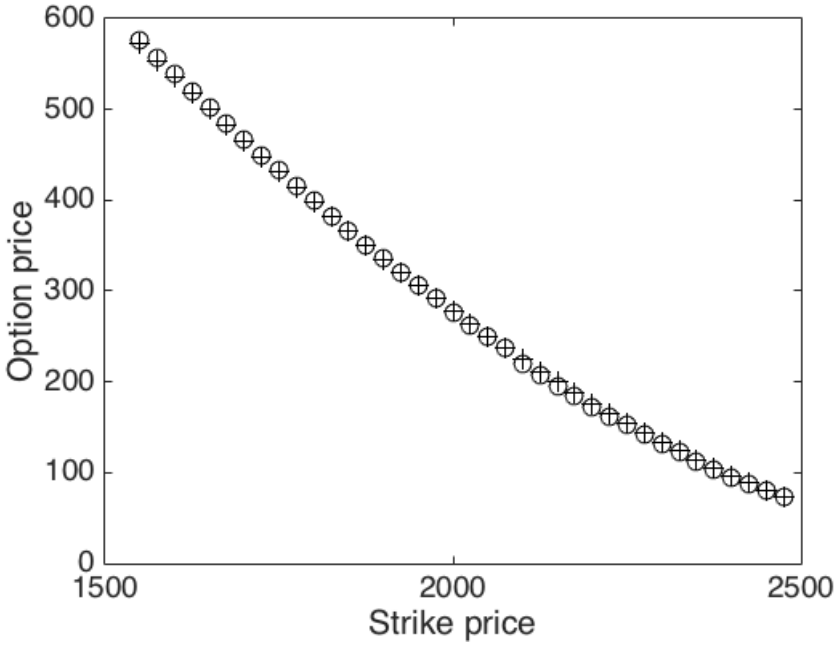


(b) The S & P 500 Index. 1004 days to maturity.

Figure 35: The variance-gamma model applied to the S & P 500 Index. Rings are market quotes, crosses are model prices.

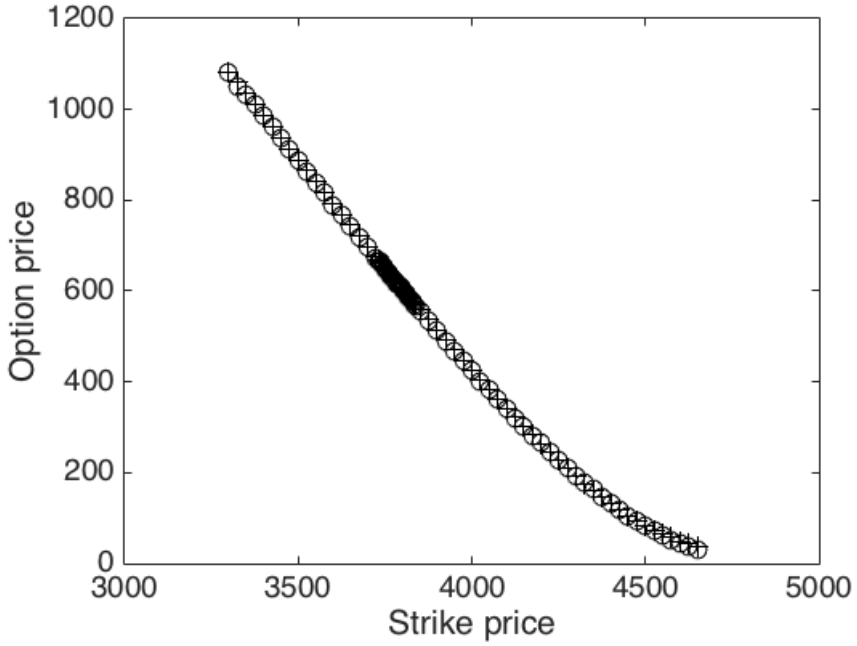


(a) The Nasdaq-100 Index. 94 days to maturity.

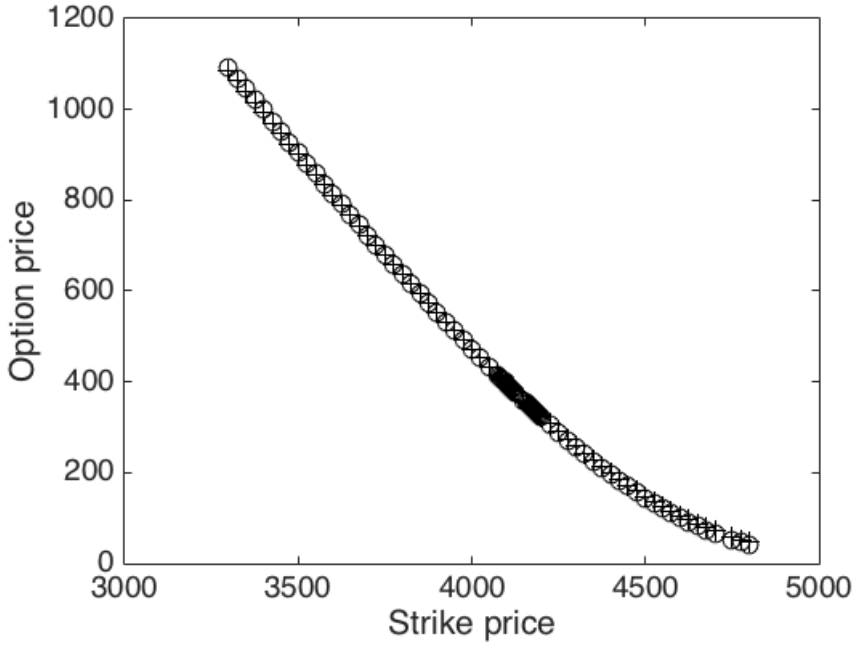


(b) The Nasdaq-100 Index. 185 days to maturity.

Figure 36: The normal-inverse Gaussian model applied to the Nasdaq-100 Index. Rings are market quotes, crosses are model prices.

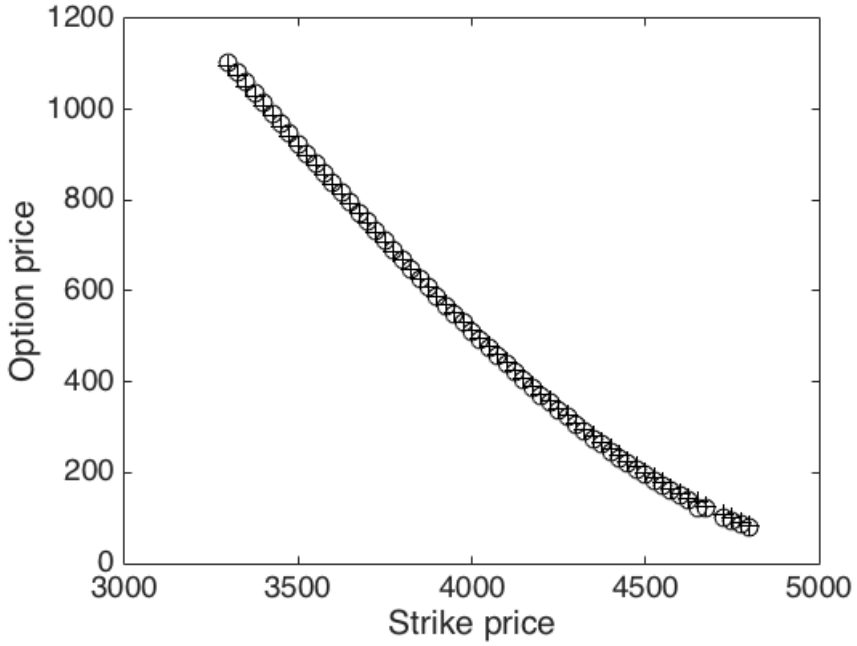


(a) The Nasdaq-100 Index. 277 days to maturity.

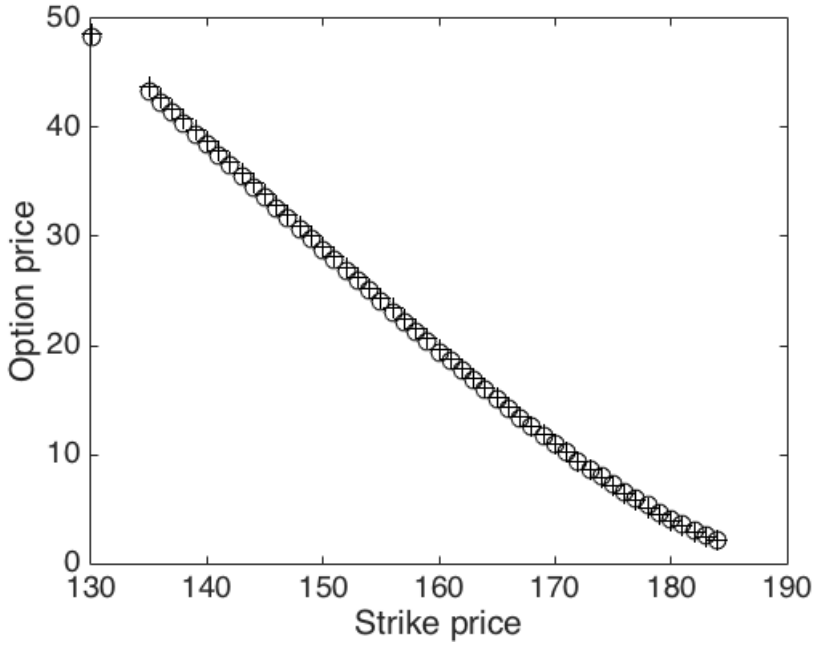


(b) The Dow Jones Industrial Average. 94 days to maturity.

Figure 37: The normal-inverse Gaussian model applied to the Nasdaq-100 Index and the Dow Jones Industrial Average. Rings are market quotes, crosses are model prices.

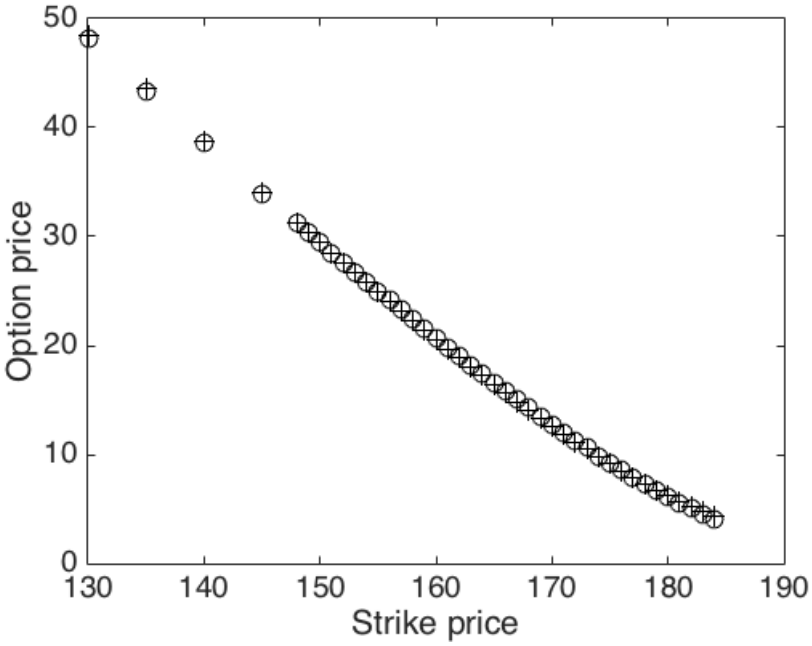


(a) The Dow Jones Industrial Average. 185 days to maturity.

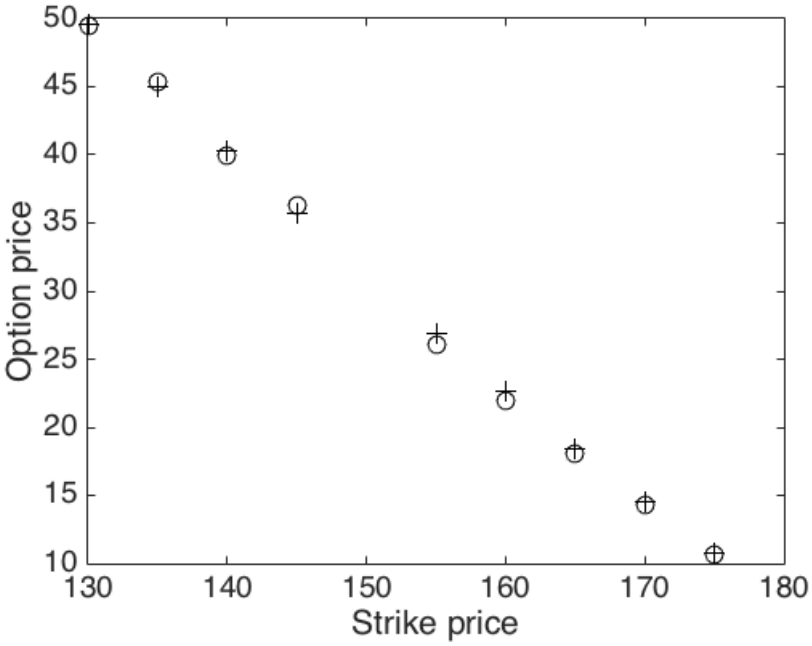


(b) The Dow Jones Industrial Average. 277 days to maturity.

Figure 38: The normal-inverse Gaussian model applied to the Dow Jones Industrial Average. Rings are market quotes, crosses are model prices.

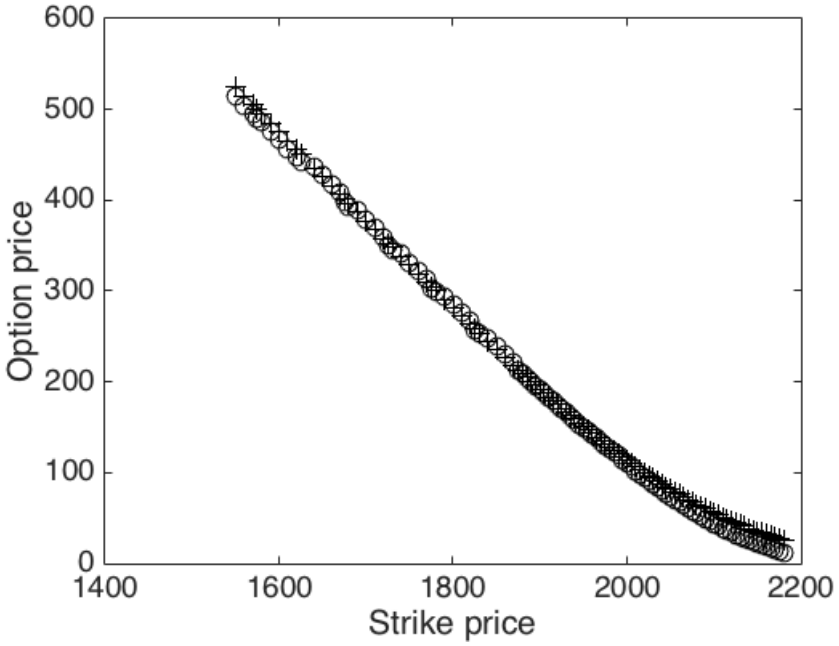


(a) The S & P 500 Index. 94 days to maturity.

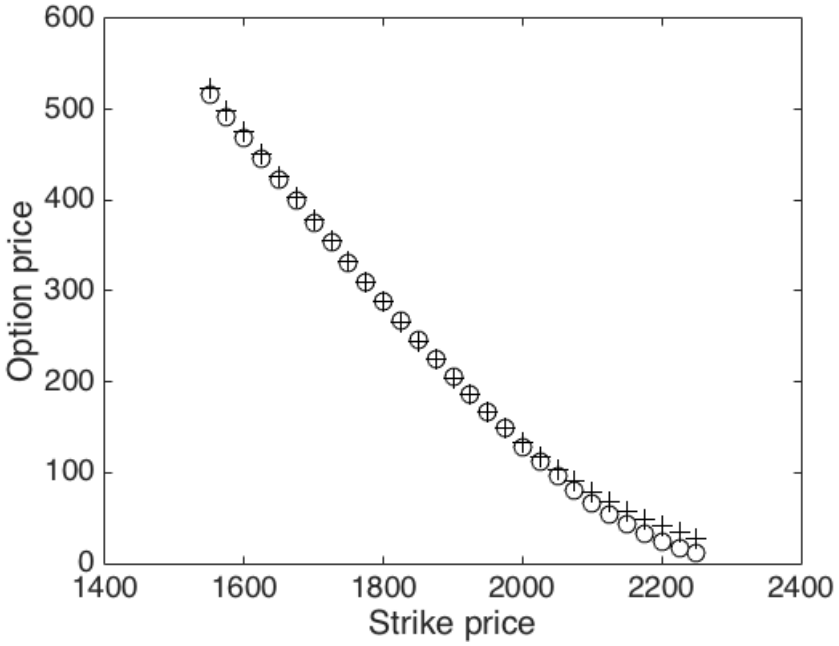


(b) The S & P 500 Index. 185 days to maturity.

Figure 39: The normal-inverse Gaussian model applied to the S & P 500 Index. Rings are market quotes, crosses are model prices.

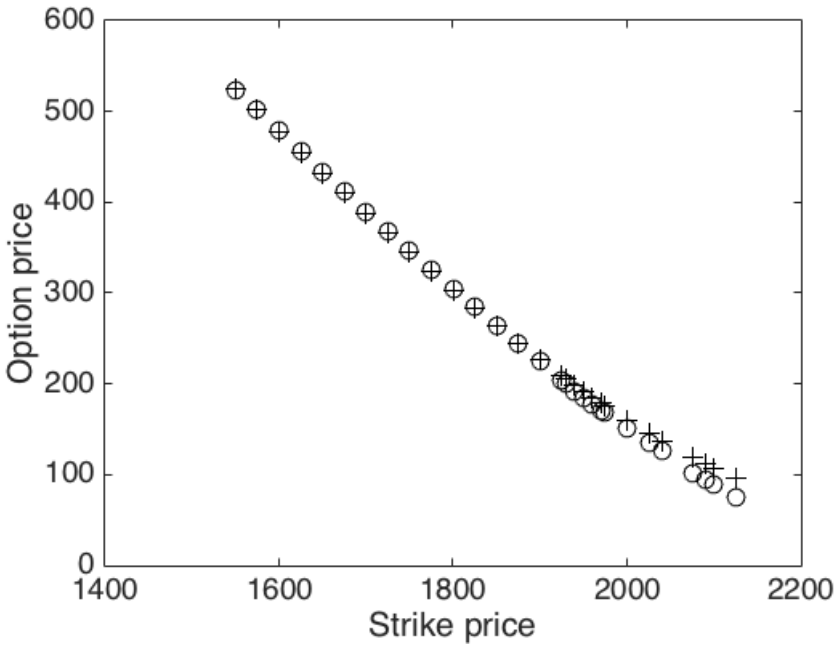


(a) The S & P 500 Index. 277 days to maturity.

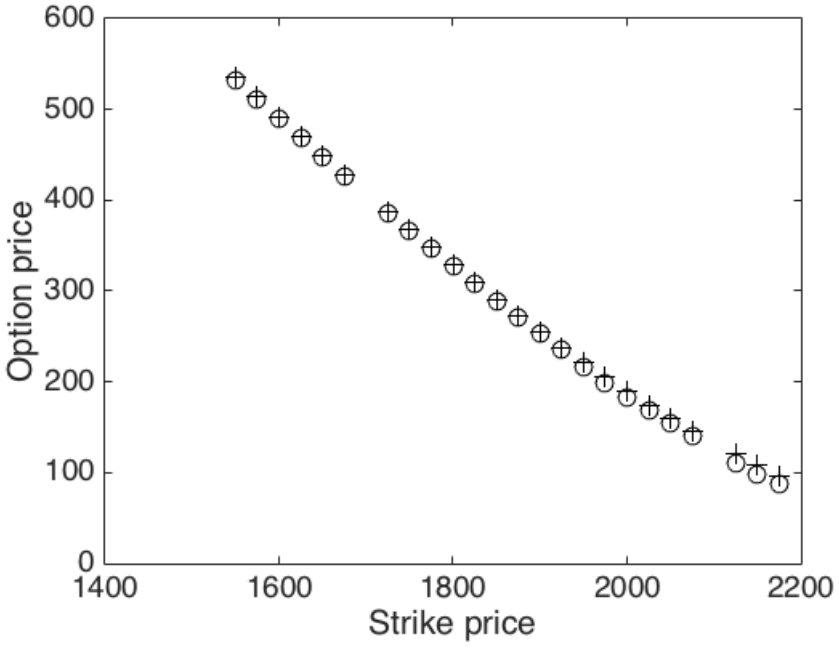


(b) The S & P 500 Index. 458 days to maturity.

Figure 40: The normal-inverse Gaussian model applied to the S & P 500 Index. Rings are market quotes, crosses are model prices.

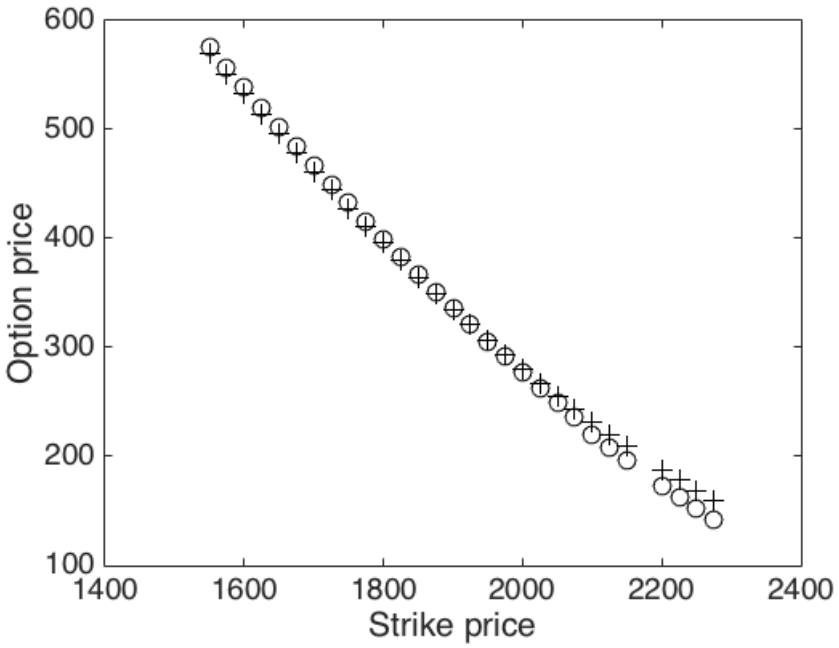


(a) The S & P 500 Index. 640 days to maturity.

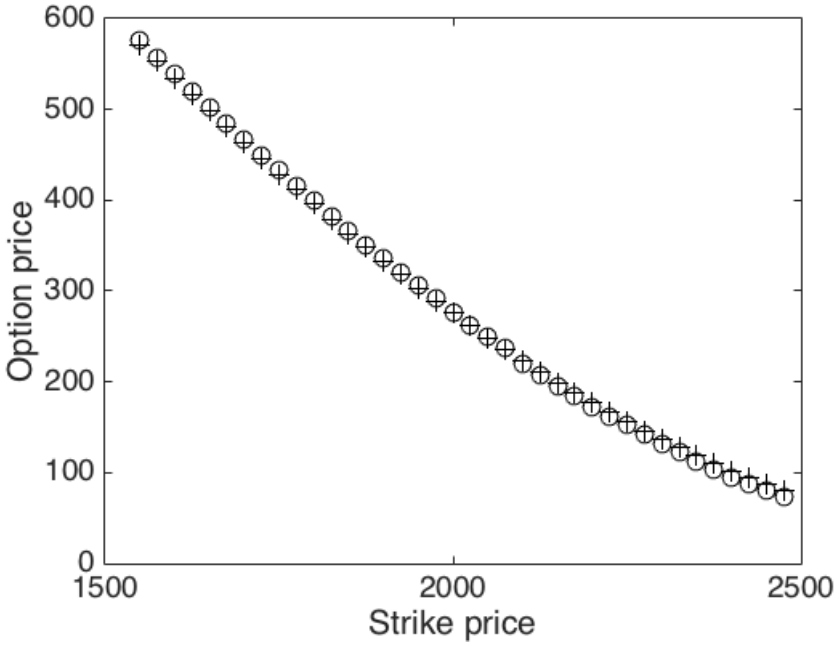


(b) The S & P 500 Index. 1004 days to maturity.

Figure 41: The normal-inverse Gaussian model applied to the S & P 500 Index. Rings are market quotes, crosses are model prices.

# 9 Discussion and Conclusions

In this thesis we talked about the shortcomings of the classical Black-Scholes model used for option pricing. As an alternative to the Black-Scholes model we introduced exponential Lévy models, namely Merton's and Kou's jump-diffusion models, and two pure jump models governed by the variance-gamma process and the normal-inverse Gaussian process. The underlying assets were the indices Nasdaq-100, Dow Jones Industrial Average, and S & P 500. The fractional fast Fourier transform was used to retrieve option prices from the corresponding characteristic functions. What separates the fractional fast Fourier transform from the regular fast Fourier transform and speaks in favor of the former is that we are given the liberty to independently choose the grid sizes of the integration and the log-strike price, and hence the characteristic function information can be used more efficiently typically yielding less function evaluations resulting in computational time savings.

The models were calibrated with the method of steepest descent and non-linear least squares. However, as was mentioned, the method of steepest descent is very much connected to the initial guess of the parameters and is relatively slow close to the minimum. Hence, an extension to this thesis could be to use another calibration method.

As seen in Chapter 8, all of the exponential Lévy models improved on the Black-Scholes model across all markets. It should however be noted that we used a very simple form of the Black-Scholes model, utilizing only a single, constant volatility parameter.

In this thesis, asset price jumps were included as a way of trying to improve on the Black-Scholes model and to capture its stylized facts. A further extension could be the inclusion of stochastic volatility, that is, to model and to calibrate option prices taking into account both the occurence of jumps and the possibility of the volatility being stochastic.

An even further extension to this thesis could be to model exotic option prices by calibrating a stochastic volatility model to vanilla option prices and then calculate the prices of more complicated options, such as barrier options etc.

An important topic we only mentioned briefly while deriving the Black-Scholes equation is that of hedging. It is a vital topic because risk is a crucial yet problematic element of investing. In complete markets, hedging is pretty straightforward since risk can be completely avoided simply by purchasing the replicating portfolio. Incomplete markets, on the other hand, necessitates additional criteria in able to determine viable hedging strategies. Thus, hedging could perhaps also be an extension to this thesis.

# REFERENCES


[1] Applebaum, D. (2009). *Lévy Processes and Stochastic Calculus*. New York: Cambridge University Press.

[2] Black, F. (1972). Capital Market Equilibrium with Restricted Borrowing. *The Journal of Business*. Vol. 45, No. 3, pp. 444-455.

[3] Carr, P. and Madan, D. (1999). Option Valuation Using the Fast Fourier Transform. *Journal of Computational Finance*. Vol. 2, No. 4, pp. 61-73.

[4] Chourdakis, K. (2004). Option Pricing Using the Fractional FFT. *Journal of Computational Finance*. Vol. 8, No. 2, pp. 1-18.

[5] Chourdakis, K. (2008). *Financial Engineering: A Brief Introduction Using the Matlab System*. Available at: <http://cosweb1.fau.edu>.

[6] Cont, R. and Tankov, P. (2002). *Calibration of Jump-Diffusion Option Pricing Models: A Robust Non-Parametric Approach. Rapport Interne CMAP Working Paper*. No. 490.

[7] Cont, R. and Tankov, P. (2004). *Financial Modelling with Jump Processes*. London: CRC Press LLC.

[8] Gerber, H. U. and Shiu E. S. W. (1994). Option Pricing by Esscher Transforms. *Transactions of Society of Actuaries*. Vol. 46, pp. 99-191.

[9] Higham, D. J. (2004). *An Introduction to Financial Option Valuation: Mathematics, Stochastics, and Computation*. New York: Cambridge University Press.

[10] Hull, J. C. (2011). *Options, Futures, and Other Derivatives*. 8th edn. Boston, MA: Prentice Hall.

[11] Klebaner, F. C. (2005). *An Introduction to Stochastic Calculus with Applications*. 2nd edn. London: Imperial College Press.

[12] Kou, S. G. (2002). A Jump-Diffusion Model for Option Pricing. *Management Science*. Vol. 48, No. 2, pp. 1086-1101.

[13] Kou, S. G. and Wang, H. (2004). Option Pricing Under a Double Exponential Jump Diffusion Model. *Management Science*. Vol. 50, No. 9, pp. 1178-1192.

[14] Krichene, N. (2005). Subordinated Lévy Processes and Applications to Crude Oil Options. *IMF Working Paper*. No. 5, pp. 1-26.

[15] Madan, D. and Seneta, E. (1990). The Variance Gamma (V.G.) Model for Share Market Returns. *The Journal of Business*. Vol. 63, No.4, pp. 511-524.

[16] Mastro, M. (2013). *Financial Derivative and Energy Market Valuation: Theory and Implementation in Matlab*. Hoboken, NJ: John Wiley & Sons, Inc.

[17] Matsuda, K. (2004). *Introduction to Merton's Jump-Diffusion Model*. Available at: <http://www.maxmatsuda.com>.

[18] Papapantoleon, A. (2008). *An Introduction to Lévy Processes with Application in Finance*. Available at: <http://page.math.tu-berlin.de>.

[19] Pender, K. (2004). SFGate. Available at: http://www.sfgate.com/business/networth/article/What-rising-interest-rates-will-mean-for-your-2765393.php.

[20] Schoutens, W. (2003). *Lévy Processes in Finance: Pricing Financial Derivatives*. Chichester, West Sussex, England: John Wiley & Sons, Ltd.

[21] Srikant, M. (2000). *The Black-Scholes Equation*. Available at: <http://srikant.org/thesis/node8.html>.

[22] Strutz, T. (2011). *Data Fitting and Uncertainty: A Practical Introduction to Weighted Least Squares and Beyond*. Wiesbaden, Germany: Vieweg+Teubner.

[23] Tankov, P. and Voltchkova, E. (2009). Jump-Diffusion Models: A Practitioner's Guide. *Banque et Marchés*. No. 99.

[24] Tankov, P. and Touzi, N. (2010) *Calcule Stochastique en Finance*. Available at: <http://www.cmap.polytechnique.fr>.

[25] Tankov, P. (2010). *Financial Modeling with Lévy Processes*. Available at: <http://www.impan.pl>.

[26] Todorov, V. and Tauchen, G. (2006). Simulation Methods for Lévy-Driven Continuous-Time Autoregressive Moving Average (CARMA) Stochastic Volatility Models. *Journal of Business & Economic Statistics*. Vol. 24, No. 4, pp. 455-469.

[27] Wikipedia (2015). *Gradient Descent*. Available at: <http://en.wikipedia.org/wiki/Gradient_descent>.

[28] Wilmott, P., Howison, S., and Dewynne, J. (1995). *The Mathematics of Financial Derivatives: A Student Introduction*. Cambridge, UK: Cambridge University Press.

[29] Øksendal, B. (2003). *Stochastic Differential Equations: An Introduction with Applications*. New York: Springer-Verlag.